



universität
wien

MASTERARBEIT

Titel der Masterarbeit

“Advanced fractionation of tropical healing plants used against
inflammation; testing of anti-neoplastic activity”

angestrebter akademischer Grad

Master of Science (M.Sc.)

Verfasserin:	Mareike Seelinger, B.Sc.
Studienkennzahl lt. Studienblatt:	A 066 838
Studienrichtung lt. Studienblatt:	Ernährungswissenschaften
Betreuer:	ao. Univ.-Prof. Dr. Georg Krupitza
Ort, Datum:	Wien, Dezember 2010

Table of Content

1	Introduction	1
2	Literature survey	3
2.1	Carcinogenesis	3
2.1.1	The multistep model	3
2.1.2	The role of oncogenes and tumor suppressor genes	5
2.1.3	Cancer and inflammation.....	6
2.2	The six hallmarks of cancer	7
2.2.1	Self sufficiency in growth signals.....	8
2.2.2	Insensitivity to antigrowth signals	9
2.2.3	Evading apoptosis	12
2.2.4	Limitless replicative potential.....	15
2.2.5	Sustained angiogenesis	16
2.2.6	Tissue invasion and metastasis	16
2.3	Leukaemia	17
2.4	Investigated activity of two ethnomedical plants from Guatemala.....	17
3	Materials and methods.....	20
3.1	Plant material	20
3.1.1	<i>P. odorata</i>	20
3.1.2	<i>S. spinosa</i>	21
3.2	General methods.....	23
3.2.1	Thin layer chromatography (TLC)	23
3.2.2	Cell culture.....	24
3.2.3	Proliferation assay.....	25
3.2.4	Apoptosis assay.....	25
3.2.5	Western Blotting	26
3.2.6	Statistical Analysis.....	29
3.3	Methods used for <i>P. odorata</i>	30
3.3.1	Chlorophyll Separation	30
3.3.2	Vacuum Liquid Chromatography (VLC)	30
3.3.3	Column chromatography (CC) and Thin Layer Chromatography (TLC)	32
3.4	Methods used for <i>S. spinosa</i>	36
3.4.1	Extraction.....	36
3.4.2	Detannification of the methanol extract.....	37
4	Results.....	38
4.1	<i>P. odorata</i>	38
4.1.1	Comparison of the 2005 and 2009 dichloromethane extract	39

Table of Content

4.1.2	Separation of chlorophyll	40
4.1.3	Vacuum Liquid Chromatography (VLC)	41
4.1.4	Column Chromatography (CC) and Thin Layer Chromatography (TLC)	49
4.1.5	Western Blot analysis	63
4.2	<i>S. spinosa</i>	69
4.2.1	Extraction	69
4.2.2	Detannification	74
4.2.3	Western Blot analysis	78
5	Conclusion	83
5.1	<i>P. odorata</i>	83
5.2	<i>S. spinosa</i>	85
6	Summary	87
7	Zusammenfassung	89
8	References	91
9	Indices	100
9.1	Index of Tables	100
9.2	Index of Figures	101
10	Danksagung	104
11	Curriculum Vitae	105
12	List of Publications	106

Abbreviation Index

ADP	Adenosine diphosphate
ALL	Acute lymphoblastic leukaemia
AML	Acute myeloid leukaemia
Apaf-1	Apoptotic protease activating factor-1
ASR	Anisaldehyd sulphuric acid reagent
ATCC	American Type Culture Collection
ATM	Ataxia-telangiectasia-mutated
ATP	Adenosine-5'-triphosphate
ATR	Ataxia telangiectasia mutated and Rad3-related
Bcl-2	B-cell lymphoma 2
CAM	Cell-to-cell adhesion molecules
CC	Column chromatography
Cdc	Cell division control
Cdk	Cyclin-dependent kinase
Chk	Check point kinases
CLL	Chronic lymphocytic leukaemia
CML	Chronic myelogenous leukaemia
DMSO	Dimethyl sulfoxide
DNA	Deoxyribonucleic acid
ECL	Enhanced chemiluminescence
ECM	Extracellular matrix
FADD	FAS-associated death domain protein
FCS	Fetal calf serum
FGF	Fibroblast growth factor
G0, G1, G2	Gap phases of the cell cycle
GTP	Guanosine-5'-triphosphate
H ₂ SO ₄	Sulfuric acid
HL-60	Human promyelocytic leukaemia cell-line
HO	Hoechst 33258
HOPI	Hoechst 33258 / propidium iodide
IGF-1/IGF-2	Insulin-like growth factors

Abbreviation Index

IL	Interleukin
MBS	Myosin-binding subunit
MLC2	Myosin light chain 2
MLCK	Myosin light chain kinase
M-phase	Mitosis-phase
mRNA	Messenger ribonucleic acid
MYPT1	Myosin-binding subunit of myosin phosphatase
NF- κ B	Nuclear factor κ B
NOS	Nitrogen species
PAGE	Polyacrylamide gel electrophoresis
PARP	ADP-ribose polymerase
PBS	Phosphate buffered saline
PDGF	Platelet-derived-growth factor
PI	Propidium iodide
PI3-kinase	Phosphatidylinositol 3-kinase
PIC	Protease inhibitor cocktail
PKB	Protein kinase B
PMSF	Phenylmethylsulfonyl fluoride
pRb	Retinoblastoma protein
PVDF	Polyvinylidene difluoride
RhoA	Ras homolog gene family member A
RNA	Ribonucleic acid
ROCK	Rho-associated kinases
ROS	Reactive oxygen species
RPMI	Roswell park memorial institute
SDS	Sodium dodecyl sulfate
S-phase	Synthesis-phase
TAM	Tumor-associated macrophages
TBS	Tris buffered saline
TGF	Transforming growth factor
TLC	Thin layer chromatography
TNF α	Tumor necrosis factor α

TRADD	TNF receptor-associated death domain protein
UV	Ultra-violet
VCR	Vincristine
VEGF	Vascular endothelial growth factor
VLB	Vinblastine
VLC	Vacuum liquid chromatography

1 Introduction

One out of three persons is affected by cancer during their lifetime (Pecorino, 2008) and more than 50 % of them die from the disease (Stewart, et al., 2003). In 2004 13 % of all deaths worldwide were caused by cancer and the number of people affected and die from cancer will increase from 7.4 million in 2004 to approximately 12 million in 2030. Despite the fact that 30 % of cancer cases could be prevented by healthy nutrition, avoiding other risk factors like tobacco, being physically active and preventing chronic infections (WHO, 2009), there is a substantial need for anti-cancer drugs at the moment and it will increase in the near future. For the treatment of many types of cancer, plants have been a source of effective drugs. Over 60 % of anti-cancer drugs originate from natural sources like plants, marine organisms and micro-organisms (Cragg, et al., 2005). For thousands of years those natural products have been administered as a therapy against several diseases (Shoeb, 2006). An estimation conducted by the WHO reveals that even today 80 % of the population in Asian and African countries rely on traditional medicine for primary health care (WHO, 2008). Important examples of drugs derived from natural products that are now used in clinic are the vinca alkaloids vinblastine (VLB) and vincristine (VCR). Both were isolated from the Madagascar periwinkle, *Catharanthus roseus* G. Don.(Apocynaceae). Semi-synthetic analogues of these agents, originally used for the treatment of diabetes, are recently applied during cancer therapy in combination with other chemotherapeutic drugs. Another agent belonging to the plant-derived chemotherapeutic drugs is called Paclitaxel (taxol®), isolated from the bark of *Taxus brevifolia* Nutt. These examples show that isolated compounds from plants traditionally used as home remedies may lead to the development of novel anti-cancer agents (Cragg, et al., 2005). Between 1983 and 1994, 60 % of anti-cancer drugs arised from natural origin (Cragg, et al., 1997). Especially the high biodiversity of the rain forests provide a framework of possible sources for new drugs (Cseke, et al., 2006). These facts established the basis for the present work with the objective of finding new potential lead compounds against cancer by investigating two ethnomedical plants from Guatemala. The two plants, *Pluchea odorata* and *Smilax spinosa*, are both used by the Maya as natural healing plants against inflammation.

Because of similar signalling pathways up-regulated in inflammation and cancer these plants were selected (Kundu, et al., 2008). Bioassay-guided fractionation of *P. odorata* and its anti-cancer activity (especially of the dichloromethane extract) were first described by Gridling et al. (2009). Therefore the activity of the dichloromethane extract was further investigated in the current work with focus on the apoptotic pathways. Not much is known about the anti-cancer activity of the second ethnomedical plant, *S. spinosa*, and therefore we started with the extraction of the plant particularly focussing on the toxic activity. Both plant extracts and fractions were tested in proliferation and apoptosis assays, using HL-60 cells. In case of *P. odorata* the bioassay-guided fractionation, using solvents of increasing polarity, was further conducted with the most active fraction of the proliferation or apoptosis assay. After bioassay-guided fractionation, mechanisms of growth inhibition and apoptosis were investigated in western blot analyses.

2 Literature survey

This chapter includes important mechanisms for the development of cancer, as well as the definition of leukaemia and facts about the use of ethnomedical plants during drug development.

2.1 Carcinogenesis

Adults consist of around 10^{13} cells. These cells are renewed and replaced constantly, but during this process alterations or damage to the genetic material can occur, which may lead to cancer if they are not being repaired (World Cancer Research Fund International, 2007). In tumor cells many alterations of deoxyribonucleic acid (DNA), including point mutations and even chromosomal aberrations such as deletions and translocations have been detected. Causes of damaged DNA are both endogenous (internal) and exogenous (environmental) and accumulate during lifetime. Most of the mutations detected in tumor cells are somatic mutations, which are not passed to the next generation, whereas germline mutations will be inherited and therefore passed to the offspring (Pecorino, 2008). 5 to 10 % of cancers are caused by inheriting genes alterations. For example defects of DNA repair mechanisms predispose persons towards cancer (World Cancer Research Fund International, 2007).

2.1.1 The multistep model

A tumor arises from one single cell and is the outcome of a long latent period involving generations of cells (Foulds, 1969) undergoing multiple steps of tumor development, (Stewart, et al., 2003) (Figure 1). Especially with increasing age, mutations accumulate, repair mechanisms fail and thus the chance for carcinogenesis to take place is rising (Till, 1999). The three steps tumor initiation (irreversible genome damage), tumor promotion (reproduction of initiated cells) and tumor progression (increasing malignity) (Nau, et al., 2003) are described in the following chapter for historical reasons. This model is outdated and replaced by concise and proven concepts based on molecular verification (see chapter 2.2 The six hallmarks of cancer).

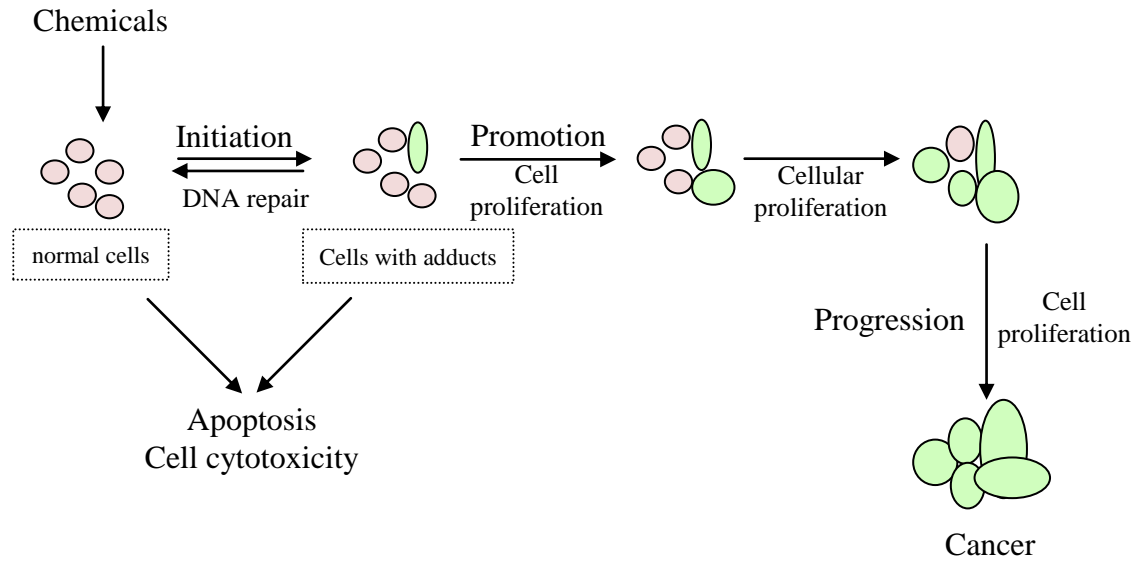


Figure 1 Multistep model of carcinogenesis (own figure, based on Oliveira, et al., 2007)

2.1.1.1 Tumor initiation

Initiation, the first step of the multistep model, includes the exposure to an agent that results in the first mutation. This mutation can be exogenous, endogenous or an inherited mutation (World Cancer Research Fund International, 2007). Endogenous carcinogenic chemicals are for example reactive oxygen species or products of lipid oxidation, both generated in metabolism (Burcham, 1999). Physical components like viruses, genotoxic or epigenetic factors belong to the exogenous cancer-causing chemicals (Davis, et al., 1993).

Somatic mutations are transferred to daughter cells during proliferation and generate the potential for neoplastic growth (World Cancer Research Fund International, 2007). An irreversible DNA damage can be acquired by a unique application of a genotoxic chemical (Nau, et al., 2003). A distinction is drawn between direct and indirect genotoxic substances: direct carcinogens are substances which directly bind to bases of the DNA (reactive oxygen species, hydroxyl radicals, and hydrogen peroxide and also external factors such as ultra-violet (UV) light) (Stewart, et al., 2003), whereas indirect ones like benzopyren, aflatoxin B1 or nitrosamines have to be activated in the metabolism before they are able to interact with the DNA (Guengerich, 2000). If critical genes like suppressor genes, oncogenes and genes involved in DNA repair are affected

by mutations, they will lead to genetic instability and loss of differentiation (Stewart, et al., 2003).

2.1.1.2 Tumor promotion

During the second step, tumor promotion, the initiated cells proliferate and become neoplastic. Tumor promoters are substances with epigenetic effects including hormones like oestrogens, androgens or phytohormones. Also polycyclic aromatic hydrocarbons are counted among tumor promoters, which all operate ‘around the gene’ and do not modify the DNA sequence. The effect of epigenetic changes is reversible and thus a repeated supply is required for tumor promotion. As a consequence proliferation of the mutated cells is stimulated and a benign tumor develops (Nau, et al., 2003).

2.1.1.3 Tumor progression

Benign tumor cells being exposed to further genotoxic substances increase their DNA damage and if DNA repair mechanisms are lacking the malignancy of the tumor increases (Nau, et al., 2003). Oncogenes have to be activated and tumor suppressor genes have to be deactivated for more and more autonomous growth of the tumor during the progression (Stewart, et al., 2003). Eventually, cancer cells become invasive and induce angiogenesis (World Cancer Research Fund International, 2007). This entire step is irreversible, just like the first step of tumor initiation (Nau, et al., 2003). This dogma is at stake, as it does not explain spontaneous remissions and ignores the fact that cells can be reprogrammed.

2.1.2 The role of oncogenes and tumor suppressor genes

Oncogenes and tumor suppressor genes are varying in function and play different roles in tumor development. During carcinogenesis proto-oncogenes are activated to oncogenes (gain of function), whereas alterations in tumor suppressor genes result in a loss of function (Stewart, et al., 2003). In the following chapters both genes and their proteins are described further.

2.1.2.1 Oncogenes

Proto-oncogenes, which are a normal part of the human genome, participate in regulation of growth and differentiation processes (Mehnert, et al., 2003). As they are dominant genes, one somatic mutation in one allele of a proto-oncogene induces the transformation into an oncogene. The oncogene thus gained its function and triggers uncontrolled proliferation and tumor promotion (Zielinski, et al., 1999). Hence, oncogenes have the ability to transform healthy cells, which is the main step in the development of sporadic tumors (Hunter, 1997). Until now, no germline mutations in oncogenes have been detected, leading to the assumption that such mutations are lethal during embryonic development (Löffler, et al., 1997). Mechanisms which may induce activation of proto-oncogenes are for example point mutations, gen amplifications or translocations (Till, 1999). Examples for oncogenes are c-Myc and Bcl-2, described in chapter 2.2.2 and 2.2.3.

2.1.2.2 Tumor suppressor genes

Tumor suppressor genes are also part of the normal human genome (Mehnert, et al., 2003). They protect the cells from unrestricted growth by guarding parts of the cell cycle as well as genes of the DNA repair system (Karlson, et al., 2005) and controlling the accuracy of cell division (Stewart, et al., 2003). The cell is then affected by genetic changes more easily (Kinzler, et al., 1997). Mutations of tumor suppressor genes are often the reason for congenital tumors, for which already one germline mutation has to be present (Zielinski, et al., 1999). Hereditary tumors thus occur at younger ages, because only one allele has to be hit by a mutation for a tumor to develop (Till, 1999). Tumor suppressor genes are for example the retinoblastoma protein (pRb) and p53 described in chapter 2.2.2 and 2.2.3, respectively.

2.1.3 Cancer and inflammation

Many chronic inflammations induced by non-infectious agents are known for their association with cancer. For example cancer caused by asbestos and also rheumatoid arthritis is linked with non-Hodgkin's lymphoma. On the other hand there also exist

cancers on the basis of virus or bacterium infections. For example hepatitis B virus and liver cancer are strongly associated and *helicobacter pylori* infections in the stomach are capable of causing stomach cancer. The link between inflammation and cancer are components causing DNA damage, produced during the inflammatory response. Macrophages for instance produce TNF α which acts as a tumor promotor when its expression, regulated by nuclear factor κ B (NF- κ B), is increased. Also reactive oxygen species (ROS) and nitrogen species (NOS) secreted by leucocytes promote carcinogenesis as they damage the DNA. The possibility of DNA damage is also enhanced by hepatitis B and *helicobacter pylori* infections, which both lead to tissue regeneration and increased cell division. Cell division is known as a procedure where DNA is susceptible to be damaged and where mutated genome can be passed to the progeny (Pecorino, 2008).

The link between cancer and inflammation continues even when the tumor has already developed. Again TNF α produced by tumor-associated macrophages (TAM) is the key for further malignancy, as it can affect cell motility and tumor metastasis (Pecorino, 2008). A very important target for anti-cancer drugs involving the inflammation causing part of the immune system is COX-2 inhibition (Stewart, et al., 2003), because the overexpression of COX-2 in epithelial cells inhibits apoptosis and increases the invasiveness of tumour cells (Gupta, et al., 2001). Close to 20 % of all cancers worldwide are estimated to be attributable to infection (Flood, et al., 2000). Thus the link between cancer and inflammation can be used for development of new therapeutics against cancer.

2.2 The six hallmarks of cancer

Approximately one hundred types of cancer from different origins are defined by now. Every type of cancer belongs either to carcinomas (cancers in epithelial cells), sarcomas (cancers from mesodermal cells) or adenocarcinomas (cancer of glandular tissues). Hanahan and Weinberg (2000) defined six hallmarks present in most cancer types: self-sufficiency in growth signals, insensitivity to anti-growth signals, evading apoptosis, limitless replicative potential and sustained angiogenesis (Figure 2). Each hallmark is a (potential) opportunity for new therapeutics to attach (Pecorino, 2008). In the following

chapters the six hallmarks are characterized. Two of them, loss of growth control and of programmed cell death control, were studied in a series of tests with extracts of the traditional healing plants *P. odorata* and *S. spinosa*.

2.2.1 Self sufficiency in growth signals

The hallmarks of growth signal autonomy, as well as evasion of growth inhibitory signals, and unlimited replication, increase cell proliferation (World Cancer Research Fund International, 2007). Unlike normal cells, cancer cells are independent from normal growth factor signalling for their division (Pecorino, 2008). Many cancer cells also produce their own growth signals, thus creating a positive signalling loop. Healthy cell types provide growth factors in a paracrine fashion to stimulate the proliferation of each other, whereas some tumor cells are able to autocrinely produce their own growth factors. Both, dependence from normal growth factors and the triggering of a positive signalling loop lead to unregulated cell growth. Examples for growth factors autocrinely produced by tumor cells are platelet-derived-growth factor (PDGF) and transforming growth factor α (TGF α) in glioblastomas and sarcomas, respectively. Cells gain this growth signal autonomy by alteration of extracellular growth signals, alteration of transcellular transducers of those signals or mutations of intracellular circuits (Hanahan, et al., 2000).

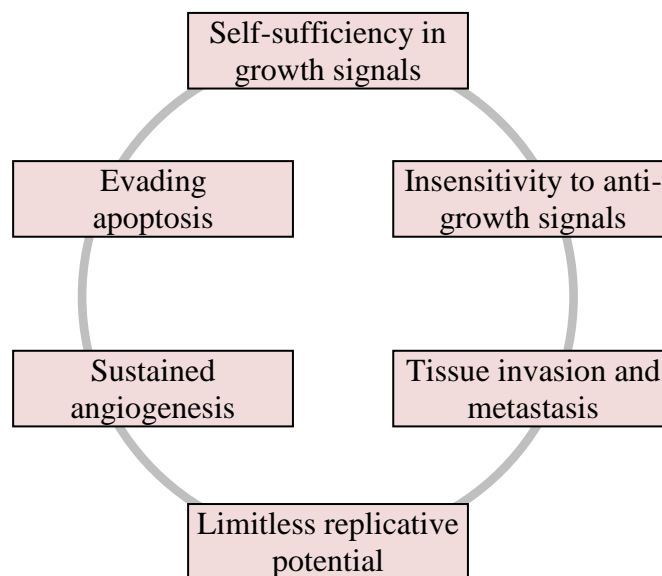


Figure 2 The six hallmarks of cancer (own figure, based on Hanahan, et al., 2000)

2.2.2 Insensitivity to antigrowth signals

Most cells of the body are quiescent and not dividing, because they achieve growth inhibitory signals to maintain homeostasis (Pecorino, 2008). Normal cells for example decrease proliferation as a result of environmental signals like contact with other cells. Anti-growth signals from nearby cells are soluble growth inhibitors or immobilized inhibitors placed in the extracellular matrix. These signals inhibit proliferation in two different ways. First, cells can be transferred into the quiescent stage of the cell cycle, G₀. Second, cells are made to give up their proliferative potential by entering postmitotic stages of the cell cycle (Hanahan, et al., 2000). Probably all anti-proliferative signals are caused by the pRb and its two relatives p107 and p130. In its hypophosphorylated stage, pRb is inactive and blocks the progression from G₁ to S phase by altering the function of E2F transcription factors (Hanahan, et al., 2000). Thus proliferation is inhibited (Figure 3). For G₁ to S phase transition, pRb has to be phosphorylated by Cyclin/Cyclin-dependent kinases (Cdks). The phosphorylation allows E2F to interact with transcription co-activators and to initiate messenger ribonucleic acid (mRNA) synthesis (Weinberg, 1995). In contrast to this acquisition, TGF β inhibits G₁ progression by preventing pRb phosphorylation (Hanahan, et al., 2000). TGF β also suppresses c-Myc which blocks Cyclin-Cdk complexes and therefore no pRb phosphorylation and no proliferation occurs (Datto, et al., 1997).

The insensitivity to antigrowth factors in different types of cancer can depend on the following mechanisms that interrupt the pRb pathway, as well as to a variety of other mechanisms regarding the pRb signalling circuit (Fyran, et al., 1993). For example TGF β responsiveness can be lost through down-regulation of TGF β receptors or the receptors themselves can be mutated (Markowitz, et al., 1995). Also, a loss of pRb function can be generated by a mutation of its gene. pRb is lost in retinoblastomas and altered in 5-10 % of all other cancers (Stewart, et al., 2003). Regarding the c-Myc oncoprotein an overexpression is noticed in many tumors. C-Myc stimulates growth, but during normal development the protein is associated with the Mad-Max complex which finally leads to differentiation-inducing signals (Foley, et al., 1999). An overexpression of c-Myc thus promotes growth and increases differentiation.

Cell cycle and cancer

The cell cycle plays an important role in tumor development and cancer therapy, because cancer is a result of an imbalance between DNA damage, repair and apoptosis. This mismatch leads to uncontrolled cell growth. The cell cycle describes the proliferation process from one cell to two daughter cells. This process is subdivided into four phases: G1, S, G2 and M (Pecorino, 2008) (Figure 3). M (mitosis) phase and S (synthesis) phase are separated by gap phases G1 and G2 (Stewart, et al., 2003).

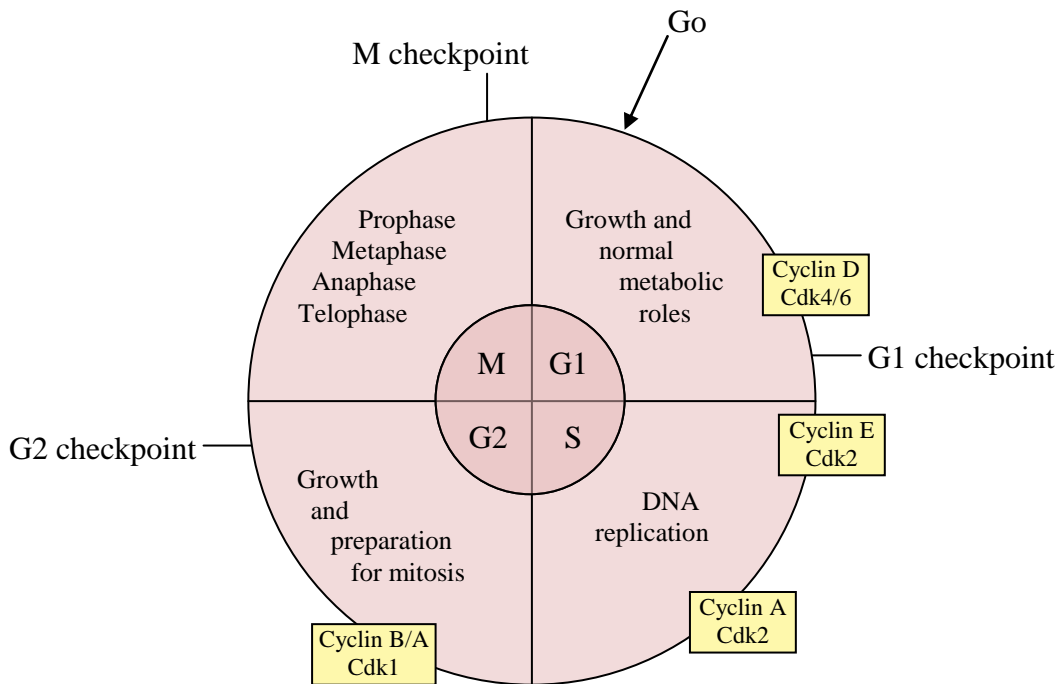


Figure 3 Cell cycle (own figure, based on Pecorino, 2008)
Cyclin-Cdk activity and checkpoints of the cell cycle

Description of the cell cycle

Usually cells are quiescent in a phase outside the cell cycle, called G0 phase. To undergo cell division these cells have to re-enter the cell cycle at G1 after being activated by growth factors or mitogens. After passing the G1 restriction point the cell cycle continues without any need of growth factors or mitogens (Pecorino, 2008). In the G1 phase two copies of every chromosome are existent (Pecorino, 2008) and here the cells grow and synthesise ribonucleic acid (RNA) and proteins to pass the G1 checkpoint. If there is no DNA damage present or DNA damage is not detected, the cell

passes the checkpoint and enters the S phase (World Cancer Research Fund International, 2007). Otherwise, the cell cycle will be arrested to stop replicating the DNA damage (Pecorino, 2008). During the S phase the two copies of every chromosome replicate and become four copies of each. After the synthesis phase, the cells continue with a gap phase (G2), in which the cells grow and synthesise proteins (World Cancer Research Fund International, 2007). After passing checkpoint G2 (ensure no DNA damage or unreplicated DNA is generated), the cells enter the M phase, where they divide in two new cells with two copies of chromosomes each (Pecorino, 2008). The M phase also contains a checkpoint which arrests the cell cycle if the DNA of a daughter cell is damaged (World Cancer Research Fund International, 2007) or in case of misalignment on the mitotic spindle (Pecorino, 2008). Every failure of a checkpoint function results in DNA-mutations which can induce carcinogenesis (Pecorino, 2008).

Because each cell that enters the cell cycle undergoes several serious challenges like completing DNA synthesis, proofreading and correcting synthesized DNA (Stewart, et al., 2003), the cell cycle is controlled by Cyclins and their specific Cdks (Pecorino, 2008). Complexes of Cyclins and Cdks activate transcription factors, which themselves activate Cyclin genes and other genes which products are needed for the next phase of the cell cycle (World Cancer Research Fund International, 2007). The first Cyclin established in the cell cycle is called Cyclin D. Cyclin D and the Cdks 4 and 6 result in passing the cell through G1. Cyclin D is also responsible for the Cyclin E gene expression, whose product is liable for the transition from G1 to S phase, as illustrated in Figure 3. According to this mechanism, Cyclin A and Cdk2 are responsible for passing the S phase and Cyclins A, B and Cdk1 for transition from G2 to M phase, also presented in Figure 3 (Pecorino, 2008).

During lifetime approximately 10^{16} cell divisions proceed. As the DNA is permanently exposed to genotoxic, epigenetic or endogenous substances damaging the DNA, each of these divisions has the chance for failures in the replicated DNA. This may lead to non-functioning genes and further to altered proteins (World Cancer Research Fund International, 2007).

2.2.3 Evading apoptosis

Definition

Apoptosis is defined as the programmed cell death. Unwanted cells are eliminated through apoptosis, a process which can be subdivided in three phases: regulation, effector phase and engulfing (Strasser, et al., 2000). It is a program of steps including disruption of cellular membranes, break down of cytoplasmic and nuclear skeletons, chromosome degradation, nucleus fragmentation and extruded cytosol (Hanahan, et al., 2000). The shrivelled cell corpse is interlocked by nearby cells and disappears (Wyllie, et al., 1980). Apoptosis differs from necrosis morphologically and functionally (Figure 4). In apoptosis only single cells are involved and it does not cause inflammation. Apoptosis is initiated usually when abnormalities like DNA damage, signalling imbalance as a result of oncogene activation, lack of survival factors or presence of hypoxia are registered (Evan, et al., 1998). Therefore apoptosis maintains tissue integrity and protects the cell from cancer (World Cancer Research Fund International, 2007).

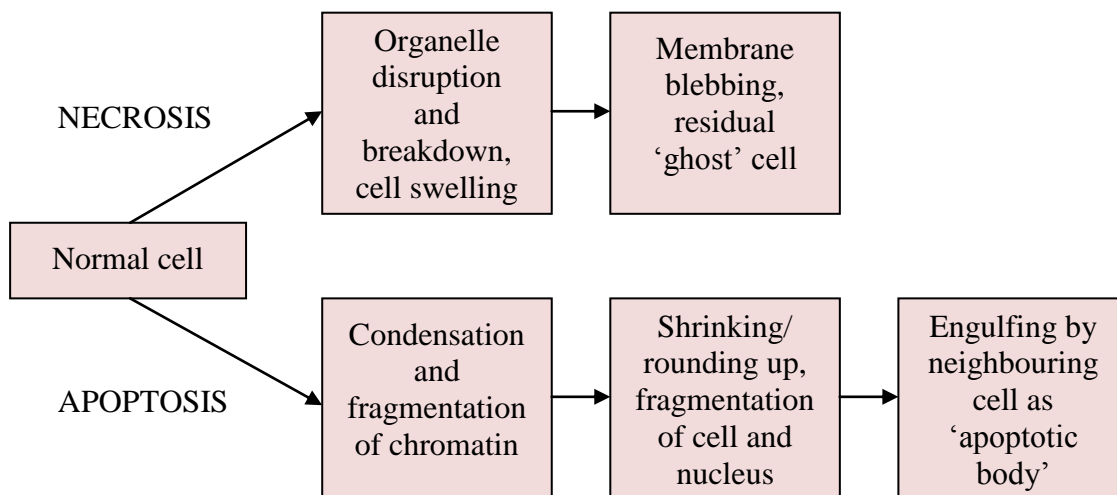


Figure 4 Apoptosis and necrosis characteristic morphological changes (own figure, based on Stewart, et al., 2003)

Mechanisms

Pathways leading to apoptosis are also included in cell proliferation, differentiation, response to stress and homeostasis (Stewart, et al., 2003). Two pathways, an extrinsic and an intrinsic pathway that induce apoptosis, are known (Pecorino, 2008).

The extrinsic pathway leads to apoptosis by activation of cell death receptors, including the activity of sensors. Sensors are described as components which evaluate the extracellular and intracellular environment and if necessary activate regulators and effectors of the apoptosis pathway (Hanahan, et al., 2000). Sentinels of this pathway are survival or death factor binding cell surface receptors. Survival signals are interfered by insulin-like growth factors (IGF-1/IGF-2) through their receptor IGF-1R and by interleukin-3 (IL-3) and the IL-3 receptor (Butt, et al., 1999), whereas death signals can be triggered by the FAS ligand binding FAS receptor or by the tumor necrosis factor α (TNF α) binding TNF-R1 (Ashkenazi, et al., 1999). After ligand binding to the cell surface receptor FAS, also called CD95 receptor, the death domain interacts with the FAS-associated death domain protein (FADD) molecule and afterwards binds procaspase 8. In case of the TNF-receptor, the death domain interacts with the intracellular adaptor protein TRADD (TNF receptor-associated death domain protein). Caspase 8 activates itself by self-cleavage and induces apoptosis by activating caspase 3 through cleaving the procaspase (Pecorino, 2008) (Figure 5). All caspases are effectors of apoptosis (Thornberry, et al., 1998). Caspase 8 and caspase 9 are called “gatekeepers” because they are activated by the death receptor FAS and cytochrome c (Hanahan, et al., 2000).

The intrinsic pathway also leads to the activation of caspase 3 by affecting the mitochondria through stimuli from inside the cell, like DNA damage or oxidative stress (Pecorino, 2008). It responds with the release of cytochrome c, when converged by signals that provoke apoptosis (Green, et al., 1998). These pro-apoptotic signals are often mediated by members of the B-cell lymphoma 2 (Bcl-2) family (Gross, et al., 1999). For example Bax, Bak, Bid and Bim have pro-apoptotic effects, whereas other members of this family have anti-apoptotic effects (Bcl-2, Bcl-XL, Bcl-W). Bcl-2 and Bcl-XL are located in the outer mitochondrial membrane (Stewart, et al., 2003), whereas Bax can be influenced by the tumor suppressor protein p53 which up-regulates the expression of Bax and induces the translocation of Bax from cytosol to the

mitochondria. There, cytochrome c is released as consequence of the translocation (Hanahan, et al., 2000). Caspases, which are playing a very important role in effecting apoptosis (Thornberry, et al., 1998) are activated by assembling a complex of apoptotic protease activating factor-1 (Apaf-1), procaspase 9 and adenosine-5'-triphosphate (ATP). Thus, caspase 9 leads to the activation of caspase 3, which induces apoptosis (Stewart, et al., 2003).

Also there are interactions between the two pathways. Caspase 9 for example is able to activate caspase 8 (Stewart, et al., 2003). Also caspase 8 is able to activate Bid (pro-apoptotic), which can stimulate the intrinsic pathway of apoptosis by activating Bax and Bak resulting in cytochrom c release and finally caspase 9 activation (Pecorino, 2008).

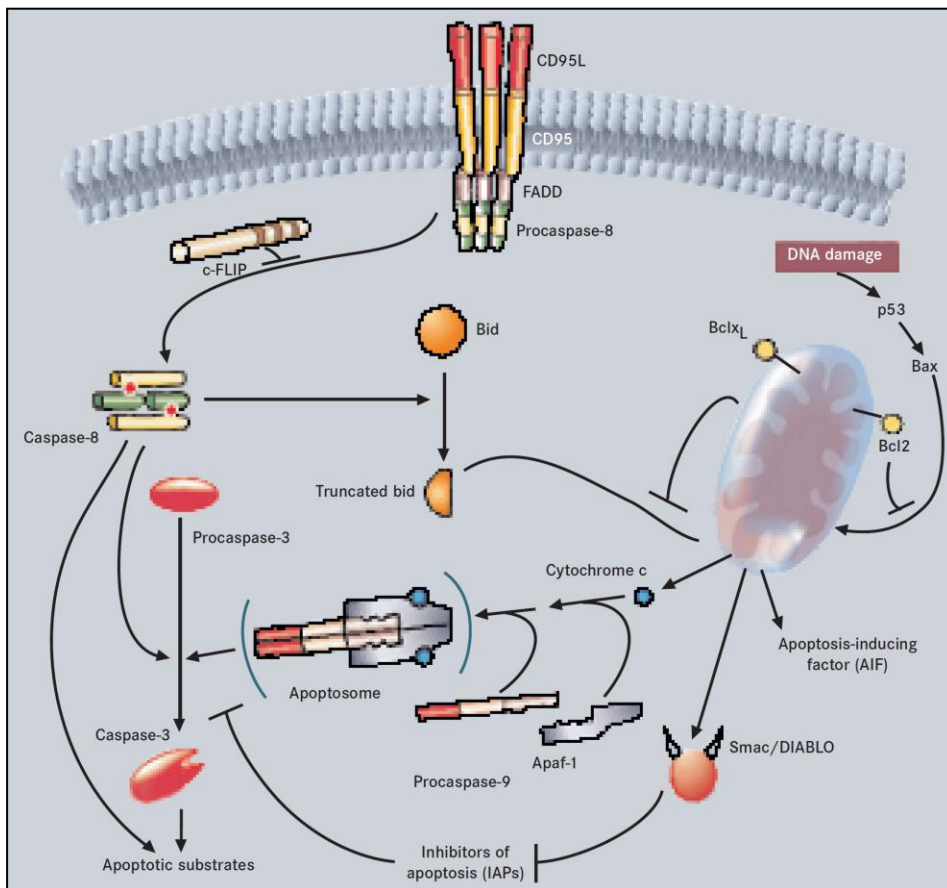


Figure 5 Intrinsic and extrinsic apoptotic pathway (Stewart, et al., 2003)

Apoptosis and tumor development

Hanahan and Weinberg (2000) assume that almost all cancer cells contain alterations to evade apoptosis (Hanahan, et al., 2000). The cell cycle is screened by tumor suppressor proteins and most cells that gain carcinogenic capacities are eliminated by apoptosis. But if tumor suppressor genes acquire mutations, the cells escape from the apoptotic pathways, survive and proliferate. In addition further mutations accumulate (Pecorino, 2008).

P53, a tumor suppressor gene, is mutated in more than 50 % of all cancers. In consequence DNA damage is not detected anymore and the apoptosis effector cascade is not induced (Harris, 1996). Also, the phosphatidylinositol 3-kinase (PI3-kinase)-AKT/protein kinase B (PKB) pathway decreases apoptosis in several human cancers, by transmitting anti-apoptotic survival signals. This pathway can be induced by extracellular factors like IGF-1/2 or IL-3 (Evan, et al., 1998) or intracellular by Ras (Downward, 1998). Also, the loss of the pTEN tumor suppressor, which usually weakens the AKT survival signal, can activate this pathway (Cantley, et al., 1999). Another mechanism in lung and colon carcinoma cell lines leading to inhibition of apoptosis is the up-regulation of a decoy receptor for the FAS ligand, which results in blocking the death-inducing signal from the FAS death receptor (Pitti, et al., 1998). If Bcl-2, a proto-oncogene, is activated and becomes an oncogene, Bcl-2 is over-expressed and thus decreases the apoptotic turnover (Pecorino, 2008). Hence Bcl-2 is connected to carcinogenesis.

2.2.4 Limitless replicative potential

Probably all mammalian cells only have the potential to replicate 60 to 70 times until an autonomous program lead to senescence (permanent growth arrest) and thus protects the cells from unlimited proliferation (Hanahan, et al., 2000). Every time the cell passes the cell cycle, the telomeric DNA diminishes. If telomeres are too small to protect the DNA, the cell undergoes apoptosis (Counter, et al., 1992). However, in cancer cells telomeric maintenance exists (Shay, et al., 1997) which admits unlimited proliferation (Hanahan, et al., 2000).

2.2.5 Sustained angiogenesis

Nutrients and oxygen are required for the proliferation of cells, including tumor cells. Angiogenesis is defined as the growth of new vessels with the objective to provide adequate supply of nutrients and oxygen for cancer cells through capillaries. Thus, angiogenesis is required for an invasive growth of the tumor (Karlson, et al., 2005) and increases the chance of generating metastasis (Fidler, et al., 1994). Therefore, proliferation and migration of endothelial cells, proteolysis of the extracellular matrix and synthesis of new matrix components are needed (Stetler-Stevenson, 1999). In healthy adults angiogenesis is induced as consequence of a pathologic situation like inflammation or hypoxia (Stetler-Stevenson, 1999) and under this condition inducers of angiogenesis and inhibitors are arranged in balance (Hanahan, et al., 2000). However, tumor cells secrete angiogenic growth factors, which block inhibitors of angiogenesis (Folkman, 1995). Signals promoting angiogenesis are the vascular endothelial growth factor (VEGF) and the fibroblast growth factor (FGF 1/2). Both bind to transmembrane tyrosine kinase receptors displayed by endothelial cells (Veikkola, et al., 1999).

2.2.6 Tissue invasion and metastasis

As a consequence of the tumor reaching the membrane encapsulating the organ, serine- and metalloproteases are secreted by cancer cells for further growth of the tumor (MacDougall, et al., 1995). These proteases digest the membrane and allow cancer cells to invade to nearby tissues and to spread all over the body by using the blood and lymphatic system (World Cancer Research Fund International, 2007). Beside proteases classes of proteins are also involved in invasion and metastasis (Hanahan, et al., 2000). Cell-to-cell adhesion molecules (CAM) and integrins, which link cells to the extracellular matrix, are noticed to be altered in metastatic tumors. Another well-documented alteration affects the adhesion molecule E-cadherin. E-cadherin normally results in conveyance of anti-growth (Christofori, et al., 1999), but a mutation of the gene that encodes for E-cadherin is found in a majority of epithelial cancers. Thus, no release of anti-growth signals occurs in these cancers. Once cancer cells escape from the origin organ and intravasated into the blood or lymphatic system, the cells stick to the

endothelial tissue and extravasate from the vessels into the target tissue (Karlson, et al., 2005). Again, angiogenesis is needed for accretion of the metastatic colony (Löffler, et al., 1997).

2.3 Leukaemia

Leukaemia is defined as the neoplastic proliferation of lymphoid or myeloid cells of the haematopoietic system (Freireich, et al., 1991). The incidence is about one to twelve cases in 100,000 people. Interestingly the incidence in industrialized countries is higher than in developing countries (Stewart, et al., 2003). The chance of getting leukaemia is the highest in the first four years of life. People affected with leukaemia have a five year survival rate of approximately 40 % in industrialized countries, whereas in low-income countries the survival rate is about 20 % (Parkin, et al., 2005). Leukaemia is associated with risk factors including tobacco use, infection with human T-cell leukaemia virus, radiation and benzene (IARC International Agency for Research on Cancer, 1987). Subcategories of the generic term leukaemia are: acute lymphoblastic leukaemia (ALL) which especially occurs in children, acute myeloid leukaemia (AML) which is the predominant form of the disease in adults, chronic myelogenous leukaemia (CML) and chronic lymphocytic leukaemia (CLL), which is the usual type of leukaemia in patients over 50 years of age.

HL-60 cells, which are used for analysing the anti-cancer effect of *P. odorata* and *S. spinosa* in the present study, are a subtype of AML.

2.4 Investigated activity of two ethnomedicinal plants from Guatemala

Ethnomedicine is defined as the use of plants as medicine. Fabricant et al. (2001) describes ethnomedicine as “highly diversified approach to drug discovery”. It involves observation, description, and experimental investigation of indigenous drugs for their possible biological or medicinal activity. The plants are selected by their botany, chemistry, biochemistry and/or pharmacology character. The selected plants are often used in traditional medicine for hundreds of years (Fabricant, et al., 2001), which is the reason why no or only little toxic effects in humans are expected. Especially in Africa

and South America traditional medicine is advised by a shaman or herbalist. He often keeps the use of the healing plants as a secret (Rastogi, et al., 1982). Therefore, not much is known about the plants used by humans for thousands of years and thus this is a great potential for drug development. Until now, only 6 % of higher plant species have been screened for their biologic activity (Fabricant, et al., 2001). But with focus on plants used in traditional medicine, the screening can be done more efficiently as it is a very expensive and time consuming work. For example in 1991 in the United States only one out of 10,000 pure compounds reached the U.S Drug Administration. The process costed \$231 million and took ten years (Vagelos, 1991). By now most of the investigated plant species were tested towards their anti-cancer or anti-HIV activity (Fabricant, et al., 2001).

The anti-neoplastic activity of *P. odorata* is described by Gridling et al. (2009) and Bauer et al. (2010). Both describe an impressive effect of the dichloromethane extract in HL-60 and MCF-7 cells. Gridling et al. (2009) first investigated the anti-cancer activity of *P. odorata* and started with the extraction of the plant. The apolar constituents contained in the dichloromethane extract showed anti-proliferative (cell cycle arrest in G2-M phase) and pro-apoptotic (caspase 3 activation) effects in both cell lines. They also led to the inhibition of inflammatory responses and exhibition of the anti-cancer activity (Gridling, et al., 2009). Bauer et al. (2010) further investigated the dichloromethane extract of *P. odorata* by using bioassay-guided fractionation. The three most active fractions of this fractionation process were highly apolar. Here the most significant anti-proliferative activity was observed at a concentration of 3 µg/ml medium after 72 hours of incubation in HL60 cells. A down-regulation of Cyclin D1 and cell division control(Cdc)25A in HL-60 cells was triggered by these apolar fractions, which is described as the mechanism for the anti-proliferative activity measured in proliferation assays, because the two down-regulated oncogenes are known as cell-cycle protagonists (Bauer, et al., 2010).

About the second plant, *S. spinosa*, not much is known yet. Until now only few pharmacological effects of *Smilax sp.* are investigated in clinical trials (Taylor, 2005). *Smilax regelii* for example has an antimicrobial activity against *Shigella dysenteria* (Caceres, et al., 1990) and a *Smilax glabra* extract had a immunomodulatory activity in

rats by decreasing the IL-1-, TNF- and NO-release of macrophages (Jiang, et al., 2003). *Smilax regelii* (syn. Sarsaparilla) is probably the most common genus of *Smilax*. It is mostly applied internally, it is for example known as medicament against arthritis, rheumatism (both causing inflammation), against psoriasis or dermatitis (skin disorders), against impotence or as a blood purifier (Taylor, 2005). An excessive dosage of *Smilax regelii* is said to cause gastrointestinal irritation (Taylor, 2005), but it is also active against snake bites (Alam, et al., 1998).

Smilax sp. (including sarsaparilla) species are especially known as saponin and other plant steroids containing plants. They can be synthesized into human steroids such as estrogen and testosterone. Also the majority of *Smilax regelii*'s activities are reported to be caused by these steroids and saponins (Taylor, 2005). Navarro et al. (2003) investigated the methanol extract of *S. spinosa* for their ability to render DPPH, OH[•] and O²⁻ radicals innocuous and inhibit lipoperoxidation. *S. spinosa* showed a significant activity for all the above listed mechanisms and it was also active against *Salmonella typhi* and *Trypanosoma cruzi*. Therefore the methanol extract has an anti-oxidative and antimicrobial activity (Navarro, et al., 2003).

As *S. spinosa* was not yet investigated towards its anti-neoplastic activity, the present work was conducted to analyse the oncolytic effects on HL-60 cells.

3 Materials and methods

3.1 Plant material

3.1.1 *P. odorata*



Figure 6 *P. odorata* plant and flower (National Park Service, 2010)

Kingdom: Plantae
Division: Magnoliophyta
Class: Magnoliopsida
SuBclassis: Asteridae
Order: Asterales
Family: Asteraceae
Genus: Pluchea cass.
Species: *Pluchea odorata* (L.) cass.

(Natural Resources Conservation Service, 2010)

P. odorata is also called saltmarsh fleabane, sweet-scent or Santa María. The plant is distributed in North and South America in the following countries: USA, Mexico, Belize, Guatemala, Panama, Cayman Islands, Guadeloupe, Jamaica, Puerto Rico, St. Lucia, Venezuela and Ecuador (GRIN Germplasm Resources Information Network, 2004). *P. odorata* grows up to 3 m. Its usual places of location are clearings or edges of the forest. The harsh plant-leaves smell oregano-like (Arvigo, et al., 1994) and flowers

of *P. odorata* look pink. In traditional medicine *P. odorata* is used for therapy of common cold, fever, flu, head colds, headache, hypertension, neuralgia, ophthalmia, palsy, pneumonia and snake bite (Arvigo, et al., 1994). Further the plant is described as being antidote, astringent, diaphoretic, emmenagogue, haemostat and stomachic (Johnson, 1999), as well as traditionally used by mothers after giving birth to decrease the risk for infections and conveyance of tissue recovery and for abatement of arthralgia (Arvigo, et al., 1994). *P. odorata* is also traditionally used by the Mayas to treat swellings, inflammation, and bruises on the skin. The medical solution is prepared by boiling two handfuls of leaves in one gallon of water and then it is frequently applied on the affected area until the inflammation subsides (Balick, et al., 2005).

For this research the aerial parts (leaves, caulis, florescence) of *P. odorata* were collected in Guatemala, Departamento Petén, in the north-western area of Lago Petén Itzá, San José, (16 59'30" N, 89 54'00" W). 6 kg of air dried plant material have been extracted with dichloromethane by Björn Feistel (Finzelberg GmbH & Co.KG, Andernach, Germany), preserved and transported to Vienna, where the investigation of the present work took place. Voucher specimens Nr. 1-2009 08. 04. 2009 were archived at the Museum of Natural History, Vienna, Austria, leg. G. Krupitza & R. O. Frisch.

3.1.2 *S. spinosa*



Figure 7 *S. spinosa* leaf (Paton, et al., 2010) and root (own picture)

Kingdom: Plantae
Division: Magnoliophyta
Class: Liliopsida
Order: Liliales
Family: Smilacaceae
Genus: Smilax
Species: Smilax spinosa

(IABIN Red Interamericana de Información sobre Biodiversidad, 2010)

Until now more than 200 *Smilax* species are identified, which makes the classification of each plant of the *Smilax* genus very difficult. In western literature not much is known about *S. spinosa*, which is the reason for general description of the *Smilax* genus (*Smilax* sp.). *Smilax* sp. is a vine growing in forests and undisturbed areas, reaching up to 6 m. The flowers of *Smilax* sp. are green and small and its fruits are 5-10 mm brown berries. The leaves are lanceolate, 9 cm long by 5 cm wide, and look shiny and smooth with paired tendrils at the axil (Arvigo, et al., 1998). *Smilax* sp. occurs in pantropical to temperate climate (Missouri Botanical Garden, 2010) especially in South America, Jamaica, the Caribbean, Mexico, Honduras, and the West Indies (Taylor, 2005). Many *Smilax* species contain stems covered with prickles. The long and tuberous root is spreading 6-8 feet wide, is odourless and almost tasteless (Taylor, 2005). Traditionally the root is used against fatigue, anaemia, acidity, toxicity, rheumatism and for skin conditions by boiling a small handful of minced root in three cups of water. If cinnamon, milk and nutmeg are added, it is said to have a positive influence on the proliferation of red blood cells. Two other ways of preparing the traditional medicine are described by Arvigo, et al.(1998). One recipe leads to a drinkable mixture by boiling a handful of the root with three cloves of garlic and three hibiscus flowers (unopened) for ten minutes. This mixture is said to stop internal haemorrhaging, which occurs after childbirth or during menstruation. The other recipe, used against male impotency, includes a handful of root and *guinweo* (a local plant) both soaked in rum and applied in shots twice a day (Arvigo, et al., 1998). Already in 1536 a *Smilax* root from Mexico was introduced into European medicine to treat syphilis and rheumatism. This is the time when the long history of the *Smilax* roots for syphilis and other sexually-transmitted diseases started (Taylor, 2005).

For the present work, the rhizome of *S. spinosa* was collected in Playa Diana, San José, Petén, Guatemala (16 59'30" N, 89 54'00" W). The root was dried and brought to Vienna, Austria. Voucher specimens Nr. 4-2009 19. 04. 2009 were archived at the Museum of Natural History, Vienna, Austria, leg. G. Krupitza & R. O. Frisch, det. B. Wallnöfer (W), 26. 01. 2010. The plant was ground before the extraction and analyses of the anti-neoplastic activity were performed.

3.2 General methods

3.2.1 Thin layer chromatography (TLC)

Thin layer chromatography (TLC) was used for detecting the best solvent combination for vacuum liquid chromatography (VLC) or column chromatography (CC), or as a finger print of new fractions. Stationary phase and mobile phases are described in Table 1. The mobile phase varied between six solvent systems. Plates were detected under UV₂₅₄, UV₃₆₆ and visible light, before and after spraying with anisaldehyd sulphuric acid reagent (ASR). ASR consisted of 0.5 ml anisaldehyd, 10 ml glacial acetic acid, 85 ml methanol and 5 ml H₂SO₄ (sulfuric acid). The sprayed plate was heated at 100 °C for five minutes and then compounds were detected at UV and visible light. Unless otherwise stated 8 µl extract or fraction were applied to the plate.

Table 1 Stationary phase, mobile phases and detection methods used for TLC

Stationary phase	silica gel plates 60 F254 (Merck, Darmstadt, Germany)	
Mobile phase	TLC system 1: chloroform: methanol: water	90:22:3.5
	TLC system 2: chloroform: methanol: water	90:3.5:0.2
	TLC system 3: chloroform: methanol: water	70:30:10
	TLC system 4: dichloromethane: ethyl acetate	80:20
	TLC system 5: dichloromethane: ethyl acetate	85:15
	TLC system 6: chloroform: methanol: water	70:22:3.5
Detection	UV ₂₅₄ , UV ₃₆₆ , visible light Anisaldehyd sulphuric acid reagent (ASR)	

3.2.2 Cell culture

HL-60 (human promyelocytic leukaemia cell) cells were purchased from American Type Culture Collection (ATCC). The cells were grown in RPMI 1640 medium which was supplemented with 10 % heat-inactivated fetal calf serum (FCS), 1 % Glutamax and 1 % Penicillin-Streptomycin. Both medium and supplements were obtained from Life Technologies. The cells were kept in humidified atmosphere at 37 °C containing 5 % CO₂.

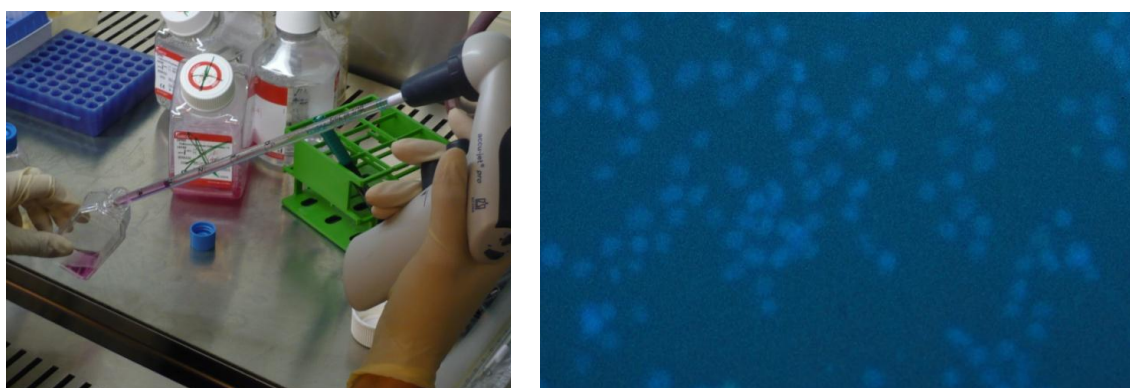


Figure 8 Cell culture work (left), HL-60 cells (right) (own pictures)

3.2.3 Proliferation assay

Proliferation assays were performed to analyse the inhibition of proliferation of HL-60 cells treated with an extract or fraction of *P. odorata* or *S. spinosa*. Extracts and fractions were either dissolved in preferably small amounts of 96 % ethanol in the case of *P. odorata* or dimethyl sulfoxide (DMSO) in the case of *S. spinosa*. HL-60 cells were seeded in 24-well plates at a concentration of 1×10^5 cells per ml RPMI medium, allowing logarithmic growth within 72 hours. Afterwards the cells were treated with at least one concentration of a plant extract or fraction. Each experiment was carried out in triplicate. The control was only treated with 96 % ethanol (in *P. odorata* experiments) or DMSO (in *S. spinosa* experiments) in the concentration of the highest extract or fraction concentration. After 24, 48 and 72 hours the number of cells was determined using the Sysmex Cell Counter (Sysmex Corp., Japan). Percentage of cell division progression compared to the untreated control was calculated by applying the following formula:

$$\frac{C_{48 \text{ or } 72 \text{ h} + \text{drug}} - C_{24 \text{ h} + \text{drug}}}{C_{48 \text{ or } 72 \text{ h} - \text{drug}} - C_{24 \text{ h} + \text{drug}}} \times 100 = \% \text{ cell division}$$

Table 2 Explanation of the formula used for calculation of proliferation assay data

Calculation		Description
$C_{48 \text{ or } 72 \text{ h}}$	+ drug	Cell number after 48 or 72 h of drug treatment
$C_{24 \text{ h}}$	+ drug	Cell number after 24 h of drug treatment
$C_{48 \text{ or } 72 \text{ h}}$	- drug	Cell number after 48 or 72 h without drug treatment
$C_{24 \text{ h}}$	- drug	Cell number after 24 h without drug treatment

3.2.4 Apoptosis assay

Determination of cell death by Hoechst 33258 (HO) and propidium iodide (PI) double staining (both Sigma, St. Louis, MO) allows identifying the amount and the type of cell death (early or late apoptosis or necrosis). Therefore HL-60 cells were seeded in a 24-well plate at a concentration of 1×10^5 cells per ml RPMI medium. Cells were treated with at least one concentration of a fraction or extract of *P. odorata* or *S. spinosa*,

whereas the control was only treated with 96 % ethanol in *P. odorata* experiments or DMSO in *S. spinosa* experiments in the concentration of the highest extract or fraction concentration. The cells were incubated for 8, 24, 48 and/or 72 hours, depending on the experiment. At each time point 100 µl cell suspension of each well were transferred into separate wells of a 96-well plate and Hoechst 33285 and propidium iodide were added at final concentrations of 5 µg/ml and 2 µg/ml, respectively. After one hour of incubation at 37 °C, stained cells were examined and photographed on a fluorescence microscope (Axiovert, Zeiss) equipped with a DAPI filter. Type and number of cell deaths were evaluated by visual examination of the photographs according to the morphological characteristics revealed by HOPI staining. Experiments were done in triplicate.



Figure 9 Fluorescence microscope (Axiovert, Zeiss) (own picture)

3.2.5 Western Blotting

3.2.5.1 Preparation of lysates

HL-60 cells were seeded in a tissue culture flask at a concentration of 1×10^6 cells per ml RPMI medium. *P. odorata* fractions F1, F4.6.3 and F5.3.6.7 and the water-methanol fraction (achieved from the detannification process) of *S. spinosa* were analysed by western blots. HL-60 cells were either incubated with 40 µg/ml F1 or with 10 µg/ml of one of the other two *P. odorata* fractions or with 120 µg/ml of the *S. spinosa* extract for

0.5, 2, 4, 8 and 24 hours. At each time point, 4×10^6 cells were harvested, placed on ice and centrifuged (1000 rpm, 4 °C, 4 min). Then, the supernatant (medium) was discarded and the pellet was washed twice with cold phosphate buffered saline (PBS, pH 7.2), and centrifuged (1000 rpm, 4 °C, 4 min). The cell pellet was lysed in a buffer containing 150 mM NaCl, 50 mM Tris (pH 8.0), 1 % Triton-X-100, 1 mM phenylmethylsulfonyl fluoride (PMSF) and 1 mM protease inhibitor cocktail (PIC) (Sigma, Schnellendorf, Germany). Afterwards the lysate was centrifuged at 12000 rpm for 20 min at 4 °C. Supernatant was transferred into a 1.5 ml tube and stored at -20 °C for further analyses.

3.2.5.2 Gel electrophoresis (SDS-PAGE) and blotting

Equal amounts of protein samples (lysate) were mixed with sodium dodecyl sulfate (SDS) sample buffer (1:1) and loaded onto a 10 % polyacrylamide gel. Proteins were separated by polyacrylamide gel electrophoresis (PAGE) at 120 Volt for approximately one hour. To make proteins accessible to antibody detection, they were electrotransferred from the gel onto a polyvinylidene difluoride (PVDF) Hybond membrane (Amersham, Buckinghamshire, UK) at 95 Volt for 80 minutes. Membranes were allowed to dry for 30 minutes to provide fixing of the proteins on the membrane. Methanol was used to remoist the membranes. Equal sample loading was checked by staining the membrane with Ponceau S (Sigma).

3.2.5.3 Protein detection

After washing with PBS or TBS (tris buffered saline, pH 7.6), membranes were blocked in PBS- or TBS-milk (5 % non-fat dry milk in PBS containing 0.5 % Tween 20 or TBS containing 0.1 % Tween 20) for one hour at room temperature. Then membranes were washed with PBS/T (PBS containing 0.5 % Tween 20) or TBS/T (TBS containing 0.1 % Tween 20), changing the washing solution four to five times every five minutes. Then every membrane was incubated with a primary antibody (1:500) in blocking solution (according to the data sheet TBS-, PBS- milk or TBS-, PBS- BSA), at 4 °C over night gently shaking. Subsequently the membrane was again washed with PBS/T or TBS/T, and incubated with the second antibody (peroxidase-conjugated goat anti-

rabbit IgG or anti-mouse IgG) diluted 1:2000 for one hour at room temperature. After washing the membranes chemiluminescence was developed with enhanced chemiluminescence (ECL) plus detection kit (Amersham, UK) (two seconds to ten minutes) and membranes were exposed to the Lumi-Imager TM F1 (Roche) for increasing times.

3.2.5.4 Antibodies

Table 3 Antibodies used for western blots *P. odorata* fractions and *S. spinosa* extracts

Antibody	Description	<i>Pluchea Smilax odorata spinosa</i>	
		P	S
Anti-acetylated tubulin clone6-11B-1	Monoclonal mouse ascites fluid, product no. T6793 (Sigma)	P	S
α tubulin (DM1A)	Sc-32293, monoclonal mouse (Santa Cruz Biotechnology, Inc.)	P	S
β tubulin (H-235)	Sc-9104, polyclonal rabbit (Santa Cruz Biotechnology, Inc.)	P	S
Anti-H2AX (pSer139)	Mouse, DR 1017 (EMD Chemicals)	P	S
Cleaved caspase 3 (Asp175)	Polyclonal rabbit, #9661 (Cell Signaling)	P	S
Cleaved caspase 8 (Asp391)	18C8 Rabbit mAb, monoclonal rabbit, #9496 (Cell Signaling)	P	S
Cleaved caspase 9 (Asp330)	Human Specific, polyclonal rabbit, #9501 (Cell Signaling)	P	S
PARP-1 (F-2)	Sc-8007, monoclonal mouse (Santa Cruz Biotechnology, Inc.)		S
Phospho-Stat3 (Tyr705)(D3A7)	Monoclonal rabbit, #9145 (Cell Signaling)	P	S
Stat3	Polyclonal Rabbit, #9132 (Cell Signaling)	P	S
Phospho-Stat5 (Tyr694)(C11C5)	Monoclonal rabbit, #9359 (Cell Signaling)		S
Stat5 (C-17)	Sc-835, polyclonal rabbit (Santa Cruz Biotechnology, Inc.)		S
c-Jun (H-79)	Sc-1694, polyclonal rabbit (Santa Cruz Biotechnology, Inc.)	P	S
Jun b (210)	Sc-73, polyclonal rabbit (Santa Cruz Biotechnology, Inc.)	P	S

c-Myc Ab-2 (9E10.3)	#MS-139-P1, monoclonal mouse (Thermo Fisher Scientific, Inc.)	P	S
p21 (C-19)	sc-397, polyclonal rabbit (Santa Cruz Biotechnology, Inc.)		S
pChk2 (Thr68)	Polyclonal rabbit, #2661 (Cell Signaling)	P	
Chk2	Polyclonal rabbit, #2662 (Cell Signaling)	P	
pCdc25A-S177	Antibody, polyclonal rabbit, Cat. #AP3046a (Abgent)	P	S
Cdc25A (F-6)	sc-7389, monoclonal mouse (Santa Cruz Biotechnology, Inc.)	P	S
Cyclin D1 (M-20)	Sc-718, polyclonal rabbit, (Santa Cruz Biotechnology, Inc.)		S
Paxillin (H-114)	Sc-5574, polyclonal rabbit, (Santa Cruz Biotechnology, Inc.)	P	
ROCK-1 (C8F7)	Monoclonal rabbit, #4035 (Santa Cruz Biotechnology, Inc.)	P	
Phospho-Myosin Light Chain 2 (Ser19)	Polyclonal rabbit, #3671 (Cell Signaling)	P	
Myosin Light Chain 2	Polyclonal rabbit, #3672 (Cell Signaling)	P	
Phospho-MYPT1 (Thr696)	Rabbit polyclonal IgG, Cat. # 07-251 (upstate cell signalling solutions)	P	
MYPT1	Polyclonal rabbit, #2634 (Cell Signaling)	P	
β actin (AC-15)	monoclonal mouse ascites fluid, Cat. No. A5441 (Sigma)	P	S

3.2.6 Statistical Analysis

For statistical analyses Excel 2003 software and Prism 5 software package (GraphPad, CA, USA) were used. The values were expressed as mean \pm standard deviation and the Student's T-test was applied to compare differences between control samples and treatment groups. Statistical significance level was set to $p < 0.05$.

3.3 Methods used for *P. odorata*

In the following chapters the methods which were only used for analysing *P. odorata* are described.

3.3.1 Chlorophyll Separation

113.66 g of the dichloromethane extract (Björn Feistel, Finzelberg GmbH & Co.KG, Andernach, Germany) were divided into four parts. Every part was dissolved in 100 ml dichloromethane and mixed with 200 ml of a water-methanol mixture (1:1). After evaporation of dichloromethane at 40 °C and 600-800 mbar (Heidolph WB 2001) the remaining solution was filtered (Schleicher & Schuell, Microscience, 595, Ref Nr 10311612 – diameter 150 nm). Collected insoluble chlorophyll of the four parts was combined and dissolved in 760 ml dichloromethane. Again the dichloromethane was evaporated like described above, as well as the water-methanol mixture at 40 °C and 100-300 mbar. The chlorophyll part and the rest of the fraction were checked by TLC.

3.3.2 Vacuum Liquid Chromatography (VLC)

Vacuum liquid chromatography was used for separating large amounts of extracts or fractions (> 5 g) of *P. odorata*.

3.3.2.1 VLC - fractionation of the chlorophyll-rich dichloromethane extract

For better separation only one third of the dichloromethane extract with chlorophyll (most active substances were still contained in the chlorophyll part) was applied to the VLC column. The extract (36 g) was dissolved in dichloromethane, mixed with 70 g silica gel and evaporated (Heidolph WB 2001) to dryness. To obtain a homogenous powder it was refined in a mortar. The 12 x 40 cm column was packed with 900 g silica gel, the silica gel containing extract, and to ballast the powdered sample it was covered with sea sand. By applying vacuum the mobile phase was passed through the column. After checking the collected fractions by TLC, those with similar bands were reunited. Table 4 shows the mobile phases used.

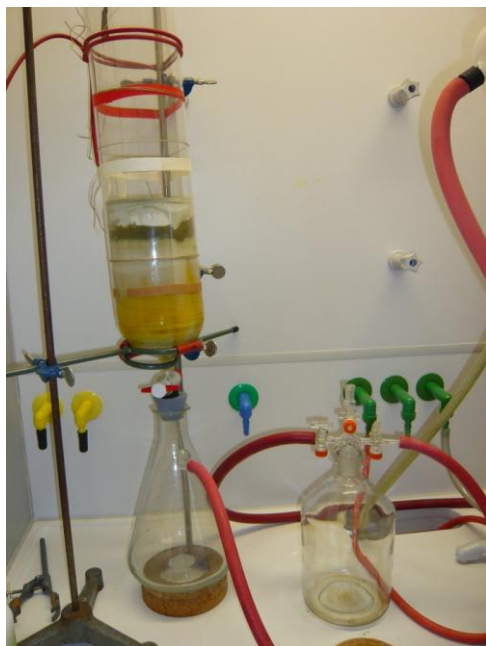


Figure 10 VLC of the chlorophyll-rich dichloromethane extract (own picture)

Table 4 Mobile phases used for VLC of the chlorophyll-rich dichloromethane extract

Mobile phase	Relation	Volume (l)
Petroleum ether		4
Petroleum ether: chloroform	9 : 1	5
Chloroform		12
Chloroform: methanol	9 : 1	9
Chloroform: methanol	7 : 3	9
Chloroform: methanol	5 : 5	9
Chloroform: methanol	3 : 7	9
Chloroform: methanol	1 : 9	9
Methanol		9

3.3.2.2 VLC – fractionation of F1

Approximately 10 g of F1 were dissolved in dichloromethane and applied to a 5 x 60 cm column to achieve a better separation compared to a column with a larger diameter and larger amount so substance. The established solution was mixed with silica gel and evaporated (Heidolph WB 2001) to dryness. After refining in a mortar it was placed on

top of the column and covered with silica gel. For elution of compounds the following mobile phases were used by applying vacuum (Table 5). Collected fractions were checked by TLC and similar fractions were reunited.

Table 5 Mobile phases used for VLC of F1

Mobile phase	Relation	Volume (l)
Dichloromethane: hexan	8 : 2	2
Dichloromethane		2
Dichloromethane: ethyl acetate	8 : 2	1
Dichloromethane: ethyl acetate	6 : 4	1
Dichloromethane: ethyl acetate	4 : 6	1
Dichloromethane: ethyl acetate	2 : 8	1
Ethyl acetate		1
Ethyl acetate: methanol	8 : 2	1
Ethyl acetate: methanol	6 : 4	1

3.3.3 Column chromatography (CC) and Thin Layer Chromatography (TLC)

For fractions with less than 2 g CC without applying vacuum and once scraping the fraction off a TLC plate were conducted.

3.3.3.1 CC – fractionation of F2.6

For fractionation of F2.6 a column a 5 x 50 cm column was used. It was filled up with silica gel mixed with dichloromethane. On top of the silica gel the whole fraction, also dissolved in dichloromethane, was added slowly and afterwards covered with silica gel. Mobile phases used are shown in Table 6. 100 ml fractions were collected, checked by TLC and those with similar band patterns were reunited.

Table 6 Mobile phases used for CC of F2.6

Mobile phase	Relation	Volume (l)
Dichloromethane	100 %	1
Dichloromethane: ethyl acetate	80 : 20	2
Dichloromethane: ethyl acetate	60 : 40	1
Dichloromethane: ethyl acetate	40 : 60	1
Dichloromethane: ethyl acetate	20 : 80	1
Ethyl acetate	100 %	1

3.3.3.2 CC – fractionation of F3.2

42.54 mg of F3.2 were separated by a 1 x 17 cm silica gel column. The column was packed with silica gel mixed with dichloromethane. Mobile phases were used as described in Table 7. Fractions were collected by hand, a few drops in each tube, depending on the solvent colour. Approximately ten drops per minute were collected. Again the new fractions were checked by TLC.

Table 7 Mobile phases used for CC of F3.2

Mobile phase	Relation	Volume (ml)
Dichloromethane	100 %	60
Dichloromethane: ethyl acetate	90 : 10	100
Dichloromethane: ethyl acetate	80 : 20	100
Dichloromethane: ethyl acetate	60 : 40	100

3.3.3.3 CC – fractionation of F4.2.2

12.15 mg of F4.2.2 were applied to a 1 x 12 cm column (trying to achieve a pure substance). Silica gel conditioned with dichloromethane was applied on top of the column. Fractions were collected by hand, a few drops in each tube, approximately ten drops per minute.

Table 8 Mobile phases used for CC of F4.2.2

Mobile phase	Relation	Volume (ml)
Dichloromethane	100 %	125
Dichloromethane: ethyl acetate	90:10	100

3.3.3.4 Scraped TLC of F5.2.2.1

This method was conducted, because only a very small amount (6.9 mg) of F 5.2.2.1 was left after column chromatography. Scraping the new fractions off the TLC plate was attempted to purify the main compounds of F5.2.2.1. For this method a silica gel TLC plate on a glass panel, measuring 20 x 20 cm, was utilized. F5.2.2.1 was dissolved in dichloromethane and applied to the centre of the plate, broadly based. As solvent TLC system 4 (dichloromethane: ethyl acetate, 80:20) was used. TLC was stopped after running three quarter over the plate. Under UV₂₅₄ and UV₃₆₆ four substances were detected, marked and scraped off with an applicator afterwards. The thus received compounds containing silica were resuspended in dichloromethane and centrifuged for ten minutes at 3000 rpm. The supernatant (dichloromethane and substance) was saved, whereas the pellet was again resuspended, centrifuged and again the supernatant was pooled. Dichloromethane was evaporated at 850 mbar and 40 °C (Heidolph WB 2001). The obtained substances were weighted.

3.3.3.5 CC – fractionation of F3.3

1.14 g of F3.3 were fractionated by a 3.5 x 40 cm column. Sephadex was used as stationary phase to eliminate the chlorophyll, because sephadex separates the compounds by molecular weight. The column was packed with sephadex mixed with methanol. On top of this the fraction dissolved in dichloromethane and methanol was applied slowly. To cover the dissolved fraction, some more sephadex was placed on top. Methanol was used as mobile phase. Fractions were collected in tubes, up to 15 ml in each tube, depending on the colour of the fractions. New fractions were checked by TLC and those with similar band patterns were reunited.

3.3.3.6 CC – fractionation of F4.3.1

Since the previous column failed to separate F3.3, all fractions from column 3.3 were reunited again (F4.3.1) and applied to a 2 x 30 cm silica gel column. F4.3.1 was dissolved in dichloromethane, placed on top of the column and covered with silica gel. Mobile phases were used as illustrated in Table 9. New fractions were checked by TLC and those with similar band patterns were reunited.

Table 9 Mobile phases used for CC of F4.3.1

Mobile phase	Relation	Volume (ml)
Dichloromethane	100 %	500
Dichloromethane: ethyl acetate	90 : 10	500
Dichloromethane: ethyl acetate	80 : 20	500
Dichloromethane: ethyl acetate	60 : 40	500
Dichloromethane: ethyl acetate	40 : 60	500
Dichloromethane: ethyl acetate	20 : 80	500
Ethyl acetate	100 %	500

3.3.3.7 CC – fractionation of F5.3.6.7

145.64 mg of F5.3.6.7 were fractionated by a 80 x 1.5 cm column. Dichloromethane was used to dissolve the F5.3.6.7 and silica gel was also conditioned with dichloromethane. After applying the fraction on top of the silica gel, the fraction was again covered with silica gel. As mobile phase one litre solvent (chloroform: methanol: water, 95:1.5:0.1) was used, until no substances were eluted anymore. Afterwards the column was washed with 300 ml methanol. Fractions were collected in tubes, ten drops per minute, and every 30 minutes the tubes were changed. New fractions were checked by TLC and those with similar band patterns were reunited.

3.3.3.8 CC – fractionation of F3.6

0.32 g of F3.6 were fractionated by a 2.5 x 40 cm column as described in chapter 3.3.3.5 (CC – fractionation of F3.3.).

3.3.3.9 CC – fractionation of F4.6.3

F4.6.3 (very oily) was further fractionated, as it contained the highest anti-proliferative and pro-apoptotic activity. The 2.5 x 15 cm column was packed with silica gel conditioned with dichloromethane. The fraction on top was also dissolved in dichloromethane. First hexan was used as mobile phase to remove the oil. Since this was not successful, a solution of dichloromethane and hexan (70:30) was applied. Further solvent systems applied are shown in Table 10. The first four systems did not elute any substances, but the last solvent system was successful. New fractions were collected by a fraction collector, collecting ten drops per minute and changing the tube every 30 minutes. New fractions were checked by TLC and those with similar band patterns were reunited.

Table 10 Mobile phases used for CC of F4.6.3

Mobile phase	Relation	Volume (ml)
Dichloromethane: hexan	70 : 30	300
Dichloromethane	100 %	125
Dichloromethane: ethyl acetate	80 : 20	300
Dichloromethane: ethyl acetate	50 : 50	700

3.4 Methods used for *S. spinosa*

3.4.1 Extraction

The root of *S. spinosa* was air dried and then milled (Moulinette ‘S’, Moulinex). Afterwards the obtained powder was extracted. 20.1 g milled root were mixed with 200 ml (1:10) of solvent (see Table 11) and treated in an ultra sonic bath for ten minutes

to break the cell walls. Then the mixture was placed on a reflux-water bath at the temperature of the boiling point of the solvent plus 10 °C (Table 11). After one hour in the water bath the solvent was filtered through a round filter (Schleicher & Schuell, Microscience, 595, Ref Nr 10311612 – diameter 150 nm). The retained plant material (residue) was dried on a sheet of paper over night, before reuse for the next extraction. The liquid phase (solvent), which contained the dissolved material, was evaporated by a rotavapor (Heidolph WB 2001) and a water bath at 40 °C to complete dryness.

Table 11 Solvents used for extraction of *S. spinosa*

Solvent	Water Bath	Rotavapor (mbar)
Petroleum ether	55 °C	570
Dichloromethane	40 °C	850
Ethyl acetate	92 °C	260
Methanol	84 °C	300
Water	100°C	70

3.4.2 Detannification of the methanol extract

As the methanol extract was the most promising extract of *S. spinosa*, separation of the tannins was conducted to make sure that the performed bio-assays were not biased by tannins contained in the extract. For the removal of tannins the methanol extract of *S. spinosa* (4.13 g) was dissolved in 60 ml of a water-methanol mixture (9:1). After triple solvent extraction with 60 ml petroleum ether for the withdrawal of chlorophyll, waxes and fats, the methanol fraction was diluted with 60 ml of water. Subsequently this aqueous solution was extracted three times with 120 ml chloroform. For isolation of the detannified extract, the collected chloroform layer was washed three times with 360 ml sodium chloride solution (1 %). After drying with sodium sulphate, the solution was filtered (Schleicher & Schuell, Microscience, 595, Ref Nr 10311612 – diameter 150 nm) and afterwards the chloroform was evaporated at 470 mbar (Heidolph WB 2001).

4 Results

The results of the experiments performed with *P. odorata* and *S. spinosa* extracts and fractions are described separately in the following chapters.

4.1 *P. odorata*

This chapter describes the fractionation process of *P. odorata* from the dichloromethane extract to the most active fractions and further to the divided activities in the daughter fractions. In the following scheme an overview of these results is illustrated. Obtained fractions were investigated towards their anti-carcinogenic potential in HL-60 cells. Bioassay (proliferation and apoptosis assay)-guided fractionation was performed to identify the most promising fractions. Finally the effects of the two most active fractions were subsequently studied in more detail by western blot analysis.

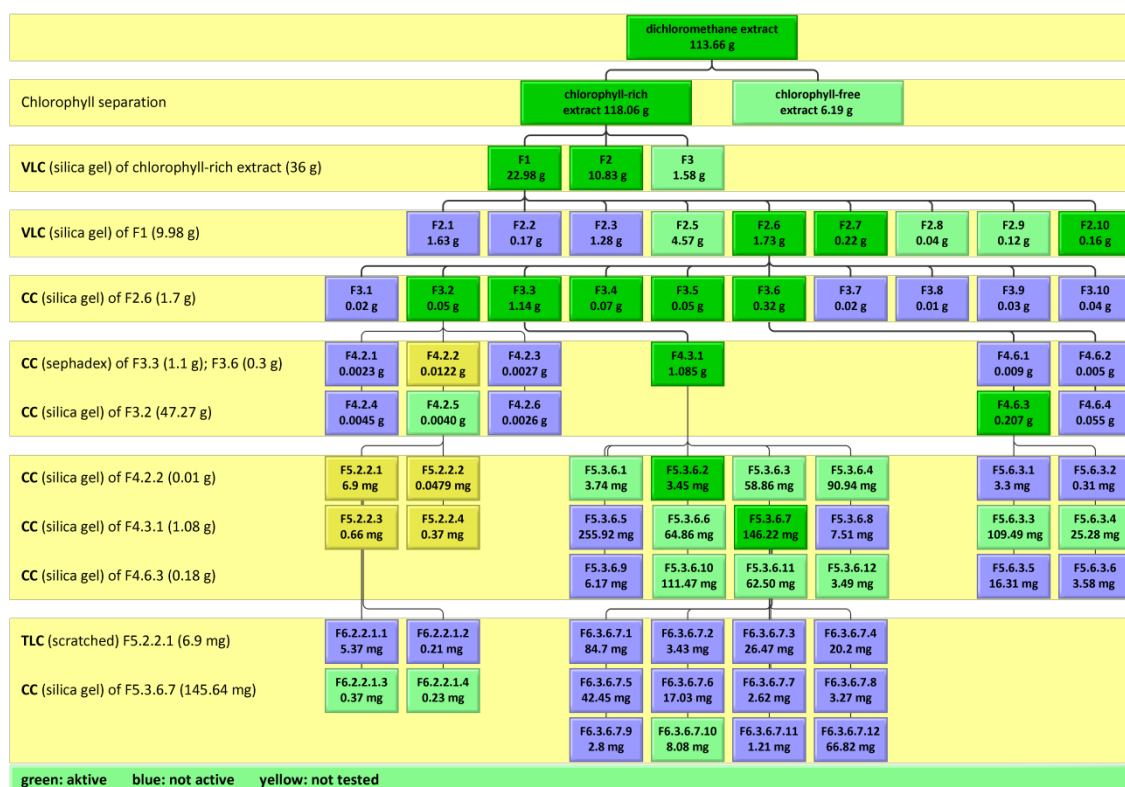


Figure 11 Fractionation overview of *P. odorata*

4.1.1 Comparison of the 2005 and 2009 dichloromethane extract

The activity of the dichloromethane extract from 2009 (extracted by Björn Feistel, Finzelberg GmbH & Co. KG, Andernach, Germany) was tested in comparison to the dichloromethane extract from 2005 (extracted by Sabine Bauer) to ascertain that the new extract is as effective as the old one. In both cases HL-60 cells were treated with 5 µg/ml, 10 µg/ml and 40 µg/ml for 24 and 72 hours and counted afterwards to measure the anti-proliferative activity as described in chapter 3.2.3. In Figure 12 the dichloromethane extract from 2009 reveals a nuance higher activity than the 2005 collected extract (yet not significant). Therefore the new dichloromethane extract was appropriate for subsequent fractionation.

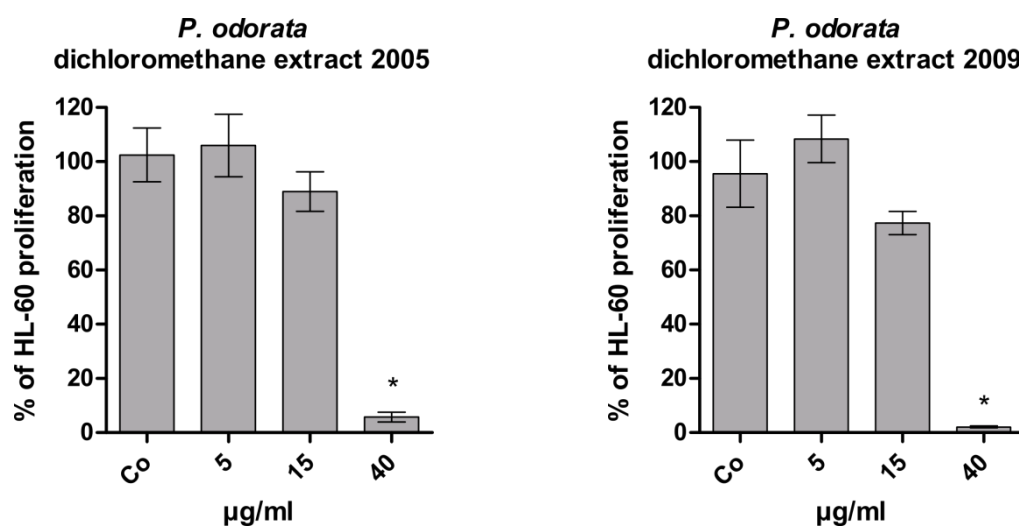


Figure 12 Anti-proliferative effect of dichloromethane extract from 2005 and of the one from 2009 HL-60 cells were seeded into 24-well plate (1×10^5 cells/ml), incubated with 5, 15 and 40 µg/ml of each extract for 72 hours. Cells were counted after 24, 48 and 72 hours of treatment. The percentage of proliferation between 24 and 72 hours was determined in comparison to control. Experiments were performed in triplicate. Asterisks indicate significance compared to untreated control ($p < 0.05$) and error bars indicate \pm SD

4.1.2 Separation of chlorophyll

Separation of chlorophyll was conducted to achieve a more concentrated extract with higher activity for further fractionation. The process of separation was performed as described in chapter 3.3.1. TLC system 3 (chloroform: methanol: water, 70:30:10) was used for TLC analysis, applying four times 5 μ l of each extract (with chlorophyll and without chlorophyll). As illustrated in Figure 13, a yet undefined amount of active compounds was still contained in the chlorophyll extract and therefore the separation of chlorophyll was not successful.



Figure 13 TLC of chlorophyll-rich (a) and chlorophyll-free dichloromethane extract (b)
Mobile phase: TLC system 3
Detection: visible light with ASR

a b

The proliferation assay performed with HL-60 cells shows that the chlorophyll-rich extract was more active than the chlorophyll-free extract. The 18-folds higher concentration of extract without chlorophyll was tested, because the amount of extract without chlorophyll was 18-folds less than the amount of extract with chlorophyll. That way both extracts were comparable. The results of the proliferation assay are presented in Figure 14 and show a proliferation rate of 80 % in HL-60 cells treated with chlorophyll-free extract in contrast to proliferation arrest in these cells treated with chlorophyll-rich extract.

P. odorata

Chlorophyll-free dichloromethane extract (CF)
Chlorophyll-rich dichloromethane extract (CR)

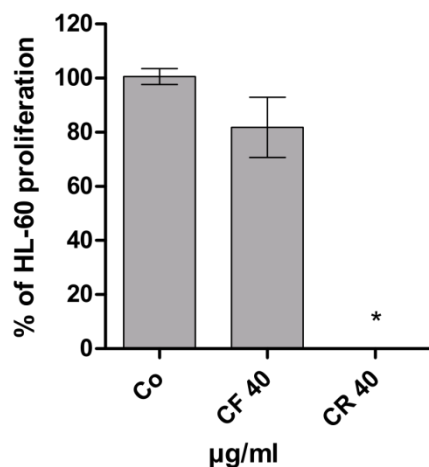


Figure 14 Anti-proliferative effect of chlorophyll-free and chlorophyll rich dichloromethane extract of *P. odorata* HL-60 cells were seeded into 24-well plate (1×10^5 cells/ml), incubated with 40 µg/ml of chlorophyll-free and chlorophyll-rich dichloromethane extract for 72 hours, respectively. Cells were counted after 24, 48 and 72 hours of treatment. The percentage of proliferation between 24 and 72 hours was determined in comparison to control. Experiments were performed in triplicate. Asterisks indicate significance compared to untreated control ($p < 0.05$) and error bars indicate \pm SD

4.1.3 Vacuum Liquid Chromatography (VLC)

In the following two chapters results of VLC of *P. odorata* are described.

4.1.3.1 VLC of the chlorophyll-rich dichloromethane extract – F1-F3

The VLC-conditions were determined empirically to achieve an optimal separation of fractions with different polarities. VLC was conducted as described in chapter 3.3.2.1. To evaluate the quality of the VLC fractionation, a TLC with TLC system 3 (chloroform: methanol: water, 70:30:10), detected under visible light, UV₂₅₄ and UV₃₆₆ was performed (Figure 15).

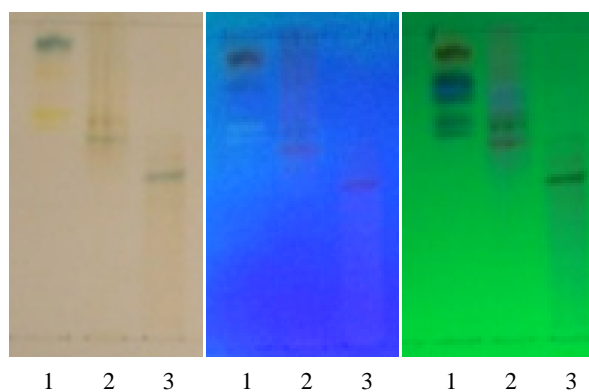


Figure 15 TLC of F1-F3
 Mobile phase: TLC system 3
 Detection: visible light with ASR (left),
 UV₂₅₄ (middle), UV₃₆₆ (right)

Results

For analytical reasons TLC system 5 (dichloromethane: ethyl acetate, 85:15) was used to achieve an improved separation with this solvent system. Three bands were visible under UV₂₅₄ and after spraying with ASR, approximately ten bands become visible in the white light.

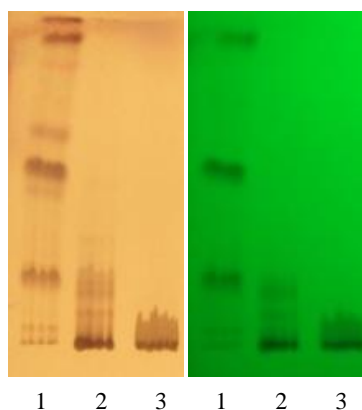


Figure 16 TLC of F1-F3
Mobile phase: TLC system 5
Detection: UV₂₅₄ (left) and visible light with ASR (right)

Table 12 Obtained amounts of fractions from VLC of the chlorophyll-rich dichloromethane extract

Fraction	F1	F2	F3
Amount in g	22.98	10.83	1.58

F1, F2 and F3 were tested in the proliferation assay with HL-60 cells at concentrations of 15 µg/ml and 40 µg/ml after 24 and 72 hours. The results of the proliferation assay are illustrated in Figure 17 and reveal F1 and F2 as the most active ones (35 % and 50 % of control when treated with 15 µg/ml), whereas the activity of F3 is much lower (95 % of control when treated with 15 µg/ml).

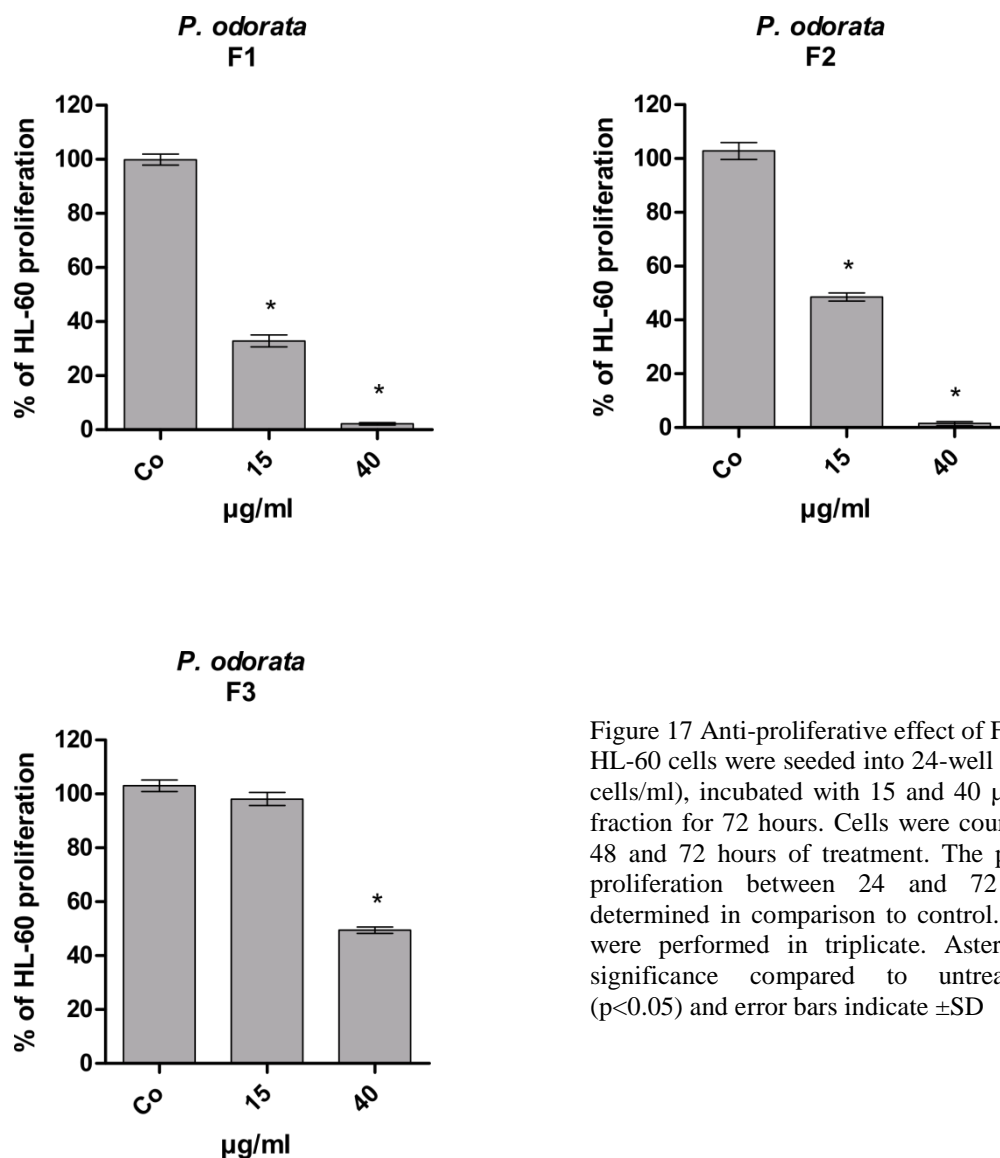
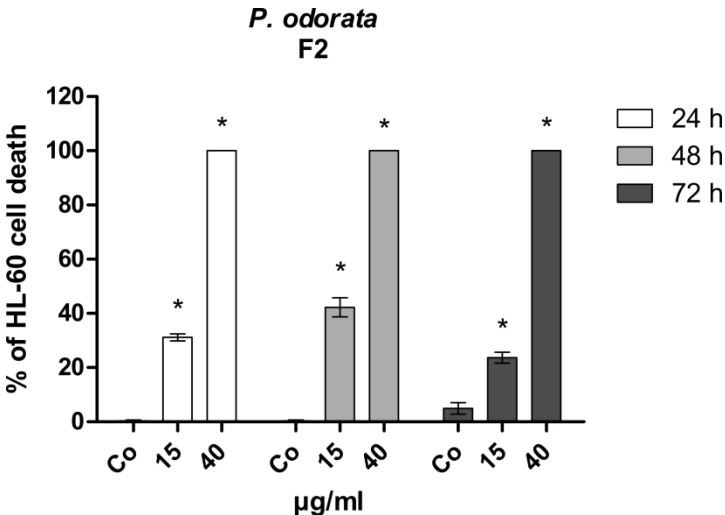
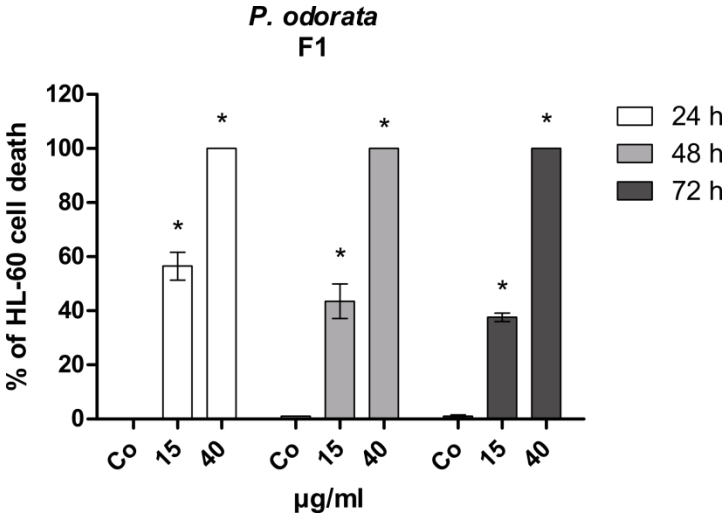


Figure 17 Anti-proliferative effect of F1, F2 and F3 HL-60 cells were seeded into 24-well plate (1×10^5 cells/ml), incubated with 15 and 40 $\mu\text{g/ml}$ of each fraction for 72 hours. Cells were counted after 24, 48 and 72 hours of treatment. The percentage of proliferation between 24 and 72 hours was determined in comparison to control. Experiments were performed in triplicate. Asterisks indicate significance compared to untreated control ($p < 0.05$) and error bars indicate $\pm\text{SD}$

To investigate whether fractions were cytotoxic, HL-60 cells were analysed for apoptotic phenotypes. Apoptosis assay of these three fractions was carried out using 15 $\mu\text{g/ml}$ and 40 $\mu\text{g/ml}$ and analysed after 24, 48 and 72 hours. Results of this assay show the same activity distribution as the proliferation assay of these fractions. After 24 hours 60 % of cells treated with F1 showed apoptosis, and 30 % of cells treated with F2 (Figure 18). The pictures taken for the apoptosis assay showed different colours of the dead cells in F1 and F2 (green) compared to F3 (light pink), which may refer to different cell death mechanisms. To assure that the greenish looking cells were dead, HL-60 cells were seeded in 24-well plates (1×10^5 cells/ml) and treated with 40 $\mu\text{g/ml}$

of F1, F2 and F3, respectively. After 48 hours of incubation the cells were centrifuged and the supernatant (old medium) was renewed. Cells were counted right after the new medium was added and then again after 3 and 6 days (72 hours and 144 hours). The result in Figure 19 shows that HL-60 cells pre-treated with F1 and F2 were dead, whereas cells pre-treated with F3 showed growth similar to the control. Therefore F1 was chosen for further fractionation, because it revealed the highest anti-proliferative and pro-apoptotic activity.



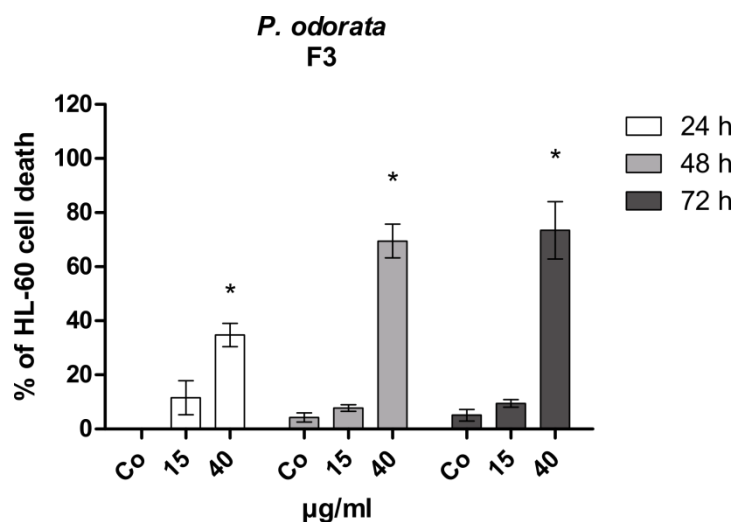


Figure 18 Induction of apoptosis by F1, F2 and F3

HL-60 cells were seeded in 24-well plates (1×10^5 cells/ml) and incubated with 15 and 40 $\mu\text{g/ml}$ of each fraction for 72 hours. Afterwards cells were double stained with Hoechst 33258 and propidium iodide and examined under the microscope with UV light connected to a DAPI filter. Nuclei with morphological changes which indicated cell death were counted and the percentages of dead cells were calculated. Experiments were performed in triplicate. Asterisks indicate significance compared to untreated control ($p < 0.05$) and error bars indicate \pm SD.

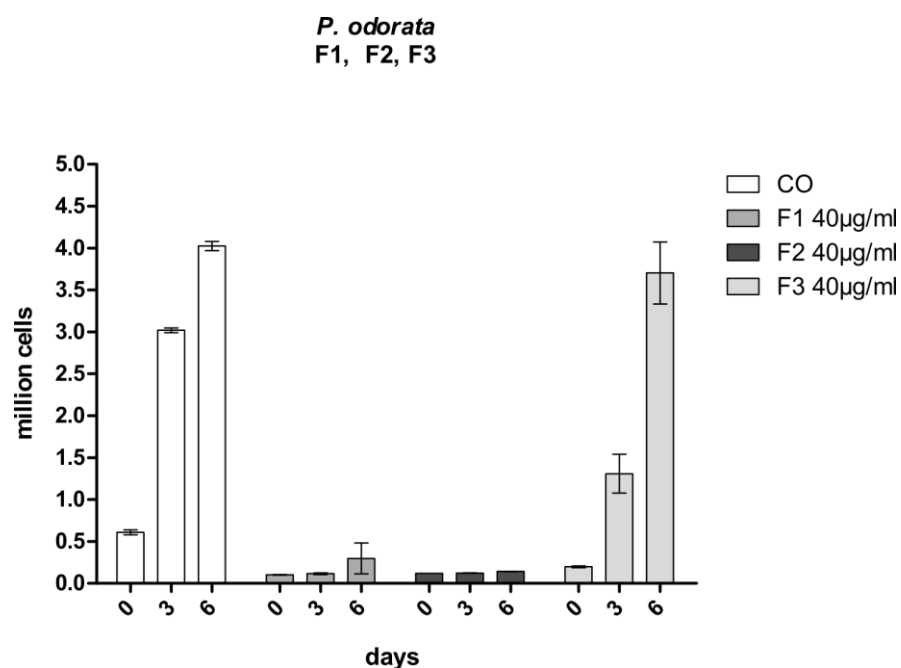


Figure 19 Analysis of proliferation of HL-60 cells pre-treated with F1, F2 and F3, respectively.

Pre-treated HL-60 cells (pre-treated in 24-well plates (1×10^5 cells/ml) with 40 $\mu\text{g/ml}$ of F1, F2 and F3, respectively; after 48 hours of incubation cells were centrifuged and old medium was replaced by new one) were counted right away after the new medium was added and after 3 and 6 days. Experiments were

performed in triplicate. Asterisks indicate significance compared to untreated control ($p < 0.05$) and error bars indicate \pm SD

To check the differences of cell death mechanisms between F1 and the most active fractions of the 2005 dichloromethane extract investigation of Bauer et al. (2010), western blot analyses were conducted of F1 with the focus on the caspase 3 apoptotic pathway. In addition to caspase 3, anti-acetylated tubulin blots were analysed. In Figure 20 the results of the western blot analysis of F1 are displayed. HL-60 cells treated with F1 did not increase acetylation of α tubulin but substantially activated caspase 3. The most active fractions investigated by Bauer et al. (2010), also led to an acetylation of α tubulin. Hence, F1 seemed to be completely different than the already investigated fractions and was therefore used for further fractionation and analyses.

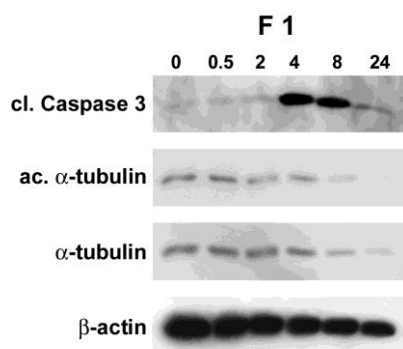


Figure 20 Western blot analysis of F1 on caspase 3 and α -tubulin

HL-60 cells (1×10^6 cells/ml) were incubated with $40 \mu\text{g/ml}$ F1 and harvested after 0.5, 2, 4, 8 and 24 h of treatment. Cells were lysed and obtained proteins samples applied to SDS-PAGE. Western blot analysis was conducted with the indicated antibodies. Equal sample loading was confirmed by Ponceau S staining and β -actin analysis.

4.1.3.2 VLC of F1 – F2.1-F2.10

For further fractionation of F1, a VLC was conducted as described in chapter 3.3.2.2. The quality of the fractionation was measured by TLC using TLC system 5 (dichloromethane: ethyl acetate, 85:15). The separation of the starting fraction F1 and the new derivative fractions F2.1-F2.9 are depicted in Figure 21. The TLC reveals that the VLC worked well in order to separate the contained compounds of F1 by polarity. F2.3 and F2.4 as well as F2.10 and F2.11 were recombined because they looked similar on the TLC. The obtained amounts of new fractions are presented in Table 13.

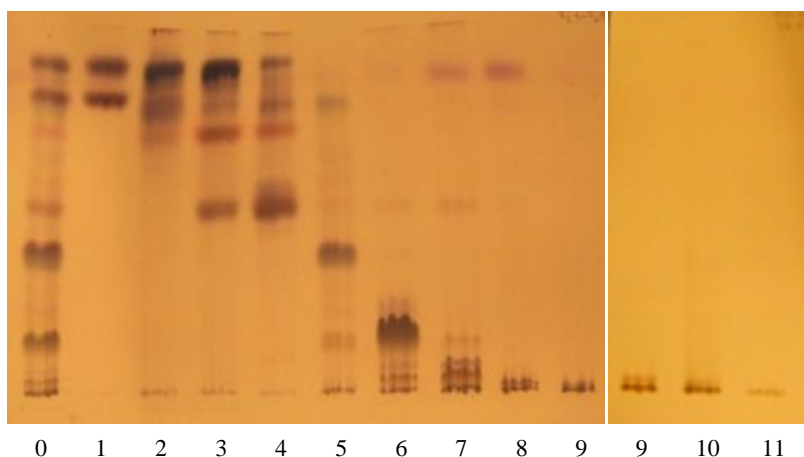


Figure 21 TLC of F2.1-F2.10
 Mobile phase: TLC system 5
 Detection: visible light with ASR (both pictures)

Table 13 Obtained amounts of fractions from VLC of F1

Fraction	F2.1	F2.2	F2.3+4	F2.5	F2.6	F2.7
Amount in g	1.63	0.17	1.28	4.57	1.73	0.22

Fraction	F2.8	F2.9	F2.10+11
Amount in g	0.04	0.12	0.16

The activity of F2.1-F2.10 was tested in HL-60 cells by analysing apoptosis. The cells were treated with a concentration of 10 $\mu\text{g/ml}$ of each fraction and incubated for 24, 48 and 72 hours, when cells were analysed (Figure 22). F2.6 (90 % apoptosis after 24 hours), F2.7 (95 % apoptosis after 24 hours) and F2.10 (95 % apoptosis after 72 hours) induced the highest rates of apoptosis, whereas the other fractions triggered the apoptosis rates to maximal 40 %. Thus, this fractionation resulted in a clear separation of cytotoxic fractions from non-toxic ones.

Figure 22 also illustrates decreasing apoptotic activity of F2.6 and F2.7 with increasing time, whereas in F2.10 the activity increases from 24 to 72 hours indicating the distinct stabilities or activities of the contained compounds.

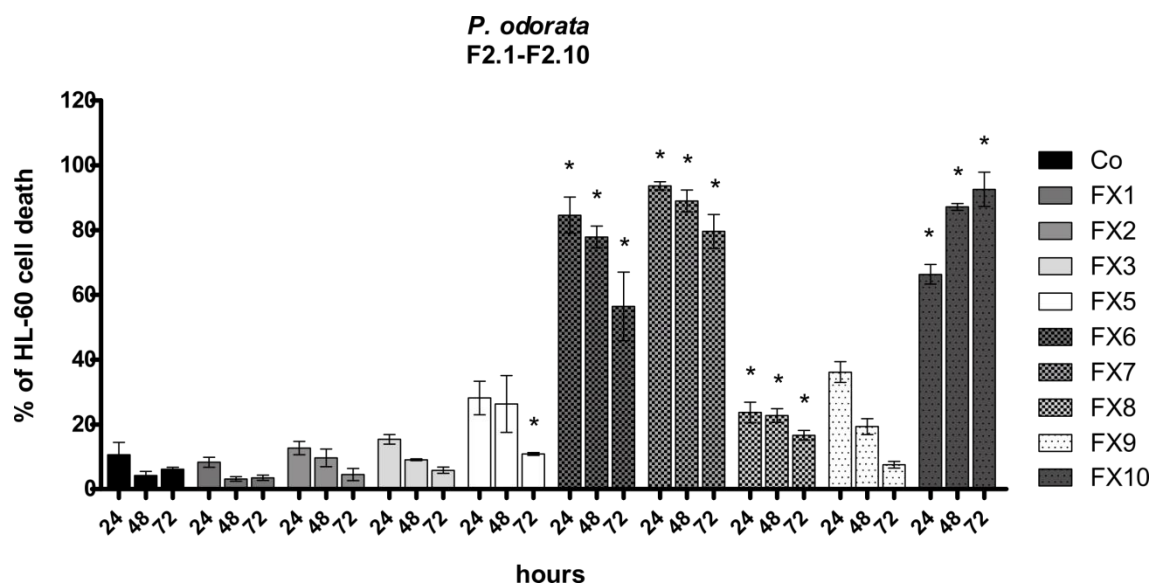


Figure 22 Induction of apoptosis by F2.1-F2.10

HL-60 cells were seeded in 24-well plates (1×10^5 cells/ml) and incubated with $10 \mu\text{g/ml}$ of each fraction for 72 hours. Afterwards cells were double stained with Hoechst 33258 and propidium iodide and examined under the microscope with UV light connected to a DAPI filter. Nuclei with morphological changes which indicated cells death were counted and the percentages of dead cells were calculated. Experiments were performed in triplicate. Asterisks indicate significance compared to untreated control ($p < 0.05$) and error bars indicate $\pm\text{SD}$.

As illustrated on the TLC of F2.6-F2.10 (Figure 23), conducted with TLC system 1 (chloroform: methanol: water, 90:22:3.5), F2.10 contains compounds which are also contained in F2.6 and F2.7. F2.10 is the last received fraction of the column. All substances left in the column, which were not eluted by previous mobile phases, are finally eluted with methanol and are now contained in F2.10. Because of this, F2.10 was not further fractionated. Instead of F2.10, the fractionation of F2.6 followed.

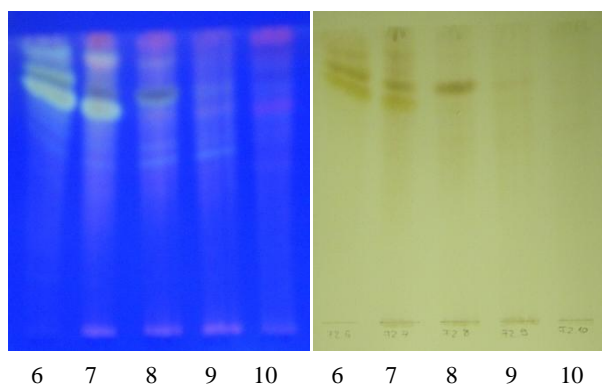


Figure 23 TLC of F2.6-F2.10
Mobile phase: TLC system 1
Detection: visible light with ASR (left),
UV₃₆₆ with ASR (right)

4.1.4 Column Chromatography (CC) and Thin Layer Chromatography (TLC)

F2.6 and F2.7 were the most active fractions and we continued with the fractionation of F2.6 because it contained 8-folds more material than F2.7. In the following chapters the results of the fractionation process, starting with F2.6 are described.

4.1.4.1 CC of F2.6 – F3.1-F3.10

Column chromatography of F2.6 was conducted as described in chapter 3.3.3.1. This time the new derivative fractions were checked by TLC system 2 (chloroform: methanol: water, 90:3.5:0.2). Figure 24 depicts the starting fraction F2.6 and the new obtained ones F3.1-F3.10. As the TLC reveals, both F3.3 and F3.6 contain a main compound, which were tried to be separated during further fractionation processes. Obtained amounts of the ten fractions are presented in Table 14.

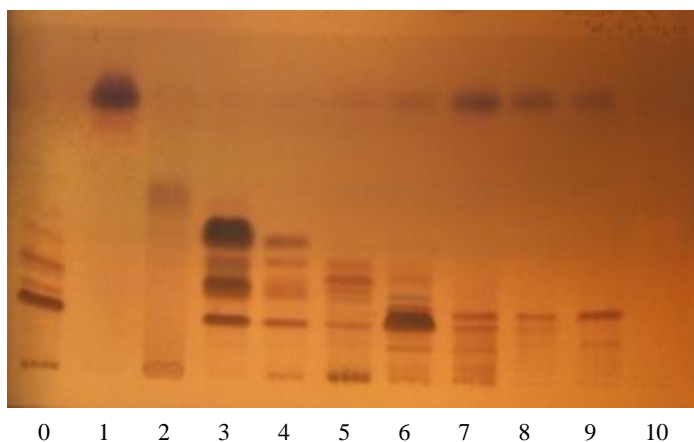


Figure 24 TLC of F3.1-F3.10
Mobile phase: TLC system 2
Detection: visible light with ASR

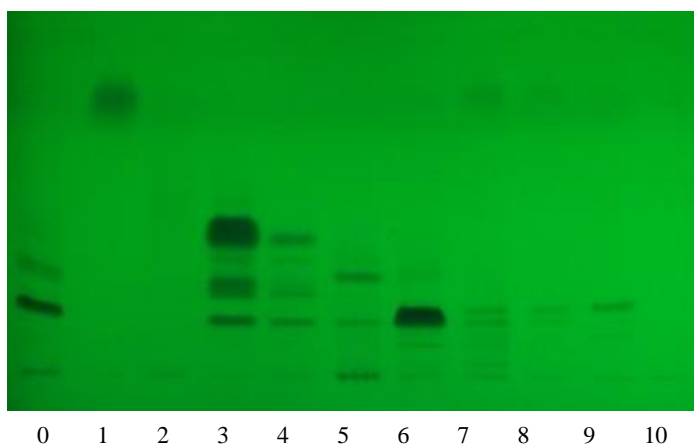


Figure 25 TLC of F3.1-F3.10
Mobile phase: TLC system 2
Detection: UV₂₅₄

Results

Table 14 Obtained amounts of fractions from CC of F2.6

Fraction	F3.1	F3.2	F3.3	F3.4	F3.5
Amount in g	0.02	0.05	1.14	0.07	0.05

Fraction	F3.6	F3.7	F3.8	F3.9	F3.10
Amount in g	0.32	0.02	0.01	0.03	0.04

In the proliferation assay, the anti-proliferative activity of F3.1-F3.10 is displayed. The assay was performed with HL-60 cells, which were treated with each fraction at the concentration of 2 $\mu\text{g/ml}$ and 10 $\mu\text{g/ml}$ and analysed after 24 and 72 hours. As Figure 26 reveals, F3.4-F3.6 had an highly anti-proliferative effect, as the three fractions suppressed proliferation by almost 100 % upon incubation with 10 $\mu\text{g/ml}$. F3.2, F3.3 and F3.6 were chosen for further fractionation because the TLC of F3.2 visualized only a few bands and F3.3 and F3.6 both contained a main compound.

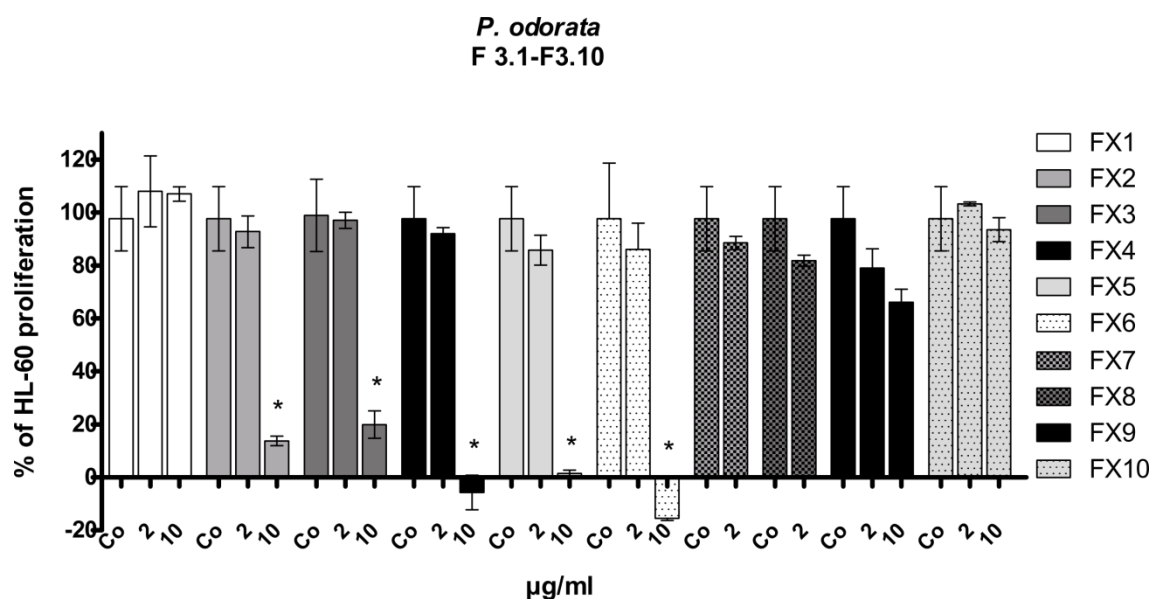


Figure 26 Anti-proliferative effect of F3.1-F3.10

HL-60 cells were seeded into 24-well plate (1×10^5 cells/ml), incubated with 2 and 10 $\mu\text{g/ml}$ of each fraction (except F2.7 and F2.8 were only applied in the concentration of 2 $\mu\text{g/ml}$) for 72 hours. Cells were counted after 24, 48 and 72 hours of treatment. The percentage of proliferation between 24 and 72 hours was determined in comparison to control. Experiments were performed in triplicate. Asterisks indicate significance compared to untreated control ($p < 0.05$) and error bars indicate \pm SD.

4.1.4.2 CC of F3.2 – F4.2.1-F4.2.6

Column chromatography of F3.2 was conducted as described in chapter 3.3.3.2. New fractions were checked by TLC system 4 (dichloromethane: ethyl acetate, 80:20). At the beginning the separation process worked well, whereas towards the end no clear separation of compounds could be spotted on the TLC. F4.2.2 appeared to be the most promising one, regarding to obtain a pure compound (Figure 27), which is the reason for further purification of this fraction. The other fractions were tested in a proliferation assay, whereas F4.2.2 was completely applied to silica gel column fractionation. The reason for not testing F4.2.2 before applying it to the column was the small amount of substance left over. Amounts of the six fractions are presented in Table 15.

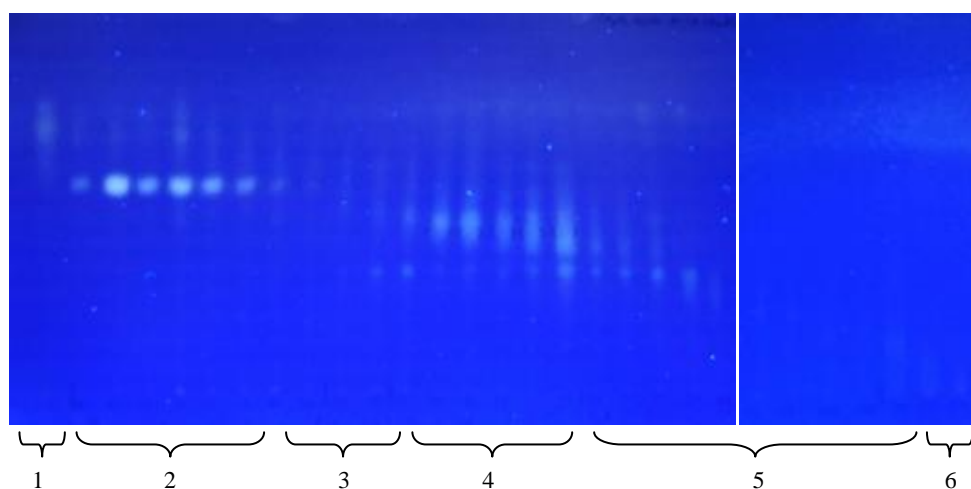


Figure 27 TLC of F4.2.1-F4.2.6
Mobile phase: TLC system 4
Detection: UV₃₆₆

Table 15 Obtained amount of fractions from CC of F3.2

Fraction	F4.2.1	F4.2.2	F4.2.3	F4.2.4	F4.2.5	F4.2.6
Amount in g	0.0023	0.0122	0.0027	0.0045	0.0040	0.0026

Proliferation assay of F4.2.1-F4.2.6 - except for F4.2.2 - is presented in Figure 28 also reveals the highest increase in proliferation in F4.2.5: up to 50 % increase in the highest concentration (5 $\mu\text{g/ml}$), compared to the control. Further fractionation of these fractions was not conducted, because unfortunately only small amounts of this fraction were left over with still a few impurities included.

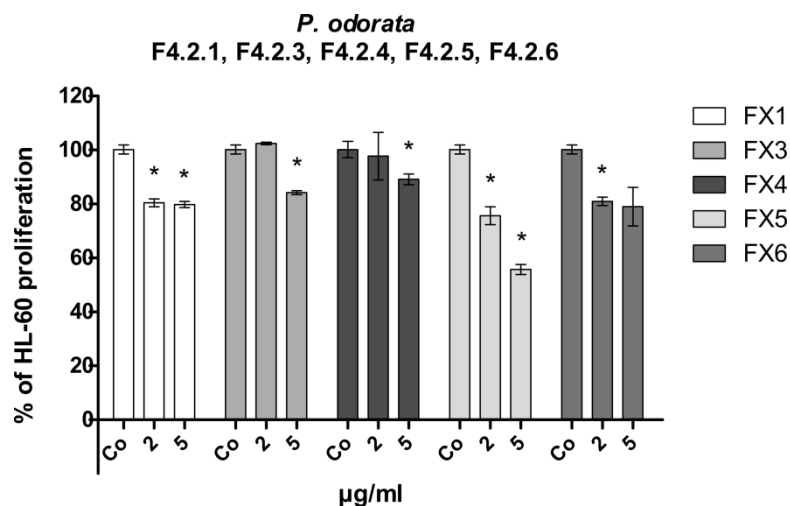


Figure 28 Anti-proliferative effect of F4.2.1, F4.2.3-F4.2.6
HL-60 cells were seeded into 24-well plate (1×10^5 cells/ml), incubated with 2 and 5 $\mu\text{g/ml}$ of each fraction for 72 hours. Cells were counted after 24, 48 and 72 hours of treatment. The percentage of proliferation between 24 and 72 hours was determined in comparison to control. Experiments were performed in triplicate. Asterisks indicate significance compared to untreated control ($p < 0.05$) and error bars indicate \pm SD.

4.1.4.3 CC of F4.2.2 – F5.2.2.1-F5.2.2.1.4

Column chromatography of F4.2.2 was conducted as described in chapter 3.3.3.3. Objective of this column was purifying the main compound of F4.2.2. TLC of F5.2.2.1, using TLC system 4 (dichloromethane: ethyl acetate, 80:20), reveals that this fraction contains a main compound, but unfortunately also some impurities. By scraping the compounds off a TLC plate (description see chapter 3.3.3.4, results see chapter 4.1.4.4), the impurities were tried to be removed, as it was not possible to purify by column chromatography with such a small amount of fraction. Amounts of the four fractions are depicted in Table 16.

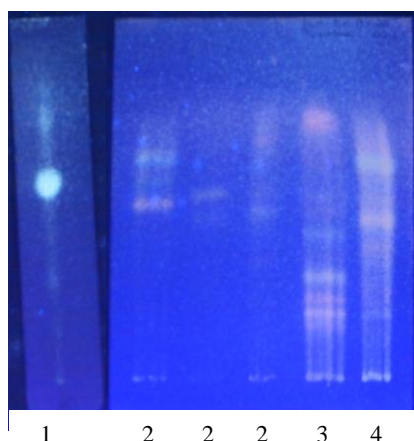


Figure 29 TLC of F5.2.2.1-F5.2.2.4
Mobile phase: TLC system 4
Detection: UV₃₆₆

Table 16 Obtained amount of fractions from CC of F4.2.2

Fraction	F5.2.2.1	F5.2.2.2	F5.2.2.3	F5.2.2.4
Amount in g	0.0069	0.000479	0.00066	0.00037

4.1.4.4 Scraped TLC of F5.2.2.1 – F6.2.2.1.1-F6.2.2.1.4

Scraping bands of F5.2.2.1 off a glass TLC plate was performed as described in chapter 3.3.3.4. Visible single bands were scraped off and a TLC of these four bands was conducted by using TLC system 4 (dichloromethane: ethyl acetate, 80:20). The obtained TLC reveals four single bands.

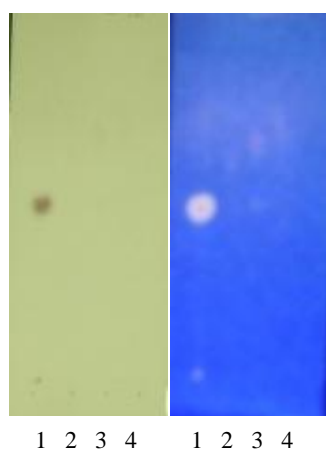


Figure 30 TLC of F6.2.2.1.1-F6.2.2.1.4
Mobile phase: TLC system 4
Detection: visible light with ASR (left), UV₃₆₆ (right)

Results

Table 17 Obtained amount of fractions from CC of F5.2.2.1

Fraction	F6.2.2.1.1	F6.2.2.1.2	F6.2.2.1.3	F6.2.2.1.4
Amount in mg	5.3	0.2	0.4	0.2

Proliferation assay of F6.2.2.1.1-F6.2.2.1.4 is presented in Figure 31. F6.2.2.1.2 and F6.2.2.1.3 are the most active fractions. Compared to the starting fraction (F3.2) they show a large decrease in activity. During the fractionation process and the conducted step of scraping the bands of F5.2.2.1 off the TLC plate, the activity was further split between the new fractions. The concentrations depicted in the proliferation graph are estimated concentrations as it was not possible to calculate the exact weight of the scraped fractions. Possibly some scraped off silica is still contained in the new fractions and therefore biasing the real fraction weights and hence the results of the proliferation analyses.

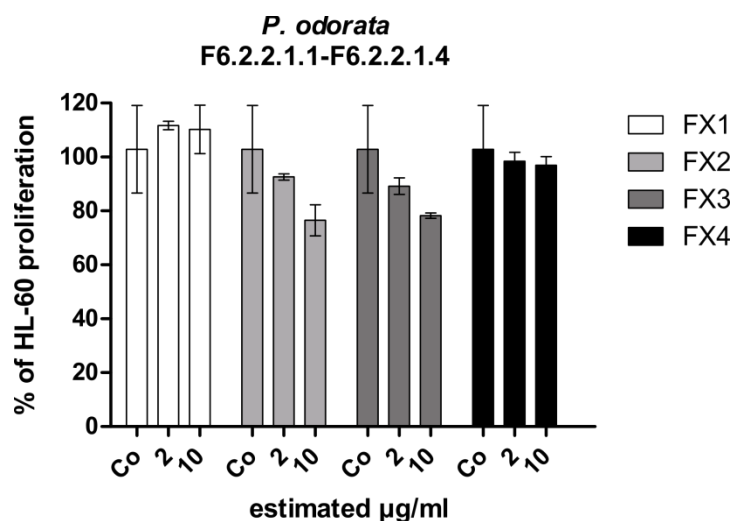


Figure 31 Anti-proliferative effect of F6.2.2.1.1-F6.2.2.1.4

HL-60 cells were seeded into 24-well plate (1×10^5 cells/ml), incubated with 2 and 10 $\mu\text{g/ml}$ of each fraction for 72 hours. Cells were counted after 24, 48 and 72 hours of treatment. The percentage of proliferation between 24 and 72 hours was determined in comparison to control. Experiments were performed in triplicate. Asterisks indicate significance compared to untreated control ($p < 0.05$) and error bars indicate \pm SD.

4.1.4.5 CC of F3.3 – F4.3.1

Column chromatography of F3.3 was performed as described in chapter 3.3.3.5. The collected fractions were checked by TLC system 2 (chloroform: methanol: water, 90:3.5:0.2). Afterwards all collected fractions were recombined, as no separation of substances was revealed by TLC (Figure 32). 1.085 g of F4.3.1 were left over after CC.

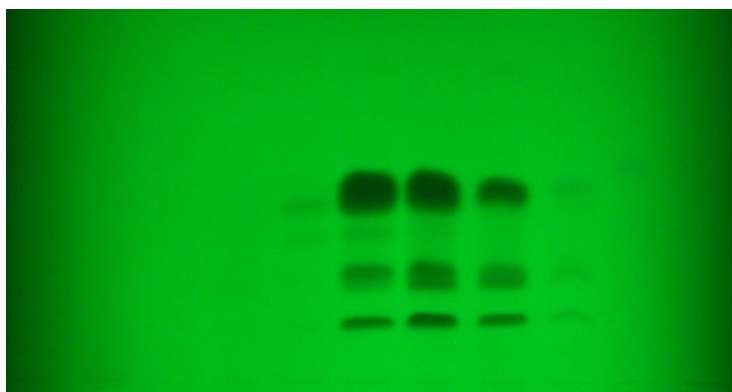


Figure 32 TLC of F4.3.1
Mobile phase: TLC system 2
Detection: UV₂₅₄

4.1.4.6 CC of F4.3.1 – F5.3.6.1-F5.3.6.12

Column chromatography of F4.3.1 was conducted as described in chapter 3.3.3.6. The TLC was performed with TLC system 2 (chloroform: methanol: water, 90:3.5:0.2). As seen by TLC (Figure 33) the compounds contained in F4.3.1 were not separated well by the CC. Amounts of the twelve fractions are presented in Table 18.

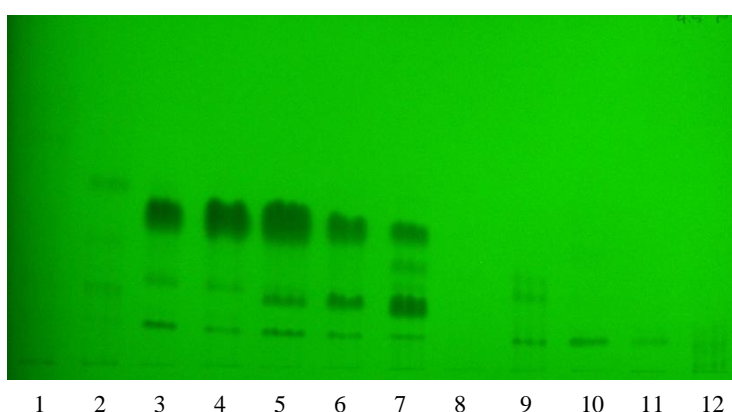


Figure 33 TLC of F5.3.6.1-
F5.3.6.12
Mobile phase: TLC system 2
Detection: UV₂₅₄

Results

Table 18 Obtained amount of fractions from CC of F4.3.1

Fraction	F5.3.6.1	F5.3.6.2	F5.3.6.3	F5.3.6.4	F5.3.6.5	F5.3.6.6
Amount in g	0.000374	0.00345	0.05886	0.09094	0.25592	0.06486

Fraction	F5.3.6.7	F5.3.6.8	F5.3.6.9	F5.3.6.10	F5.3.6.11	F5.3.6.12
Amount in g	0.14622	0.00751	0.00617	0.11147	0.06250	0.00349

Proliferation and apoptosis assay (Figure 34 and Figure 35), performed at concentrations of 5 $\mu\text{g/ml}$ and 10 $\mu\text{g/ml}$, were both analysed after 24 and 48 hours. The apoptosis assay was only conducted with F5.3.6.1, F5.3.6.2, F5.3.6.6, F5.3.6.7, F5.3.6.10 and F5.3.6.11, because these fractions revealed the strongest growth inhibition in the proliferation assay. Especially F5.3.6.2 and F5.3.6.7 decreased cell proliferation: in the highest concentration (10 $\mu\text{g/ml}$) both fractions inhibit proliferation by almost 100 % compared to the control. Also, the apoptosis assay reflects this result with an almost 100 % cell death rate induced by these fractions. The most active F5.3.6.7 was chosen for further fractionation.

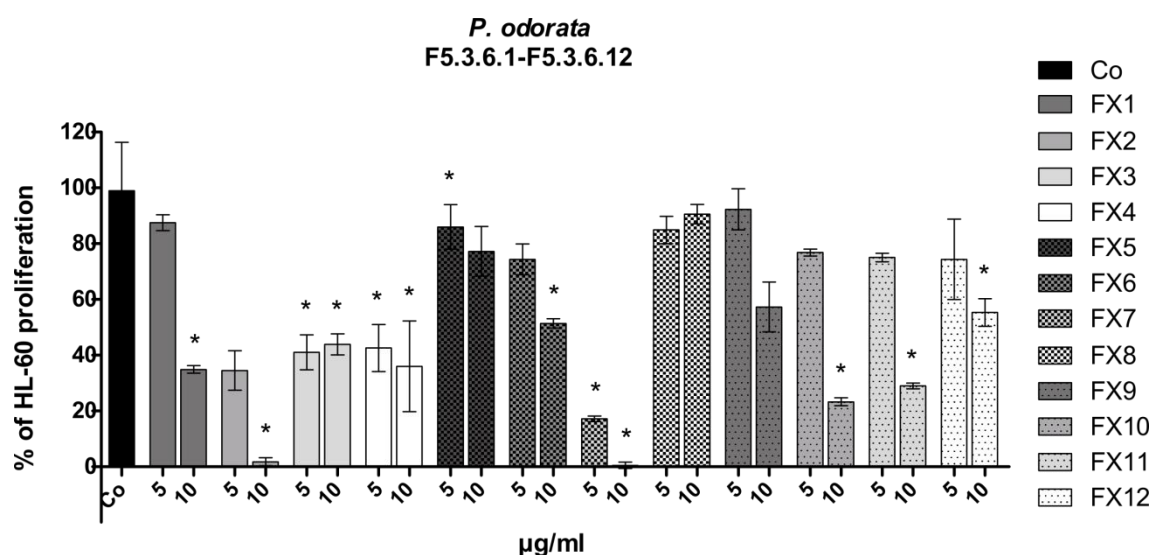
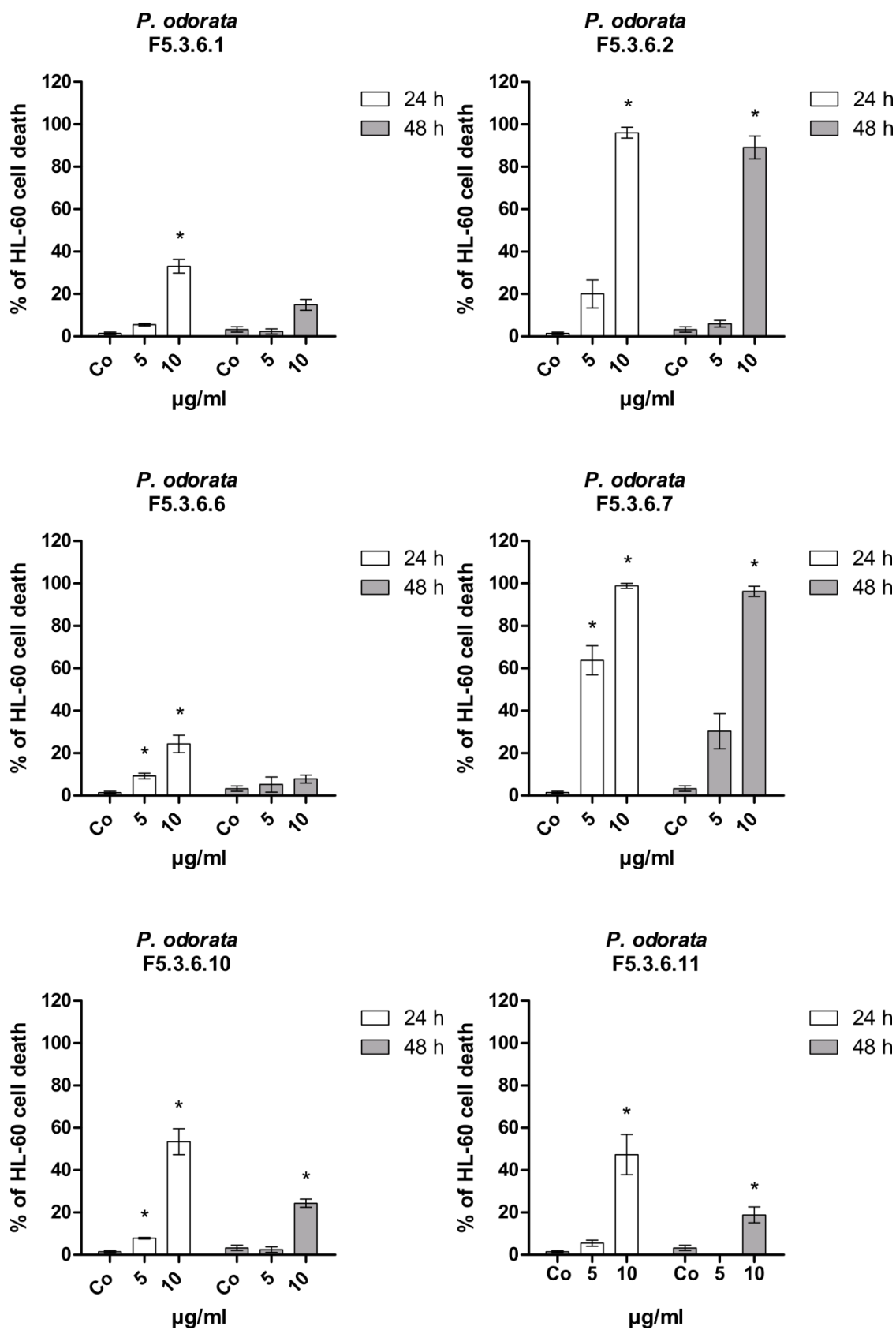


Figure 34 Anti-proliferative effect of F5.3.6.1-F5.3.6.12
HL-60 cells were seeded into 24-well plate (1×10^5 cells/ml), incubated with 5 and 10 $\mu\text{g/ml}$ of each fraction for 48 hours. Cells were counted after 24 and 48 hours of treatment. The percentage of proliferation between 24 and 48 hours was determined in comparison to control. Experiments were performed in triplicate. Asterisks indicate significance compared to untreated control ($p < 0.05$) and error bars indicate \pm SD.



Results

Figure 35 Induction of apoptosis by F5.3.6.1, F5.3.6.2, F5.3.6.6, F5.3.6.7, F5.3.6.10 and F5.3.6.11
HL-60 cells were seeded in 24-well plates (1×10^5 cells/ml) and incubated with 5 and 10 $\mu\text{g/ml}$ of each fraction for 48 hours. Afterwards cells were double stained with Hoechst 33258 and propidium iodide and examined under the microscope with UV light connected to a DAPI filter. Nuclei with morphological changes which indicated cell death were counted and the percentages of dead cells were calculated. Experiments were performed in triplicate. Asterisks indicate significance compared to untreated control ($p < 0.05$) and error bars indicate $\pm\text{SD}$.

4.1.4.7 CC of F5.3.6.7 – F6.3.6.7.1-F6.3.6.7.12

Column chromatography of F5.3.6.7 was performed as described in chapter 3.3.3.7. TLC system 2 (chloroform: methanol: water, 90:3.5:0.2) was utilized for a fingerprint of the newly received fractions (Figure 36). The TLC reveals that F6.3.6.7.3, F6.3.6.7.4 and F6.3.6.7.5 included main compounds, but also many impurities, which were not separated by the CC. Amounts of the twelve fractions are presented in Table 19.

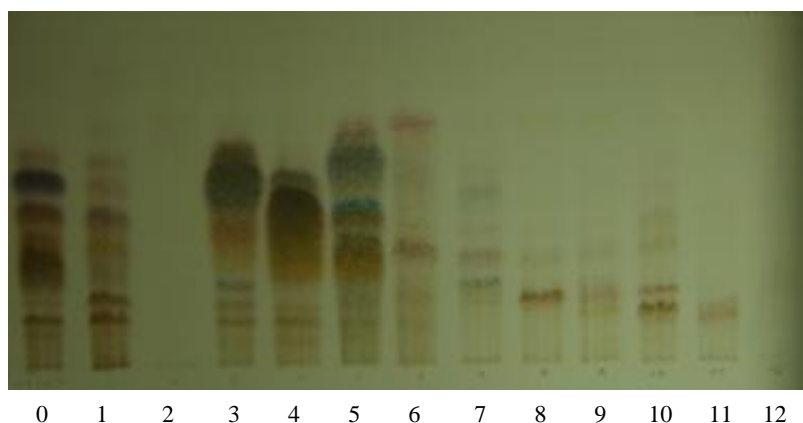


Figure 36 TLC of F6.3.6.7.1-F6.3.6.7.12
Mobile phase: TLC system 2
Detection: visible light with ASR (top), UV_{254} (bottom)

Table 19 Obtained amount of fractions from CC of F5.3.6.7

Fraction	F6.3.6.7.1	F6.3.6.7.2	F6.3.6.7.3	F6.3.6.7.4
Amount in g	0.0847	0.00343	0.02647	0.0202

Fraction	F6.3.6.7.5	F6.3.6.7.6	F6.3.6.7.7	F6.3.6.7.8
Amount in g	0.04245	0.01703	0.00262	0.00327

Fraction	F6.3.6.7.9	F6.3.6.7.10	F6.3.6.7.11	F6.3.6.7.12
Amount in g	0.00280	0.00808	0.00121	0.06682

The apoptosis assay of the received fractions was performed in the concentrations of 2 µg/ml and 5 µg/ml and cells were photographed after 24 hours. Unfortunately, the activity of the starting fraction F5.3.6.7 was split up into the new fractions, and therefore decreased in comparison to the starting fraction F5.3.6.7, which reached an apoptotic rate of 60 % in the concentration of 5 µg/ml after 24 hours of incubation. This is the reason for not further fractionating these newly received fractions.

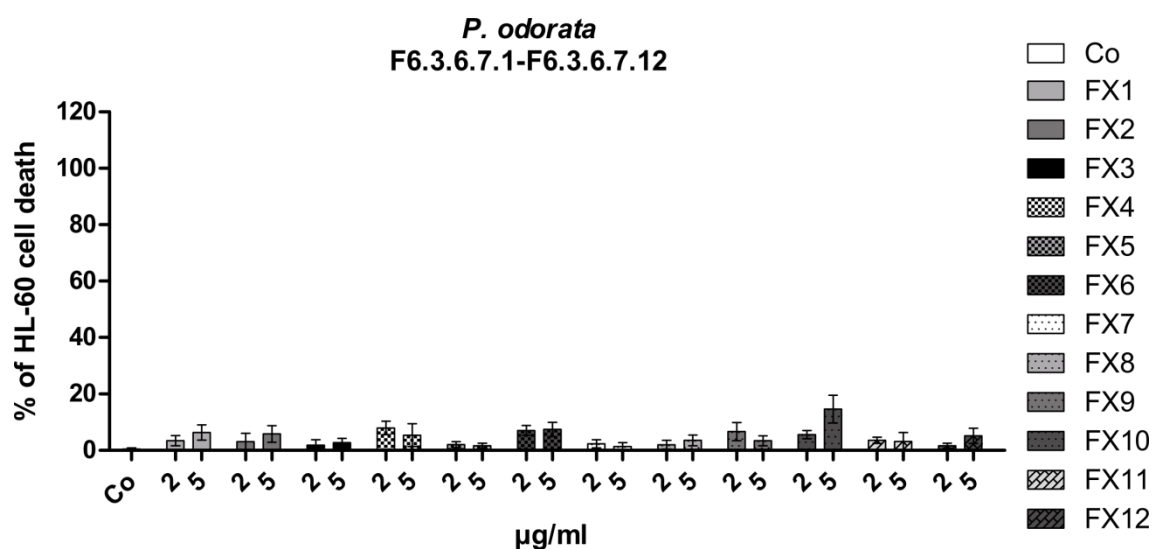


Figure 37 Induction of apoptosis by F6.3.6.7.1-F6.3.6.7.12

HL-60 cells were seeded in 24-well plates (1×10^5 cells/ml) and incubated with 2 and 5 µg/ml of each fraction for 24 hours. Afterwards cells were double stained with Hoechst 33258 and propidium iodide and examined under the microscope with UV light connected to a DAPI filter. Nuclei with morphological changes which indicated cell death were counted and the percentages of dead cells were calculated. Experiments were performed in triplicate. Asterisks indicate significance compared to untreated control ($p < 0.05$) and error bars indicate \pm SD.

4.1.4.8 CC of F3.6 – F4.6.1-F4.6.4

Fractionation of 3.6 was performed as described in chapter 3.3.3.8. For TLCs of the new fractions, TLC system 2 (chloroform: methanol: water, 90:3.5:0.2) was used. Figure 38 shows an oily fraction 4.6.3 including one main compound.

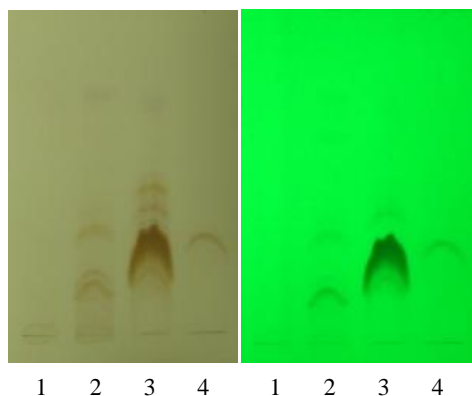
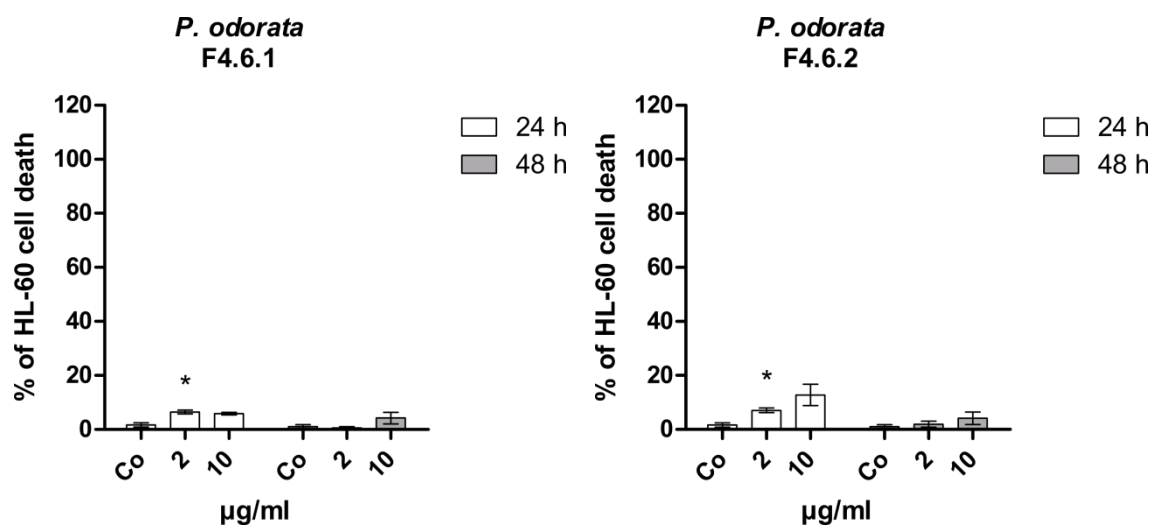


Figure 38 TLC of F4.6.1-F4.6.4
 Mobile phase: TLC system 2
 Detection: visible light with ASR (left), UV₂₅₄ (right)

Table 20 Obtained amount of fractions from CC of F3.6

Fraction	F4.6.1	F4.6.2	F4.6.3	F4.6.4
Amount in g	0.00933	0.00486	0.20695	0.05479

As illustrated in Table 20, F4.6.3 is the one with the highest amount of left over active material. HL-60 cells were treated with 2 µg/ml and 10 µg/ml for 24 and 48 hours to measure the apoptotic effect F4.6.1-F4.6.4. F4.6.3 shows an apoptosis rate of 90 % in the highest concentration (10 µg/ml) after 24 hours of incubation, whereas the other fractions induced only 20 % of apoptosis at the most. Consequently, F4.6.3 was further fractionated.



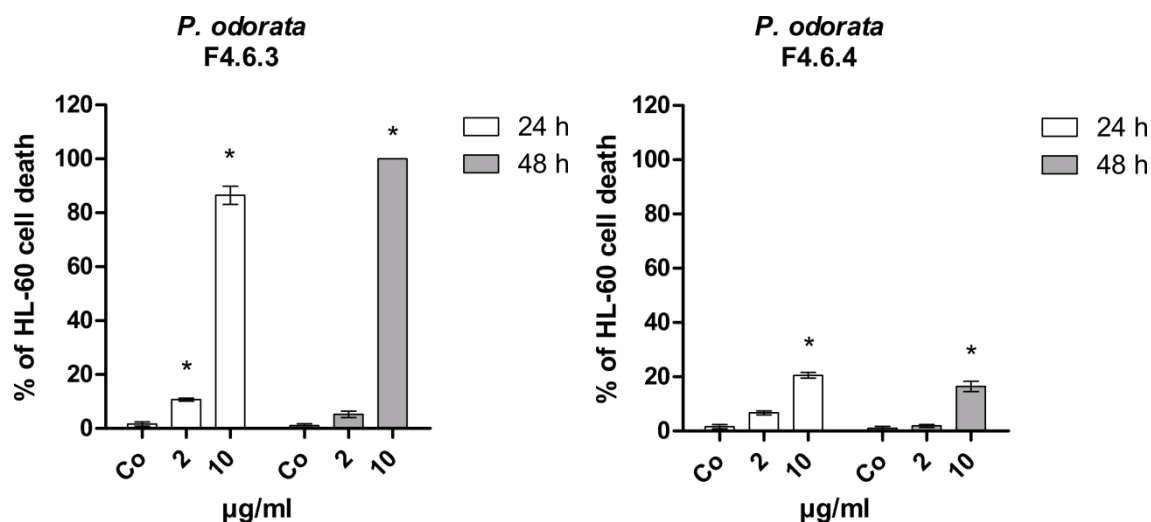


Figure 39 Induction of apoptosis by F4.6.1-F4.6.4

HL-60 cells were seeded in 24-well plates (1×10^5 cells/ml) and incubated with 2 and 10 µg/ml of each fraction for 48 hours. Afterwards cells were double stained with Hoechst 33258 and propidium iodide and examined under the microscope with UV light connected to a DAPI filter. Nuclei with morphological changes which indicated cell death were counted and the percentages of dead cells were calculated. Experiments were performed in triplicate. Asterisks indicate significance compared to untreated control ($p < 0.05$) and error bars indicate \pm SD.

4.1.4.9 CC of F4.6.3 – F5.6.3.1-F5.6.3.6

Column chromatography of F4.6.3 was performed as described in chapter 3.3.3.9. TLC of the new fractions was conducted with TLC system 2 (chloroform: methanol: water, 90:3.5:0.2) as presented in Figure 40. F5.6.3.1 is depicted on the TLC as one band, whereas F5.6.3.3 and F5.6.3.4 show main compounds, but also many impurities. The amounts of the new fractions in mg are listed in Table 21.

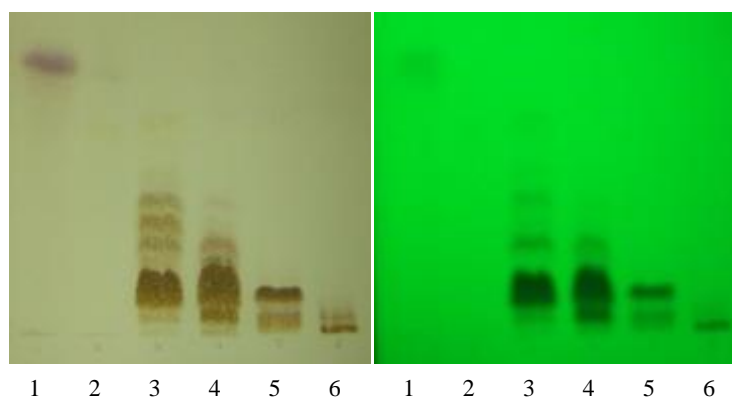


Figure 40 TLC of F5.6.3.1-F5.6.3.6
Mobile phase: TLC system 2
Detection: visible light with ASR (left), UV₂₅₄ (right)

Results

Table 21 Obtained amount of fractions from CC of F4.6.3

Fraction	F5.6.3.1	F5.6.3.2	F5.6.3.3	F5.6.3.4	F5.6.3.5	F5.6.3.6
Amount in mg	3.33	0.31	19.49	25.28	16.31	3.58

Apoptosis assay was performed after 8 and 24 hours in concentrations of 2 $\mu\text{g/ml}$ and 5 $\mu\text{g/ml}$. Figure 41 illustrates the rate of apoptosis after 24 hours. Only the pictures taken after 24 hours were analysed as there was no 100 % apoptosis rate in these cells. As shown in the graph, the apoptosis rate of the starting fraction was split to the daughter fractions, even fraction F5.6.3.1 did not show an enrichment of activity. Therefore no further fractionation process was performed with these fractions.

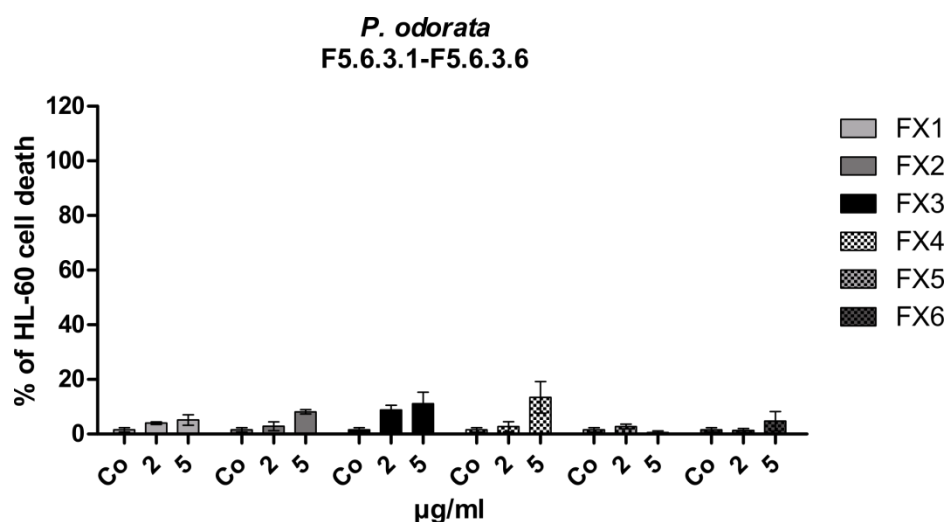


Figure 41 Induction of apoptosis by F5.6.3.1-F5.6.3.6

HL-60 cells were seeded in 24-well plates (1×10^5 cells/ml) and incubated with 2 and 5 $\mu\text{g/ml}$ of each fraction for 24 hours. Afterwards cells were double stained with Hoechst 33258 and propidium iodide and examined under the microscope with UV light connected to a DAPI filter. Nuclei with morphological changes which indicated cell death were counted and the percentages of dead cells were calculated. Experiments were performed in triplicate. Asterisks indicate significance compared to untreated control ($p < 0.05$) and error bars indicate \pm SD.

4.1.5 Western Blot analysis

Western blot analyses were conducted with the two most active fractions (F4.6.3 and F5.3.6.7) received by two different tracks of the bio-assay guided fractionation process. Both fractions showed a significant pro-apoptotic effect after 48 hours of about 100 % in HL-60 cells treated with 10 μ g/ml of F4.6.3 and about 90 % in HL-60 cells treated with F5.3.6.7. Also the anti-proliferative effect of 10 μ g/ml F5.3.6.7 was close to 100 %. Proteins for the western blot analyses were chosen with a main focus on cell cycle stress, apoptosis induction and cell motility.

4.1.5.1 Analysis of the cell cycle and its checkpoint regulators

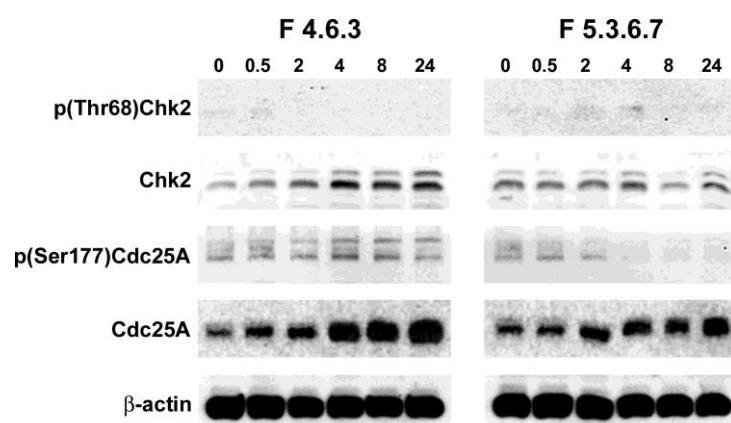


Figure 42 Analysis of cell cycle and checkpoint regulators
HL-60 cells (1×10^6 cells/ml) were incubated with 10 μ g/ml F4.6.3 and F5.3.6.7, respectively and harvested after 0.5, 2, 4, 8 and 24 h of treatment. Cells were lysed and obtained proteins samples applied to SDS-PAGE. Western blot analysis was conducted with the indicated antibodies. Equal sample loading was confirmed by Ponceau S staining and β -actin analysis

Chk2, Cdc25A: DNA damage generally leads to the activation of ataxia-telangiectasia-mutated (ATM) and ATM-and Rad3-related (ATR)-kinases, which themselves activate the effector kinases Chk1 and Chk2 (check point kinases) (Kiyokawa, et al., 2008). The Chk1/Chk2 phosphorylation results in the inactivation of Cdc25A phosphatase (Kiyokawa, et al., 2008) which causes the inactivation of Cyclin E-Cdk2. On the other hand an increased expression of Cdc25A accelerates the G1-S transition by increasing the Cdk2/Cyclin E activity (Blomberg, et al., 1999). Cdc25A activates also Cdk2/CyclinA necessary for DNA replication during S phase (Kiyokawa, et al., 2008)

(see chapter 2.2.2). Cdc25A is also a critical regulator for the G2-M transition and is required for Cdk1/Cyclin B activation. But in the G2-M transition also Cdc25C is involved, whereas the G1-S progression is predominantly controlled by Cdc25A and Cdc25B. Increased levels of Cdc25A and Cdc25B are often observed in various human cancer tissues, because the deregulated expression of these phosphatases allows cells to pass DNA damage-induced checkpoints and therefore lead to genomic instability (Kiyokawa, et al., 2008).

The analysis of the above described cell cycle and checkpoint regulators in HL-60 cells that were treated with F4.6.3 or with F5.3.6.7 showed differences in their expression patterns, because 10 µg/ml F4.6.3 caused the de-phosphorylation of Chk2, whereas F5.3.6.7 caused the phosphorylation of Chk2 after 4 hours concomitant with caspase 3 activation. Therefore, both fractions seem to be free of genotoxic compounds. Interestingly, Chk2 protein expression becomes induced. Whether this is sufficient to induce growth arrest is unlikely, because its target Cdc25A becomes strongly induced instead of degraded. In exposure to F5.3.6.7 the constitutive phosphorylation of Cdc25A was undetectable after 2 hours of incubation, which is an indicator for the stabilization of the protein (Madlener, et al., 2009). Indeed, Cdc25A protein levels increased, although not quite as high as upon treatment with F4.6.3. The phosphorylation and protein expression patterns clearly indicate that different compounds are contained in the two fractions and both fractions contain active principles free of genotoxic activity.

4.1.5.2 Analysis of apoptosis related proteins

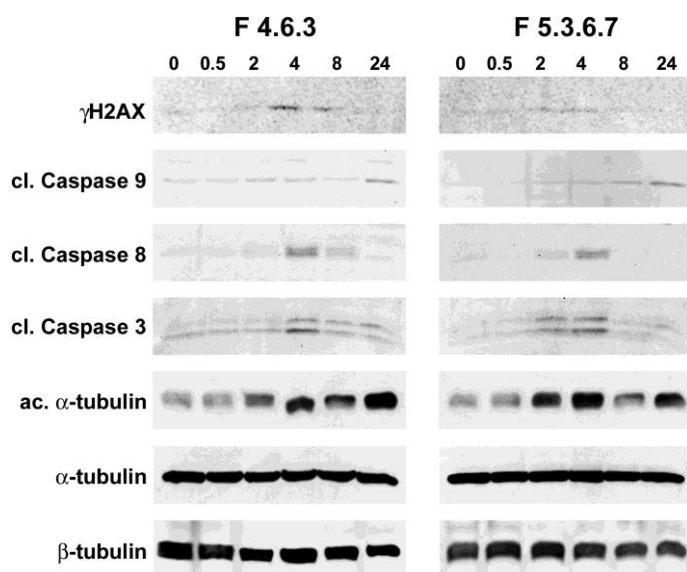


Figure 43 Analysis of apoptosis related proteins

HL-60 cells (1×10^6 cells/ml) were incubated with $10 \mu\text{g/ml}$ F4.6.3 and F5.3.6.7, respectively and harvested after 0.5, 2, 4, 8 and 24 h of treatment. Cells were lysed and obtained proteins samples applied to SDS-PAGE. Western blot analysis was conducted with the indicated antibodies. Equal sample loading was confirmed by Ponceau S staining and β -tubulin analysis

H2AX: γ H2AX is the most commonly used and sensitive marker for detecting DNA-double-strand breaks (Paull, et al., 2000), which is the reason for using the γ H2AX antibody for detecting the mechanism of apoptosis generated by F4.6.3 and F5.3.6.7. As shown in Figure 43 F4.6.3 induced the phosphorylation of H2AX with a peak after 4 hours and then slowly disappearing. F5.3.6.7 only induced a slight phosphorylation of H2AX, completely disappearing after 4 hours of incubation. However, H2AX phosphorylation was not caused by DNA damage induced by both fractions, but due to caspase 3 activity that induces DNA fragmentation through endonuclease G.

Caspases: Also cleaved caspases 8 and 9 were analysed (for their function during apoptosis see chapter 2.2.3 Evading apoptosis). F4.6.3 induced the cleavage of caspase 9 especially after 2 hours of incubation, whereas caspase 8 and caspase 3 were cleaved after 4 hours of incubation. Thus the cleavage of caspase 9 and the cleavage of caspase 8 resulted in the cleavage of caspase 3, which is a direct effector of apoptosis (see Figure 5). This activation cascade after 4 hours of incubation perfectly matches the γ H2AX, pCHK2 and pCdc25A activation after 4 hours. F5.3.6.7 showed a different

effect on the caspase cascade then F4.6.3. F5.3.6.7 first induces the cleavage of caspase 3 (after 2 hours of incubation) and therefore caspase 8 (with a peak at 4 hours and then completely disappearing) and caspase 9 (slightly increasing with a peak at 24 hours of incubation) were cleaved. This leads to the assumption that apoptosis caused by F5.3.6.7 is not induced by the caspase cascade, but independent of caspase 8 and 9.

α -tubulin: F.4.6.3 and F5.3.6.7 induced an increasing acetylation of α -tubulin, which implicates the stabilization of microtubules (Piperno, et al., 1987), and is reminiscent of the mechanism of taxol and therefore it triggers mitotic arrest and apoptosis, which was in fact observed at a concentration of 10 μ g/ml after 48 hours. Tilting the fine-tuned equilibrium of polymerized/de-polymerized microtubule is incompatible with normal cell division and this causes not only cell cycle arrest, but also apoptosis.

Unexpectedly, α -tubulin-targeting property was enriched in both fractions that was initially undetectable in the starting fraction F1.

4.1.5.3 Analysis of mobility related proteins

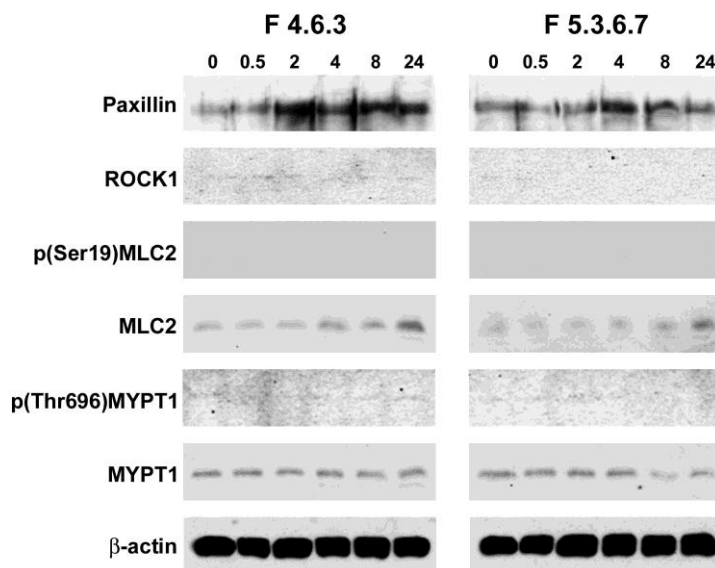


Figure 44 Analysis of mobility proteins
 HL-60 cells (1×10^6 cells/ml) were incubated with 10 μ g/ml F4.6.3 and F5.3.6.7, respectively and harvested after 0.5, 2, 4, 8 and 24 h of treatment. Cells were lysed and obtained proteins samples applied to SDS-PAGE. Western blot analysis was conducted with the indicated antibodies. Equal sample loading was confirmed by Ponceau S staining and β -actin analysis

Paxillin: Paxillin is the key regulator of cell migration (Paulitschke, et al., 2010), signal transduction, regulation of cell morphology (Salgia, et al., 1995), and it is an focal adhesion associated adaptor protein (Schaller, 2001). Thus paxillin is included in regulation of cell spreading and cell motility, both coordinated by signalling events by paxillin associated proteins (Schaller, 2001). For example it is a key coordinator of the Rho guanosine-5'-triphosphate (GTP)-ase family (Rho, Rac, Cdc42), which signalling cascades are responsible for cell spread and migration (Paulitschke, et al., 2010) and involved in cancer cell invasion.

The paxillin expression showed an increase in HL-60 cells treated with F4.6.3 whereas treatment with F5.3.6.7 left paxillin levels virtually unaffected. As paxillin is a focal adhesion phosphoprotein and necessary for the cell-extracellular matrix (ECM) contact (Deakin, et al., 2008), HL-60 cell motility was probably increased by F4.6.3.

ROCK-1: Two isoforms of Rho-associated kinases (ROCK-1 and ROCK-2) are known (Nakagawa, et al., 1996). Both are downstream effectors of RhoA (ras homolog gene family, member A) (Leung, et al., 1996), which is a small guanosine triphosphate-binding protein mediating various cellular physiologic functions such as cell proliferation, migration, adhesion, apoptosis and contraction (Hidaka, et al., 2010).

The RhoA/ROCK pathway is probably implicated in the pathophysiology of diverse cardiovascular diseases (Noma, et al., 2006), including myocardial hypertrophy (Satoh, et al., 2003), hypertension (Uehata, et al., 1997), atherosclerosis (Mallat, et al., 2003), and ischaemia/reperfusion injury (Bao, et al., 2004). Especially ROCK-1 creates a direct link from RhoA to cell morphology through the phosphorylation of MLC. The ROCK activity in peripheral leukocytes can be assayed by western blot analysis using a specific antibody to phospho-myosin-binding subunit (MBS) on myosin light-chain phosphatase, which is a downstream target of ROCK (Hidaka, et al., 2010). ROCKs are also able to generate an amoeboid movement by causing the formation of actin stress fibres and focal adhesions (Sahai, et al., 2003).

During the western blot analysis of the mobility proteins, the expression of ROCK-1 was unaffected by F4.6.3 in HL-60 cells. F5.3.6.7 showed an inhibiting effect on ROCK-1, which completely disappeared after 2 hours of incubation. In contrast, cells treated with F4.6.3 still expressed ROCK-1. The pMLC2 expression was completely undetectable at all conditions tested. Thus, F5.3.6.7 may have the effect of decreasing

the mobility of HL-60 cells and therefore decreasing the chance for cancer cell invasivity.

MLC2: Myosin light chain kinase (MLCK) phosphorylates myosin light chain 2 (MLC2) at Thr18 and Ser19 in smooth muscle (Ikebe, et al., 1985), which results in myosin ATPase activity and smooth muscle contraction (Tan, et al., 1992). Also ROCK is able to phosphorylate Ser19 of smooth muscle MLC2, which regulates the assembly of stress fibres (Totsukawa, et al., 2000).

As described above, MLC2 was not phosphorylated by both fractions, which is an indicator for the absence of cell mobility.

MYPT1: MYPT1 (myosin-binding subunit of myosin phosphatase) is a subunit of the myosin phosphatase. In response to signals of the GTPase Rho it regulates the interaction of actin and myosin (Feng, et al., 1999). One signalling pathway leading to the inhibitory phosphorylation of MYPT1 is the Rho/Rho kinase pathway, in which the activated GTPase Rho binds to Rho kinase and in consequence activates the kinase (Matsui, et al., 1996). In consequence, the activated Rho kinase phosphorylates MYPT1 and thus inhibits the myosin phosphatase (Kimura, et al., 1996). Phosphorylation of MYPT1 is essential for motility, mitosis, apoptosis, and smooth muscle contractility (Vetterkind, et al., 2010). MYPT1 was slightly phosphorylated within 24 hours after incubation with F4.6.3. F5.3.6.7 suppressed constitutive MYPT1 phosphorylation after 8 hours of incubation. Thus the cell mobility indicator pMYPT1 and MYPT were decreased by F5.3.6.7 but not by F4.6.3. The data indicate that F5.3.6.7 contains an anti-invasive-activity.

4.2 *S. spinosa*

This chapter includes the results of *S. spinosa*. The following scheme is an overview of results of the fractionation processes of *S. spinosa*. Lyophilized leaves of *S. spinosa* were subjected to sequential extraction with five solvents of increasing polarity. The obtained extracts were investigated for their anti-carcinogenic potential in HL-60 cells. Proliferation and apoptosis assays were performed to identify the most promising extract which afterwards went through a detannification process. Furthermore the effects were studied in more detail by western blot analysis.

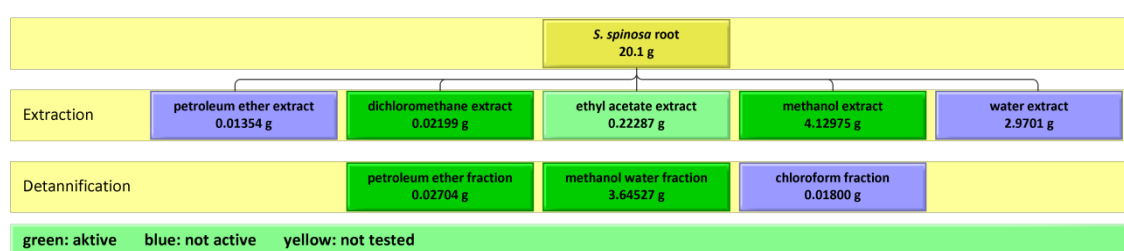


Figure 45 Fractionation steps overview

4.2.1 Extraction

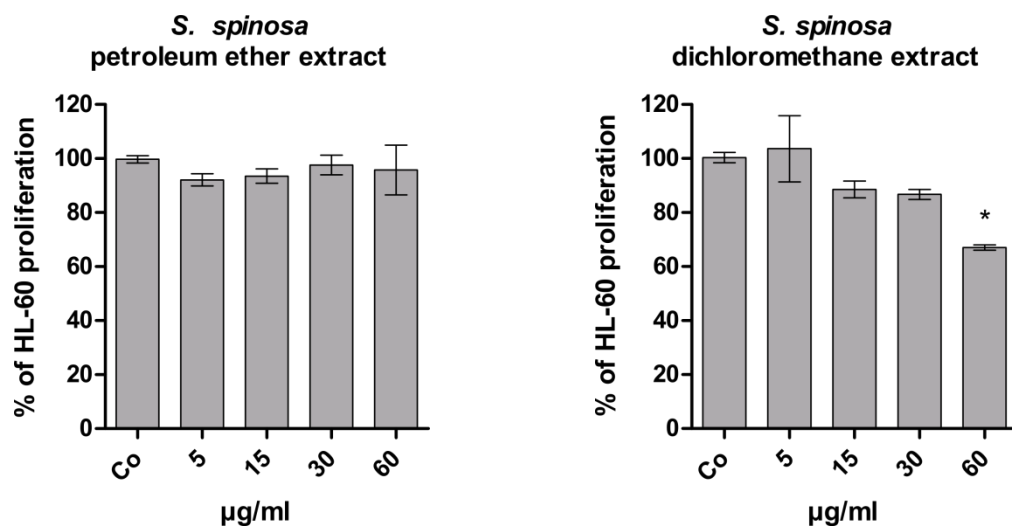
The root of *S. spinosa* was weighted before and after air drying. After air drying (625 g) the weight corresponded to 76.78 % of the weight before the drying process (814 g). Thus, air drying reduces the weight by 23.22 %. The extraction of *S. spinosa* was performed as described in chapter 3.4.1. The extract weights obtained from serial extraction of 20.1 g air dried root of *S. spinosa* with five solvents of increasing polarity are presented in Table 22. The table illustrates that the weight of the methanol extract corresponds to 20.55 % of dried plant.

Results

Table 22 Obtained amounts of extracts of *S. spinosa*

Solvent	Extract weight corresponding to 20.1 g dried plant (g)	Extract weight corresponding to 1 mg dried plant (μg)
Petroleum Ether	0.01354	0.6736
Dichloromethane	0.02199	1.0940
Ethyl acetate	0.22287	11.0881
Methanol	4.12975	205.4602
Water	2.9701	147.7662

To determine the anti-proliferative effects in HL-60 cells, extracts were applied with increasing concentrations (5 $\mu\text{g/ml}$, 10 $\mu\text{g/ml}$, 30 $\mu\text{g/ml}$, 60 $\mu\text{g/ml}$) for 24 and 72 hours. Results of the proliferation assay are presented in Figure 46. The methanol extract revealed a 45 % decrease in proliferation compared to the control and therefore was the most anti-proliferative extract of *S. spinosa*. Thus, values of the methanol extract were calculated in two more ways. In Figure 46 the 24 hours values were compared to the 72 hours values, whereas in Figure 47 the 24 hour values were compared to 48 hours values and in Figure 48 the 48 hour and 72 hours values were compared.



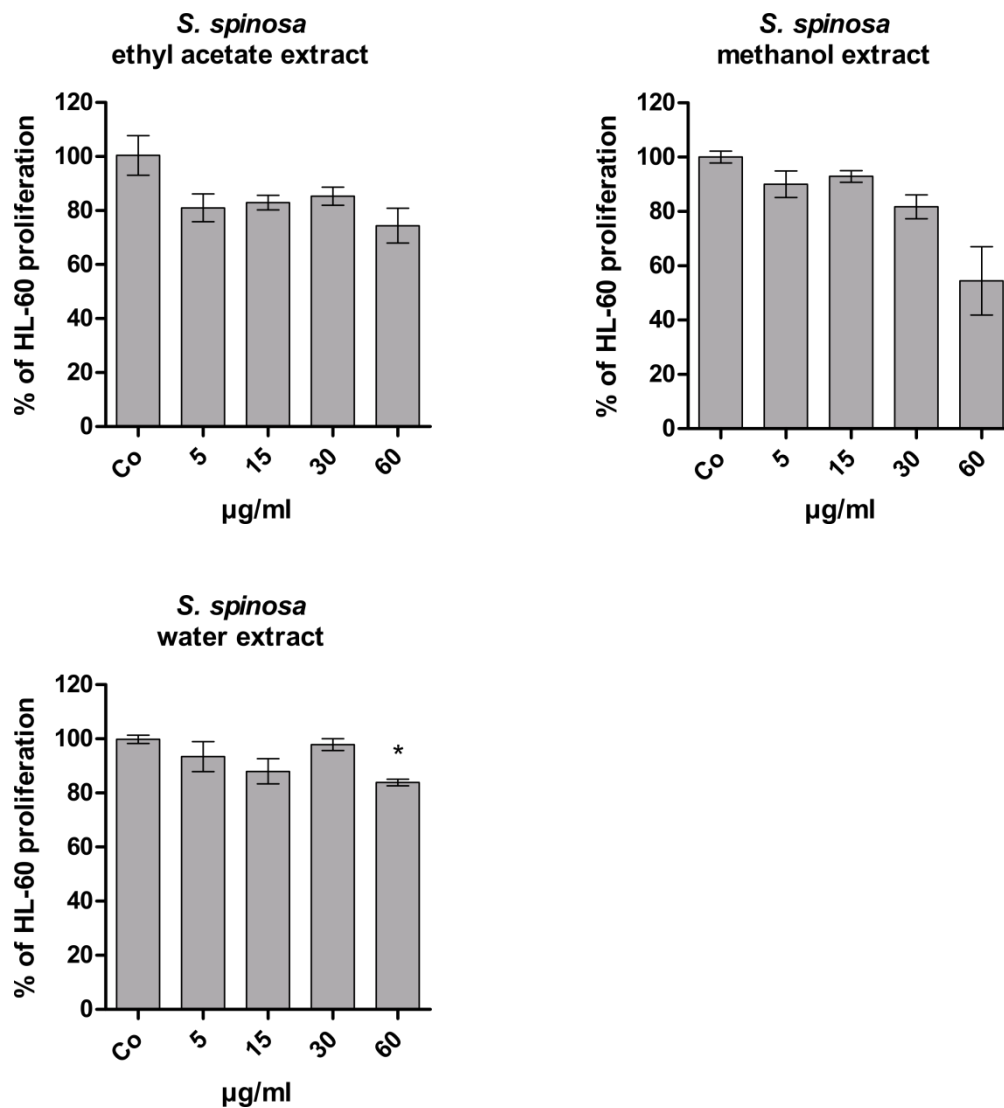


Figure 46 Anti-proliferative effect of extracts (petroleum ether, dichloromethane, ethyl acetate, methanol and water)

HL-60 cells were seeded into 24-well plate (1×10^5 cells/ml), incubated with 5, 15, 30 and 60 µg/ml of each extract for 72 hours. Cells were counted after 24 and 72 hours of treatment. The percentage of proliferation between 24 and 72 hours was determined in comparison to control. Experiments were performed in triplicate. Asterisks indicate significance compared to untreated control ($p < 0.05$) and error bars indicate \pm SD.

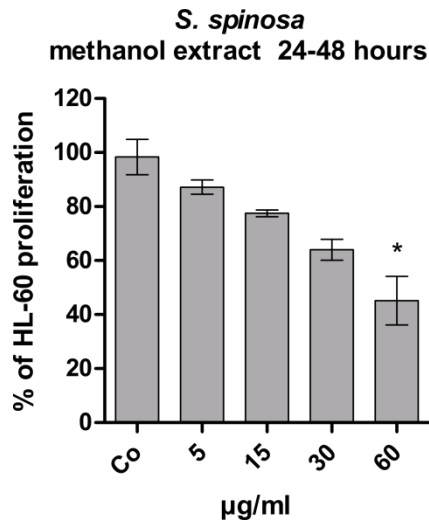


Figure 47 Anti-proliferative effect of methanol extract

HL-60 cells were seeded into 24-well plate (1×10^5 cells/ml), incubated with 5, 15, 30 and 60 µg/ml of the methanol extract for 48 hours. Cells were counted after 24 and 48 hours of treatment. The percentage of proliferation between 24 and 48 hours was determined in comparison to control. Experiments were performed in triplicate. Asterisks indicate significance compared to untreated control ($p < 0.05$) and error bars indicate \pm SD.

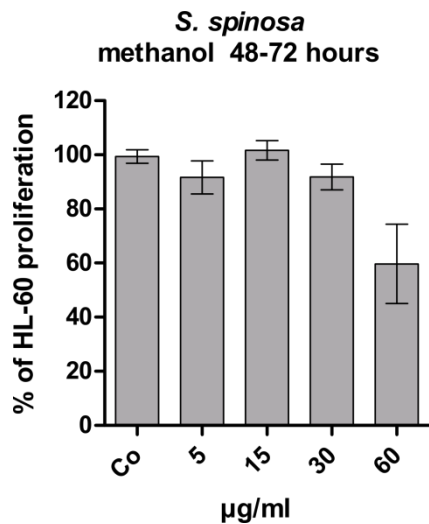


Figure 48 Anti-proliferative effect of methanol extract

HL-60 cells were seeded into 24-well plate (1×10^5 cells/ml), incubated with 5, 15, 30 and 60 µg/ml of the methanol extract for 72 hours. Cells were counted after 48 and 72 hours of treatment. The percentage of proliferation between 48 and 72 hours was determined in comparison to control. Experiments were performed in triplicate. Asterisks indicate significance compared to untreated control ($p < 0.05$) and error bars indicate \pm SD.

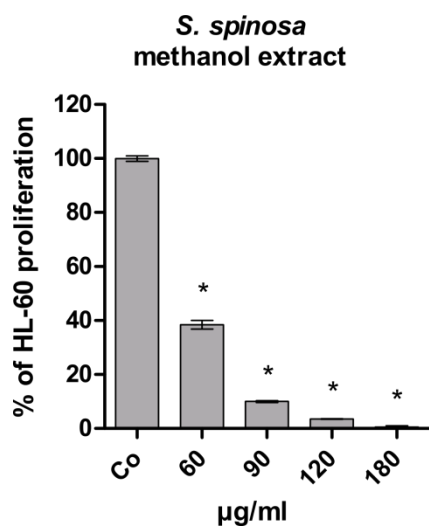


Figure 49 Anti-proliferative effect of methanol extract

HL-60 cells were seeded into 24-well plate (1×10^5 cells/ml), incubated with 60, 90, 120 and 180 µg/ml of the methanol extract for 72 hours. Cells were counted after 24 and 72 hours of treatment. The percentage of proliferation between 24 and 72 hours was determined in comparison to control. Experiments were performed in triplicate. Asterisks indicate significance compared to untreated control ($p < 0.05$) and error bars indicate \pm SD.

Figure 47 (24-48 h) illustrates a linear decrease of cells alive compared to the control over the time. Figure 48 does not show this linear effect, which leads to the assumption that the methanol extract mainly inhibited proliferation in the first 48 hours. Further the methanol extract was tested in higher concentrations (60 $\mu\text{g/ml}$, 90 $\mu\text{g/ml}$, 120 $\mu\text{g/ml}$, 180 $\mu\text{g/ml}$). As presented in Figure 49, the activity of the methanol extract increased in higher concentrations up to nearly 100 % in cells treated with 180 $\mu\text{g/ml}$ (24 and 72 hours values are compared in this figure). Still remaining that the methanol extract weighted almost one fifth of the whole lyophilized root substance, it was a promising plant concerning anti-carcinogenic activity.

Also, a cell death assay (apoptosis and necrosis) of the methanol extract in the concentrations of 60 $\mu\text{g/ml}$, 90 $\mu\text{g/ml}$ and 120 $\mu\text{g/ml}$ was performed. It is presented in Figure 50. An apoptosis rate of 70 % after 72 hours in the highest concentration (120 $\mu\text{g/ml}$) was measured. Therefore the methanol extract was subject of further analyses.

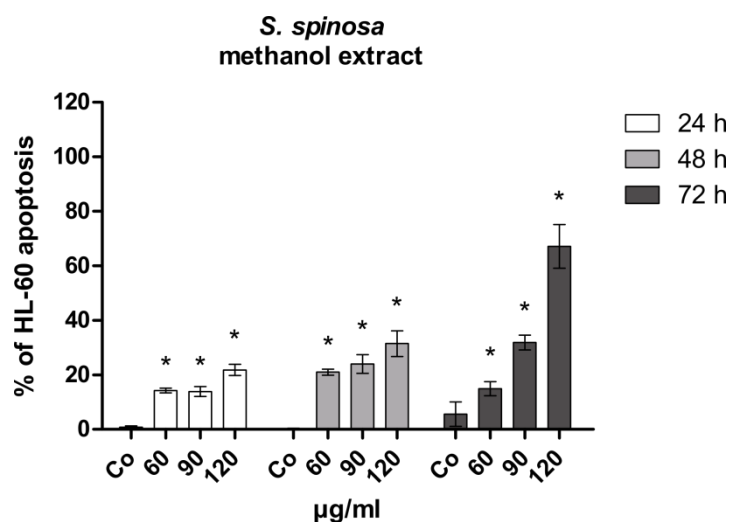


Figure 50 Induction of apoptosis by methanol extract

HL-60 cells were seeded in 24-well plates (1×10^5 cells/ml) and incubated with 60, 90 and 120 $\mu\text{g/ml}$ of each extract for 72 hours. Afterwards cells were double stained with Hoechst 33258 and propidium iodide and examined under the microscope with UV light connected to a DAPI filter. Nuclei with morphological changes which indicated apoptosis were counted and the percentage of apoptotic cells was calculated. Experiments were performed in triplicate. Asterisks indicate significance compared to untreated control ($p < 0.05$) and error bars indicate $\pm\text{SD}$.

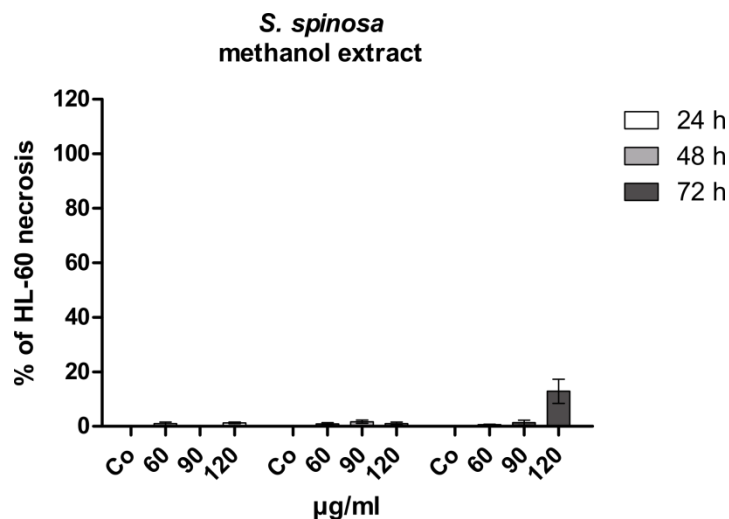


Figure 51 Induction of necrosis by methanol extract

HL-60 cells were seeded in 24-well plates (1×10^5 cells/ml) and incubated with 60, 90 and 120 $\mu\text{g/ml}$ of the methanol extract for 72 hours. Afterwards cells were double stained with Hoechst 33258 and propidium iodide and examined under the microscope with UV light connected to a DAPI filter. Nuclei with morphological changes which indicated necrosis were counted and the percentage of necrotic cells was calculated. Experiments were performed in triplicate. Asterisks indicate significance compared to untreated control ($p < 0.05$) and error bars indicate \pm SD.

4.2.2 Detannification

Detannification (separation of tannins) of methanol extract of *S. spinosa* was conducted as described in chapter 3.4.2. Approximately 10 % of the starting extract were lost during the process.

Table 23 Obtained amounts of fractions after detannification of the methanol extract

Fraction	Substances contained in the fraction	Amount
1 Petroleum ether	Chlorophyll, wax, resin, apolar substances	0.02704 g
2 Water-methanol	Tannins und polar substances	3.64527 g
3 Chloroform	All other substances soluble in chloroform	0.01800 g

The TLCs were performed with TLC system 6 (chloroform: methanol: water, 70:22:3.5). On the TLC (Figure 52), the petroleum ether extract from the beginning and the petroleum ether fraction from the detannification process seemed to contain almost the same substances. However, the substances only contained in the petroleum ether

fraction but not in the petroleum ether extract are probably reason for the increased activity of this fraction compared to the extract. Tannins should have washed out in with the water-methanol mixture, but are undetectable in this received fraction. In contrast, the water-methanol fraction contained active substances, which were actually expected to be found in the chloroform layer. Apparently the substances seemed to have almost the same polarity as the tannins which was the reason why they were washed out in the water-methanol mixture.

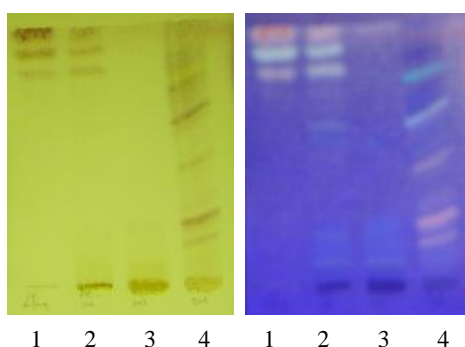


Figure 52 TLC of petroleum ether extract (1), petroleum ether fraction (2), water-methanol fraction (3) and chloroform fraction(4)
Mobile phase: TLC system 6
Detection: visible light with ASR (left), UV₃₆₆ with ASR (right)

A proliferation assay and an apoptosis assay were performed after the detannification process to measure the anti-carcinogenic activity. HL-60 cells were treated with 30 $\mu\text{g/ml}$ and 60 $\mu\text{g/ml}$ of each fraction achieved from the layers of the detannification process to measure the anti-proliferative activity and with 60 $\mu\text{g/ml}$, 90 $\mu\text{g/ml}$ and 120 $\mu\text{g/ml}$ to measure the apoptotic activity. In both experiments the cells were incubated for 24 and 48 hours. Figure 53 shows the highest decrease in proliferation in cells treated with fraction of the petroleum ether layer. It inhibited proliferation up to 40 % in the highest concentration (60 $\mu\text{g/ml}$) compared to the control, whereas the petroleum ether extract from the beginning did not show an anti-proliferative effect in HL-60 cells. Therefore the activity of the petroleum ether fraction resulted from the invisible substances on the TLC. In the apoptosis assay most apoptotic cells were counted in cells treated with fraction of the water-methanol layer, up to 95 % in the concentration of 120 $\mu\text{g/ml}$.

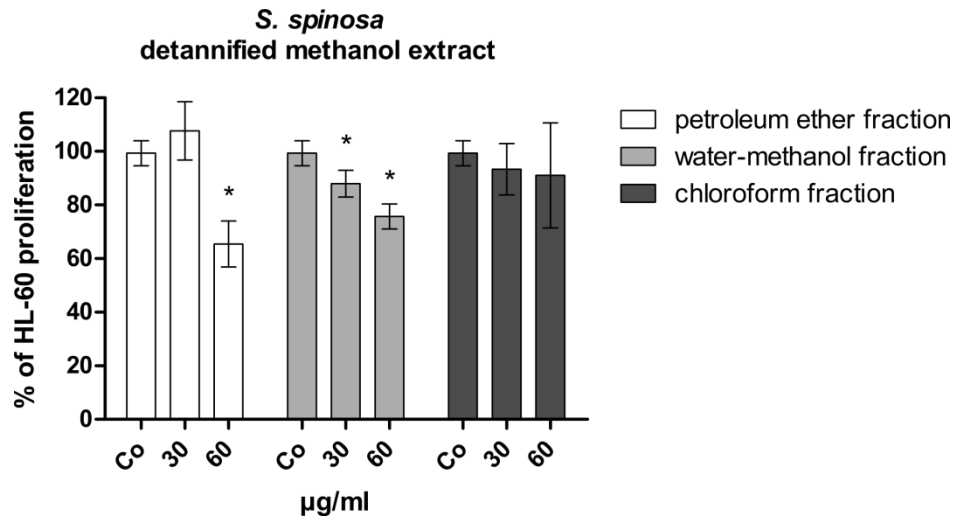
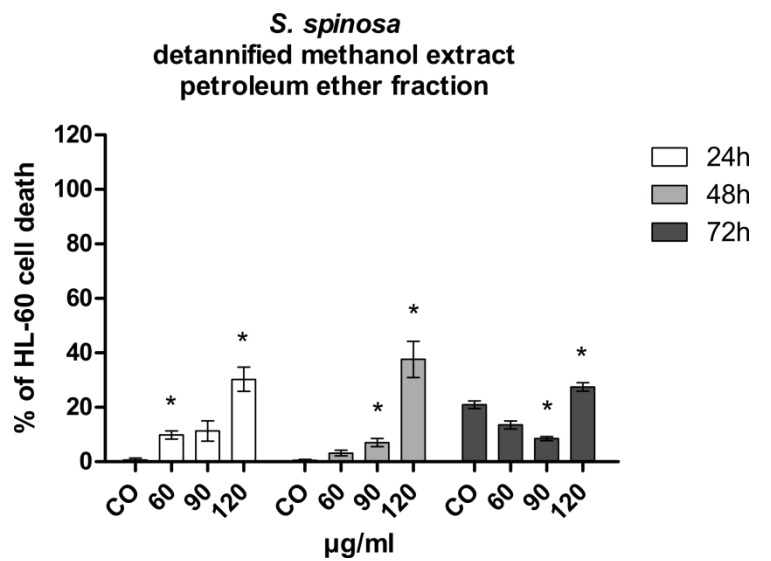


Figure 53 Proliferation assay of petroleum ether fraction, water-methanol fraction and chloroform fraction achieved from the detannification process
 HL-60 cells were seeded into 24-well plate (1×10^5 cells/ml), incubated with 30 and 60 $\mu\text{g/ml}$ of each fraction achieved from the detannification process for 48 hours. Cells were counted after 24 and 48 hours of treatment. The percentage of proliferation between 24 and 48 hours was determined in comparison to control. Experiments were performed in triplicate. Asterisks indicate significance compared to untreated control ($p < 0.05$) and error bars indicate \pm SD.



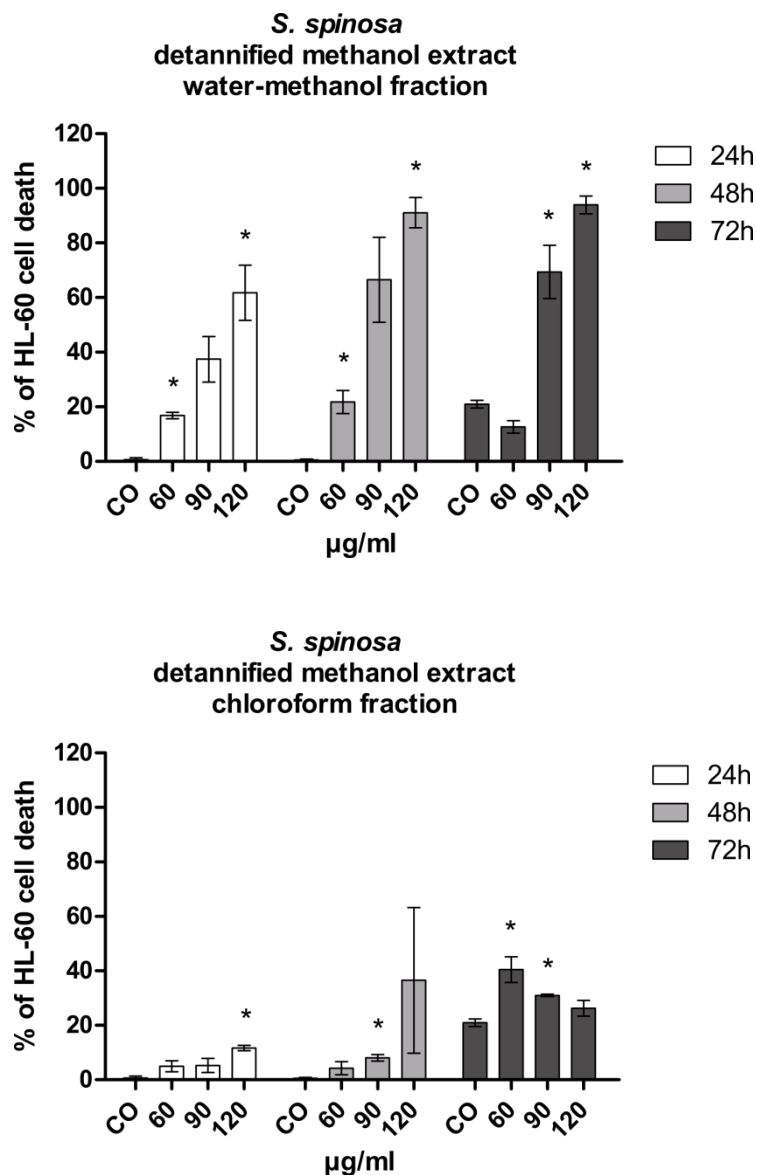


Figure 54 Induction of apoptosis by petroleum ether fraction, water-methanol fraction and chloroform fraction achieved from the detannification process

HL-60 cells were seeded in 24-well plates (1×10^5 cells/ml) and incubated with 60, 90 and 120 µg/ml of each extract for 48 hours. Afterwards cells were double stained with Hoechst 33258 and propidium iodide and examined under the microscope with UV light connected to a DAPI filter. Nuclei with morphological changes which indicated cell death were counted and the percentages of dead cells were calculated. Experiments were performed in triplicate. Asterisks indicate significance compared to untreated control ($p < 0.05$) and error bars indicate \pm SD.

4.2.3 Western Blot analysis

Western blot analyses were conducted with the most active fraction, the water-methanol fraction achieved from the detannification process of the methanol extract. The fraction showed a significant pro-apoptotic effect after 48 hours of about 90 % in HL-60 cells treated with 120 µg/ml. The anti-proliferative effect of the fraction was about 20 % in cells treated with 60 µg/ml for 48 hours. Proteins for the western blot analysis were chosen with a main focus on cytotoxic markers, cell cycle regulators, apoptosis inducers and oncogenes.

4.2.3.1 Analysis of the cell cycle and its checkpoint regulators

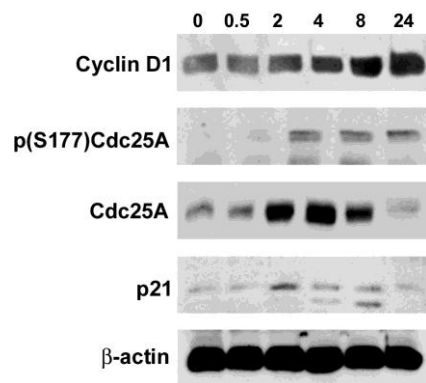


Figure 55 Analysis of cell cycle regulators HL-60 cells (1×10^6 cells/ml) were incubated with 120 µg/ml of the water-methanol fraction and harvested after 0.5, 2, 4, 8 and 24 h of treatment. Cells were lysed and obtained proteins samples applied to SDS-PAGE. Western blot analysis was conducted with the indicated antibodies. Equal sample loading was confirmed by Ponceau S staining and β-actin analysis

Cyclin D1: The proto-oncogene Cyclin D1 is necessary for the G1 to S phase transition as described in chapter 2.2.2. Cyclin D1 is involved in cell growth, metabolism, and cellular differentiation. Therefore an overexpression of Cyclin D1 plays a key role in the development of several cancers (Fu, et al., 2004). Cyclin D1 expression was clearly increased after 2 hours of treatment with the water-methanol fraction. This is indicative for cell cycle activation.

Cdc25A: Cdc25A is especially involved in G1-S transition. An inactivation of Cdc25A phosphatase (Kiyokawa, et al., 2008) causes the inactivation of Cyclin E-Cdk2. (Blomberg, et al., 1999). For further description see chapter 4.1.5.1. HL-60 cells treated with the *S. spinosa* water-methanol fraction caused a slight phosphorylation of Cdc25A at serine177, which was reported to trigger the recruitment of the proteasome and

consequently degradation of Cdc25A. This is an indicator for cell cycle arrest in the G1 phase (Madlener, et al., 2009) and stands in sharp contrast to Cyclin D1 up-regulation. Contradicting cell cycle signalling can be considered as pro-apoptotic condition.

P21: P21 is a Cdk-inhibitor protein. It silences the Cdk2/Cyclin E kinase, which normally triggers the G1-S transition. Thus p21 is thereby causing G1 arrest (Kastan, et al., 2004). Additionally, p21 binds to the Cdk4/Cyclin D complex. This results in a hypophosphorylation and activation of pRb and thereby suppression of the E2F pathway and cessation of the cell cycle (Meeran, et al., 2008). An important inducer of p21 transcription is p53, but this pathway is excluded because HL-60 cells are proven to be p53 deficient (Wolf, et al., 1985). P21 can also be regulated by p53-independent pathways (Abukhdeir, et al., 2008); its transcription for example can be regulated by the oncogene c-Myc (Coller, et al., 2000). During incubation of HL-60 cells with the *S. spinosa* extract, p21 was expressed at all times within the 24 hours of incubation. The peak of the expression was reached after 2 hours. The expression is an indicator for cell cycle arrest in G1 phase.

4.2.3.2 Analysis of apoptosis related proteins

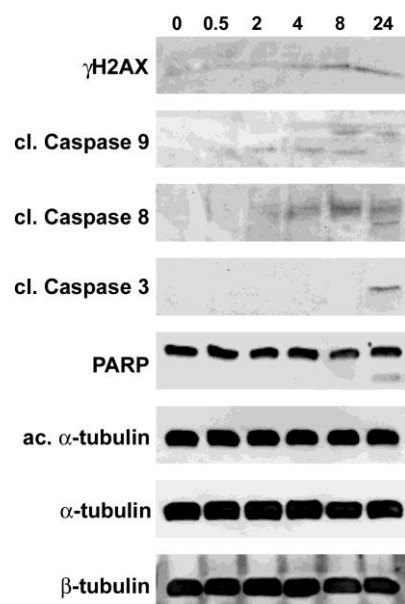


Figure 56 Analysis of apoptosis related proteins
HL-60 cells (1×10^6 cells/ml) were incubated with 120 $\mu\text{g/ml}$ of the water-methanol fraction and harvested after 0.5, 2, 4, 8 and 24 h of treatment. Cells were lysed and obtained proteins samples applied to SDS-PAGE. Western blot analysis was conducted with the indicated antibodies. Equal sample loading was confirmed by Ponceau S staining and β -tubulin analysis

γ H2AX: γ H2AX is the most commonly used and sensitive marker for detecting DNA-double-strand breaks (Paull, et al., 2000). During this experiment the phosphorylation of H2AX was induced after 8 and 24 hours.

Caspases: During the analysis of apoptosis related proteins, also cleaved caspase 3, 8 and 9 were analysed. For their function during apoptosis (see chapter 2.2.3 Evading apoptosis). The increased cleavage of caspase 9 was observed after 2 hours till 8 hours of incubation, whereas caspase 8 was cleaved after 4 hours till 24 hours of incubation with the *S. spinosa* extract. In result of caspase 8 and 9 cleavage, apoptosis inducing caspase 3 was activated after 24 hours.

PARP: Poly (Adenosine diphosphate (ADP)-ribose) polymerase (PARP) is activated by DNA strand breaks. It is a nuclear enzyme, which participated in DNA repair (Pieper, et al., 1999). During apoptosis, PARP is cleaved by caspase 3 into a 85 kDa fragment (Chang, et al., 2010). In HL-60 cells treated with the *S. spinosa* extract, the PARP cleavage occurred after 24 hours and thus exactly correlated with the cleavage and activation of caspase 3. Both protein cleavages are indicators of apoptosis. The data infer that the water-methanol fraction contains a genotoxic property, but caspase 9 (intrinsic apoptosis pathway) was activated by another mechanism, because it was cleaved before phosphorylation of H2AX.

α -tubulin: The water-methanol fraction induced a persistent acetylation of α -tubulin for the time of incubation, which implicates the stabilization of microtubules (Piperno, et al., 1987), which is incompatible with normal cell division and causes cell cycle arrest and apoptosis.

4.2.3.3 Analysis of oncogenes

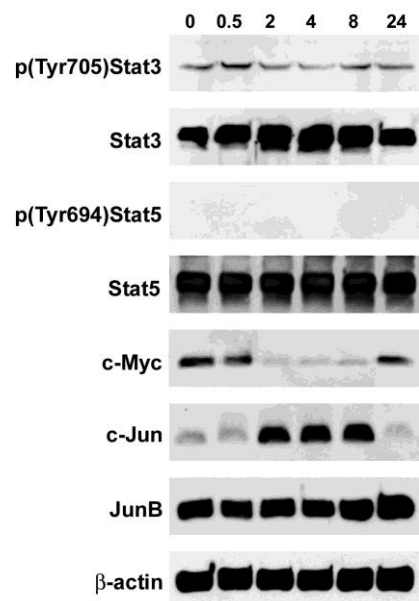


Figure 57 Analysis of oncogenes

HL-60 cells (1×10^6 cells/ml) were incubated with 120 $\mu\text{g/ml}$ of the water-methanol fraction and harvested after 0.5, 2, 4, 8 and 24 h of treatment. Cells were lysed and obtained proteins samples applied to SDS-PAGE. Western blot analysis was conducted with the indicated antibodies. Equal sample loading was confirmed by Ponceau S staining and β -actin analysis

Stat3: The Stat3 oncogene product is the most activated Stat protein in human cancers (Jackson, et al., 2009). Stat family proteins are transcription factors involved in normal and pathological cellular processes. Stat3 is especially included in cell cycle progression, apoptosis, angiogenesis and immune evasion (Grisko, et al., 2006). The activation of Stat3 leads to the prevention of apoptosis and increasing cell proliferation (Kanda, et al., 2004) and an overexpression of Stat3 was found in leukaemia, breast cancer, pancreatic cancer, prostatic cancer and melanoma. The phosphorylated Stat3 is able to migrate into the nucleus and to activate the transcription of target genes there (Deng, et al., 2010). In HL-60 cells treated with the extract of *S. spinosa*, the Stat3 phosphorylation decreased after 2 hours of incubation. Thus the oncogenic potential and the anti-apoptotic activity were decreased.

Stat5: Stat5 oncogene product is described to be activated by IL3 (Mui, et al., 1995) and to induce anti-apoptotic genes and cell proliferation (Gündogdu, et al., 2010). The Stat5 protein has a specific binding site on the Bcl-X promoter, and thus regulates Bcl-XL. Bcl-XL is known to be an anti-apoptotic protein which maintains cell survival under stresses such as genotoxic drugs (Jinawath, et al., 2010). In the experiment Stat5 was not phosphorylated at all when HL-60 cell were treated with the *S. spinosa* extract.

C-Myc: C-Myc is described to influence cell proliferation, differentiation and apoptosis (Dominguez-Sola, et al., 2007). An increase in c-Myc expression triggers an abnormal proliferation rate and is recognized in many tumor types. C-Myc is described in more detail in chapter 2.2.2 (Insensitivity to antigrowth signals). The expression of c-Myc is strongly suppressed by the extract of *S. spinosa* in HL-60 cells after 2 hours of incubation.

C-Jun, Jun B: C-Jun and junB are both products of the Jun family genes and components of the activating protein-1 transcription factor complexes. Those complexes are important in cell growth, differentiation, and neoplastic transformation. C-Jun and junB are usually promoting cell proliferation, but if activated, especially c-Jun is found to function in cell cycle progression and neoplastic transformation (Wang, et al., 2000). During incubation of HL-60 cells with the *S. spinosa* extract, c-Jun expression was immensely increased during the first 0.5 hours of treatment, whereas the junB expression stayed stable during the whole 24 hours of incubation. Thus the extract has an important impact on the de-regulation of various oncogenes: up-regulation of Cyclin D1 and c-Jun and down-regulation of Cdc25A, Stat3, c-Myc, as well as the up-regulation of the tumor suppressor p21.

5 Conclusion

In the present work the anti-neoplastic activity of the dichloromethane extract from aerial parts of *P. odorata*, and of extracts of the *S. spinosa* root was investigated. The two plants are ethnomedical healing remedies used especially against inflammation by the Maya.

5.1 *P. odorata*

We started the *P. odorata* investigation with the bio-assay guided fractionation of the dichloromethane extract, which was already examined by Gridling et al. (2009) and Bauer et al. (2010), who both discovered a strong anti-neoplastic activity in some of the extracts and fractions. The current bio-assay guided fractionation indicated that the apoptotic activity of the plant was induced by highly apolar components, matching the outcome of the investigation conducted by Bauer et al. (2010), who investigated especially the anti-proliferative effect of the apolar dichloromethane extract.

Interestingly the highest anti-neoplastic activity was found in two fractions (F4.6.3 and F5.3.6.7), containing different compounds. Four respectively five fractionation steps, including vacuum liquid chromatography (VLC) and column chromatography (CC), had to be performed to achieve the two most active fractions. In between the fractionation steps, especially apoptosis assays, but also proliferation assays were performed to detect the most promising fractions for further fractionation processes. HL-60 cells treated with 10 µg/ml of F4.6.3 and F5.3.6.7 for 48 hours showed an almost a 100 % and 90 % apoptotic rate, respectively.

The analysis of the cell cycle proteins Chk2 and Cdc25A revealed a weak phosphorylation of Chk2 and the phosphorylation of Cdc25A serine 177 by F4.6.3, whereas F5.3.6.7 de-phosphorylated Cdc25A at the amino acid. The phosphorylation of serine 177 of Cdc25A is known to promote the degradation of Cdc25A by the proteasome. Cdc25A is required for the activation of the CyclinE/Cdk2 complex, which is needed for the transition of the G1-S phase of the cell cycle (Blomberg, et al., 1999). However, for unknown reasons, Cdc25A was even up-regulated by F4.6.3, despite

induction of serine 177 phosphorylation. In contrast, F5.3.6.7 de-phosphorylated serine 177 and this was in accordance with moderate Cdc25A stabilization (up-regulation). Taking together, the expression of pChk2 and pCdc25A varied between both fractions, which indicated that different bio-active compounds were contained in F4.6.3 and F5.3.6.7. F4.6.3 included compounds for causing the early (yet weak) phosphorylation of Chk2 and transient phosphorylation of Cdc25A. In contrast, upon treatment with the more apolar fraction F5.3.6.7 the phosphorylation of Chk2 occurred later, but the inhibiting (degrading) phosphorylation of Cdc25A was blocked in HL-60 cells.

Regarding apoptosis related proteins the two extracts did not differ too much. γ H2AX was activated by both extracts, although stronger in cells treated with F4.6.3, indicating DNA-double-strand breaks in both cases. This was not due to genotoxicity (Paull, et al., 2000), but correlated with caspase 3 and concomitant apoptotic signature type DNA fragmentation. Even caspase 3 was activated differently by the two extracts. F5.3.6.7 led to the cleavage of caspase 3 first and afterwards induced an activation of caspase 8 and 9. In contrast, F4.6.3 induced the activation of the caspase cascade by both ways, the extrinsic by activation of caspase 8 leading to an activation of caspase 3 and the intrinsic apoptotic pathway by activation of caspase 9 also resulting in the activation of caspase 3, which in the end induces apoptosis (Stewart, et al., 2003). The acetylation of α -tubulin, which implicates the stabilization of microtubules (Piperno, et al., 1987) and therefore cell cycle arrest and most likely apoptosis, was increased by both extracts, but was earlier decreased by F5.3.6.7.

Markers of cell mobility, which is a hallmark property for the invasive/metastatic potential of cancer cells, were decreased by F5.3.6.7, whereas increased by F4.6.3. Regarding paxillin, a key regulator of cell migration (Paulitschke, et al., 2010), F5.3.6.7 did not induce this protein to a level observed by exposure to F4.6.3, which strongly increased the paxillin expression after 2 hours of incubation and which persisted thereafter at somewhat reduced level.

The effects on cell mobility by F4.6.3 and F5.3.6.7 are also recognized by the expression of ROCK-1, which is known to be generating an amoeboid movement (Sahai, et al., 2003) and therefore being able to promote metastasis. F5.3.6.7 led to a quick inhibition of the ROCK-1 expression, whereas cells treated with F4.6.3 still

slightly expressed ROCK-1 for the duration of incubation. But pMLC2, which is phosphorylated by ROCK-1, was not phosphorylated by both fractions. MYPT was only slightly constitutively phosphorylated and F5.3.6.7 led to a complete inhibition of the phosphorylation. Even the total MYPT protein expression was down-regulated by F5.3.6.7, whereas F4.6.3 affected neither phosphorylation nor protein expression. Therefore, F5.3.6.7 positively influenced paxillin, ROCK-1, pMLC2 and pMYPT1 expression and activity, whereas F4.6.3 did not exhibit such an activity.

Summing up, two fractions of the dichloromethane extract of *P. odorata* have pro-apoptotic, anti-proliferative and anti-metastatic effects on HL-60 cells, with a more mobility decreasing activity in F5.3.6.7.

5.2 *S. spinosa*

The investigation of the root of *S. spinosa* started with the extraction by using solvents of increasing polarity. Afterwards the extracts were tested in proliferation and apoptosis assays. The methanol extract was detected to be the most active extract by decreasing cell proliferation by 90 % in the concentration of 90 µg/ml and apoptosis by 70 % in the concentration of 120µg/ml, after 72 hours of incubation. Tannins that may have contaminated the methanol extract were tried to be separated from the extract. From the detannification process three different layers of solvents (fractions) were received, but no tannins were visually detected in the separated fractions. The most active compounds were found in the water-methanol fraction, where also the tannins were expected but not observed. The fraction obtained from the water-methanol layer, inhibited proliferation up to 40 % in the concentration of 60 µg/ml and induced apoptosis up to 95 % in the concentration of 120 µg/ml after 48 hours of incubation, and therefore was the most active fraction after the detannification process.

The water-methanol fraction increased the expression of the cell cycle protagonists Cyclin D1 and Cdc25A and also increased the phosphorylation of Cdc25A, which resulted in the decrease of Cdc25A protein after 24 hours. P21, a tumor suppressor protein, which silences the Cdk2/Cyclin E kinase resulting in the inhibition of G1-S transition (Kastan et al., 2004), was up-regulated by the water-methanol fraction. Thus,

these are all indicators that this fraction caused cell cycle disturbances leading to growth arrest.

Besides cell cycle arrest, the fraction was also figured out to promote apoptosis by a genotoxic mechanism as γ H2AX levels, a marker for DNA-double strand breaks (Paull, et al., 2000), was increased concomitant or before the activation of caspase 3. The caspase cascade i.e. cleaving of caspase 9 and 8, which both result in cleavage of caspase 3 and in addition leading to apoptosis (Stewart, et al., 2003) and the cleavage of PARP in the late stage (Chang, et al., 2010), suggested that the fraction induced the intrinsic pathway. The cleavage of PARP is known as an indicator for apoptosis.

Also the activity of the transcription factor Stat3 was down-regulated by the investigated *S. spinosa* fraction, which decreases the anti-apoptotic potential of the cancer cells. Besides this, the water-methanol fraction strongly suppressed the expression of the oncogene c-Myc and which has an impact on abnormal cell-proliferation.

In summary, the water-methanol fraction of *S. spinosa* had a positive impact on HL-60 cells, especially regarding the inactivation of oncogenesis, but was also acting pro-apoptotic and decreased cell-proliferation.

6 Summary

The facts that one out of three persons is affected by cancer during their lifetime (Pecorino, 2008) and that more than 50 % of them die from the disease (Stewart, et al., 2003) show that there is a substantial need for anti-cancer drugs.

Plants have been a source of effective drugs for the treatment of cancers, and generally over 60 % of anti-cancer drugs originate from natural sources (Cragg, et al., 2005). For this reason two ethnomedical plants, used by the Mayas of Guatemala, were investigated towards their anti-neoplastic activity. Ethnomedical plants have a large impact in cancer research, because those natural products have been administered as a therapy against several diseases for hundreds of years (Shoeb, 2006). The two plants investigated in this study, *P. odorata* and *S. spinosa*, are originally used against inflammation. Reason for the investigation of plants with anti-inflammatory effects is that both, inflammation and cancer up-regulate similar signalling pathways (Kundu, et al., 2008). The dichloromethane extract of *P. odorata* is already known to contain an anti-neoplastic activity, as described by Gridling et al. (2009) and Bauer et al. (2010). Therefore the bio-assay guided fractionation of *P. odorata* started with the dichloromethane extract. After four, respectively five steps of fractionation using vacuum liquid chromatography or column chromatography with in-between testing the pro-apoptotic and anti-proliferative effect on HL-60 cells, the fractionation process resulted in two very active fractions; F4.6.3 and F5.3.6.7. The two fractions were then further analysed by western blot analysis with focus on cytotoxic effects. In the concentration of 10 µg/ml both fractions had strong cytotoxic effects. F4.6.3 induced apoptosis by 100 % in HL-60 cells after 48 hours; F5.3.6.7 induced an apoptosis rate of 90 %. The western blot analysis revealed that F4.6.3 was the fraction with the stronger γ H2AX activation, indicating DNA-double-strand breaks. For this reason the fraction showed also the activation of the caspase cascade and inhibition of the cell cycle progression by phosphorylation of Chk2 and Cdc25A. In contrast, F5.3.6.7 had a stronger impact on the cell mobility proteins like decreasing the expression of paxillin and ROCK-1. This and the complete inhibition of pMYPT are indicative for decreased cell mobility, decreasing the chance for metastasis.

The air-dried root of the second ethnomedical plant from Guatemala, *S. spinosa*, was first milled and then extracted by solvents with increasing polarity. Afterwards proliferation and apoptosis assays were conducted. The most active extract, the methanol extract was then subjected to detannification. The anti-proliferative and pro-apoptotic activity was found in the water-methanol layer, which should also include the tannins that however have not been detectible. The extract inhibited proliferation up to 40 % in the concentration of 60 µg/ml and induced apoptosis up to 95 % in the concentration of 120 µg/ml after 48 hours of incubation. Proteins relating cell cycle progression, apoptosis and oncoproteins were investigated by western blotting. The fraction especially had a great impact on oncogenes. It decreased pStat3 as well as c-Myc, which are all indicators for abnormal cell growth. Further the water-methanol fraction led to cell cycle disturbances leading to growth arrest by decreasing the expression of Cdc25A after 24 hours and increasing the level of p(Ser177)Cdc25A and p21. Apoptosis indicating proteins like γ H2AX and the caspase cascade including caspase 8, 9 and in the end the cleavage of caspase 3, which itself results in a PARP cleavage were up-regulated by the extract of *S. spinosa*.

In summary, both investigated plants clearly showed anti-neoplastic effects on HL-60 cells, and therefore confirm that ethnomedical plants, used against inflammation for hundreds of years are suitable to discover novel anti-cancer drugs.

7 Zusammenfassung

Während des Lebens erkrankt durchschnittlich eine von drei Personen an Krebs (Pecorino, 2008) und mehr als 50 % der betroffenen Personen sterben an der Krankheit (Stewart, et al., 2003). Allein diese beiden Fakten zeigen die große Notwendigkeit für Medikamente gegen Krebs auf.

60 % der Medikamente zur Tumorbehandlung stammen von Pflanzen ab, womit Pflanzen eine wichtige Grundlage für die Entwicklung dieser Medikamente bilden (Cragg, et al., 2005). Aus diesem Grund wurden die zwei ethnomedizinischen Pflanzen, die von den Maya in Guatemala verwendet werden, auf ihre anti-neoplastische Wirkung hin untersucht. Ethnomedizinische Pflanzen sind deshalb so wichtig in der Krebsforschung, da diese Pflanzen über Jahrhunderte hinweg gegen verschiedene Krankheiten verwendet wurden (Shoeb, 2006). Die zwei in dieser Studie untersuchten Pflanzen, *P. odorata* and *S. spinosa*, wurden ausgewählt, da sie ursprünglich zur Behandlung von Entzündungen verwendet wurden und bei Entzündungen und Krebs ähnliche Signalwege angesprochen werden (Kundu, et al., 2008).

Das Dichlormethan-Extrakt der *P. odorata* ist bekannt dafür anti-neoplastisch zu wirken, wie Gridling et al. (2009) und Bauer et al. (2010) bereits beschrieben. Deshalb wurde die „Bio-Assay Guided Fractionation“ der *P. odorata* mit dem Dichlormethan-Extrakt begonnen. Nach vier bzw. fünf Fraktionierungsschritten mit Vakuum-Flüssigkeitschromatographie bzw. normaler Säulenchromatographie, wurden zwei sehr aktive Fraktionen erhalten; F4.6.3 und F5.3.6.7. Zwischen den jeweiligen Fraktionierungsschritten wurde die pro-apoptotische und anti-proliferative Aktivität der Fraktionen an HL-60 Zellen getestet. Die zytotoxischen Effekte dieser zwei Fraktionen waren erheblich, in der Konzentration von 10 µg/ml rief F4.6.3 nach 48 Stunden eine Apoptoserate von 100 % in HL-60 Zellen hervor, F5.3.6.7 von 90 %. Mittels Western Blots wurden diese Effekte weiter analysiert. Hier zeigte F4.6.3 einen etwas stärkeren Effekt auf die γ H2AX Aktivierung, welche auf eine höhere Anzahl an DNA-Doppelstrangbrüchen hinweist. Als Konsequenz wurde die Caspase-Kaskade in Gang gesetzt, und der Zellzyklus durch die Phosphorylierung von Chk2 und Cdc2A angehalten. Im Gegensatz zu F4.6.3 zeigte F5.3.6.7 einen größeren Einfluss auf

Mobilitätsproteine. F5.3.6.7 verminderte die Expression von Paxillin und ROCK-1 und hemmte die Phosphorylierung von MYPT, welche allesamt für eine Einschränkung der Zellmobilität stehen und damit den Weg für eine Metastasierung erschweren.

Die getrocknete Wurzel der zweiten ethnomedizinischen Pflanze, *S. spinosa*, wurde zuerst gemahlen und anschließend mit Lösungsmitteln mit steigender Polarität extrahiert. Danach wurden Proliferations- und Apoptose-Assays durchgeführt und das aktivste Extrakt - das Methanol-Extrakt - einer Detannifizierung unterzogen. Nach dem Detannifizierungs-Prozess war die anti-neoplastische Aktivität in der Wasser-Methanol-Fraktion zu finden, in welcher auch die Tannine enthalten sein sollten. Die Tannine konnten jedoch nicht detektiert werden. Die Proliferation von HL-60 Zellen wurde durch die neu erhaltene Wasser-Methanol-Fraktion nach 48 Stunden in einer Konzentration von 60 µg/ml um 40 % gehemmt. Apoptose wurde in der Konzentration von 120 µg/ml nach 48 Stunden in 95 % der HL-60 Zellen induziert. Auf Grund dieses Ergebnisses wurden Onkoproteine, bzw. Proteine die am Zellzyklus oder der Apoptose beteiligt sind, mittels Western Blots näher untersucht. Die Fraktion hatte vor allem großen Einfluss auf Onkogene wie beispielsweise Stat3 und c-Myc. Die Phosphorylierung von Stat3 wurde durch die Wasser-Methanol-Fraktion vermindert, ebenso wie die c-Myc-Expression, welche beide als Indikatoren für abnormales Zellwachstum bekannt sind. Außerdem führte die Fraktion zu Unterbrechungen des Zellzyklus durch verminderte Expression von Cdc25A nach 24 Stunden und erhöhte Expression von p(Ser177)Cdc25A und p21. Ebenfalls wurden Indikatoren für Apoptose durch die Fraktion von *S. spinosa* beeinflusst. Die γ H2AX Expression stieg und zusätzlich wurde die Caspase-Kaskade in Gang gesetzt, bei der es durch Aktivierung von Caspase 8 und 9 zur Spaltung von Caspase 3 kommt. Caspase 3 ist bekannt für die Induktion von Apoptose und für die Aktivierung von PARP, welches ebenfalls ein Apoptose Indikator ist.

Zusammenfassend kann gesagt werden, dass beide untersuchten Pflanzen deutliche anti-neoplastische Effekte in HL-60 Zellen zeigten und deshalb untermauern, dass ethnomedizinische Pflanzen, die seit Jahrhunderten als Medikament gegen Entzündung in Verwendung sind, eine gute Grundlage für die Forschung nach neuen Krebsmedikamenten bilden.

8 References

- Abukhdeir, A M and Park, B H. 2008.** P21 and p27: roles in carcinogenesis and drug resistanc. *Expert Rev Mol Med.* July 1, 2008, 10, p. e19.
- Alam, M I and Gomes, A. 1998.** Adjuvant effects and antiserum action potentiation by a (herbal) compound 2-hydroxy-4-methoxy benzoic acid isolated from the root extract of the Indian medicinal plant 'sarsaparilla' (Hemidesmus indicus R. Br.). *Toxicon.* October 1998, 36(10), pp. 1423-1431.
- Arvigo, R and Balick, M. 1994.** *Die Medizin des Regenwaldes. Heilende Kräfte der Maya-Medizin. Die 100 heilenden Kräuter von Belize.* Aitrag : Windpferd Verlagsgesellschaft mbH, 1994. pp. 185-187.
- . **1998.** *Rainforest Remedies. One Hundred Healing Herbs of Belize.* second edition. Twin Lakes WI : Lotus Press, 1998. pp. 72-73.
- Ashkenazi, A and Dixit, V M. 1999.** Apoptosis control by death and decoy receptors. *Curr Opin Biol.* April 1999, 11(2), pp. 255-260.
- Balick, M and Lee, R. 2005.** Inflammation and ethnomedicine: looking to our past. *Explore (NY).* September 2005, 1(5), pp. 389-392.
- Bao, W, et al. 2004.** Inhibition of Rho-kinase protects the heart against ischemia/reperfusion injury. *Cardiovasc Res.* February 15, 2004, 61(3), pp. 548-558.
- Bauer, S, et al. 2010.** Separation of anti-neoplastic activities by fractionation of a *Pluchea odorata* extract. 2010.
- Blomberg, I and Hoffmann, I. 1999.** Ectopic expression of Cdc25A accelerates the G(1)/S transition and leads to premature activation of cyclin E- and cyclin A-dependent kinases. *Mol Cell Biol.* September 1999, 19(9), pp. 6183-6194.
- Burcham, P C. 1999.** Internal hazards: baseline DNA damage by endogenous products of normal metabolism. *Mutat Res.* July 15, 1999, 443, pp. 11-36.
- Butt, A J, Firth, S M and Baxter, R C. 1999.** The IGF axis and programmed cell death. *Immunol Cell Biol.* June 1999, 77(3), pp. 256-262.
- Caceres, A, et al. 1990.** Plants used in Guatemala for the treatment of gastrointestinal disorders. 1. Screening of 84 plants against enterobacteria. *J Ethnopharmacol.* August 1990, 30(1), pp. 55-73.

- Cantley, L C and Neel, B G. 1999.** New insights into tumor suppression: PTEN suppresses tumor formation by restraining the phosphoinositide 3-kinase/AKT pathway. *Proc Natl Acad Sci USA*. April 13, 1999, 96(8), pp. 4240-4245.
- Chang, C, et al. 2010.** Involvement of mitochondrial pathway in NCTD-induced cytotoxicity in human hepG2 cells. *J Exp Clin Cancer Res*. November 9, 2010, 29, p. 145.
- Christofori, G and Semb, H. 1999.** The role of the cell-adhesion molecule E-cadherin as a tumour-suppressor gene. *Trends Biochem Sci*. February 1999, 24(2), pp. 73-76.
- Coller, H A, et al. 2000.** Expression analysis with oligonucleotide microarrays reveals that MYC regulates genes involved in growth, cell cycle, signaling, and adhesion. *Proc Natl Sci USA*. March 28, 2000, 97(7), pp. 3260-3265.
- Counter, C M, et al. 1992.** Telomere shortening associated with chromosome instability is arrested in immortal cells which express telomerase activity. *EMBO J*. May 1992, 11(5), pp. 1921-1929.
- Cragg, G M and Newman, D J. 2005.** Plants as a source of anti-cancer agents. *J Ethnopharmacol*. August 22, 2005, 100(1-2), pp. 72-79.
- Cragg, G M, Newman, D J and Snader, K M. 1997.** Natural products in drug discovery and development. *J Nat Prod*. January 1997, 60(1), pp. 52-60.
- Cseke, L J, et al. 2006.** *Natural products from plants*. second edition. Boca Raton : CRC Press, 2006.
- Datto, M B, et al. 1997.** The viral oncoprotein E1A blocks transforming growth factor beta-mediated induction of p21/WAF1/Cip1 and p15/INK4B. *Mol Cell Biol*. April, 1997, 17(4), pp. 2030-2037.
- Davis, D L, et al. 1993.** Medical hypothesis: xenoestrogens as preventable causes of breast cancer. *Environ Health Perspect*. October 1993, 101(5), pp. 372-377.
- Deakin, N O and Turner, C E. 2008.** Paxillin comes of age. *J Cell Sci*. August 1, 2008, 121(Pt 15), pp. 2435-2444.
- Deng, J Y, et al. 2010.** Stat-3 correlates with lymph node metastasis and cell survival in gastric cancer. *World J Gastroenterol*. November 14, 2010, 16(42), pp. 5380-5387.
- Dominguez-Sola, D, et al. 2007.** Non-transcriptional control of DNA replication by c-Myc. *Nature*. July 26, 2007, 448(7152), pp. 445-451.

- Downward, J. 1998.** Mechanisms and consequences of activation of protein kinase B/Akt. *Curr Opin Cell Biol.* April 1998, 10(2), pp. 262-267.
- Evan, G and Littlewood, T. 1998.** A matter of life and cell death. *Science.* August 28, 1998, 281(5381), pp. 1317-1322.
- Fabricant, D S and Farnsworth, N R. 2001.** The Value of Plants Used in Traditional Medicine for Drug Discovery. *Environ Health Perspect.* March 2001, 109(1), pp. 69-75. Review.
- Feng, J, et al. 1999.** Inhibitory phosphorylation site for Rho-associated kinase on smooth muscle myosin phosphatase. *J Biol Chem.* December 24, 1999, 274(52), pp. 37385-37390.
- Fidler, I J and Ellis, L M. 1994.** The implications of angiogenesis for the biology and therapy of cancer metastasis. *Cell.* October 21, 1994, 79(2), pp. 185-188.
- Flood, D M, et al. 2000.** Colorectal cancer incidence in Asian migrants to the United States and their descendants. *Cancer Causes Control.* May 2000, 11(5), pp. 403-411.
- Foley, K P and Eisenman, R N. 1999.** Two MAD tails: what the recent knockouts of Mad1 and Mx1 tell us about the MYC/MAX/MAD network. *Biochim Biophys.* 1999, 1423(3), pp. 37-47.
- Folkman, J. 1995.** Clinical Applications of Research on Angiogenesis. *N Engl J Med.* December 28, 1995, 333, pp. 1757-1763.
- Foulds, L. 1969.** Neoplastic Development. [ed.] Academic Press. *Science.* April 3, 1969, pp. 106-107.
- Freireich, E J and Lemak, N. 1991.** *Milestones in Leukemia Research and Therapy.* s.l. : Johns Hopkins University Press, 1991.
- Fu, M, et al. 2004.** Minireview: Cyclin D1: normal and abnormal functions. *Endocrinology.* December 2004, 145(12), pp. 5439-5447.
- Fynan, T M and Reiss, M. 1993.** Resistance to inhibition of cell growth by transforming growth factor-beta and its role in oncogenesis. *Crit Rev Oncog.* 1993, 4(5), pp. 493-540.
- Green, D R and Reed, J C. 1998.** Mitochondria and apoptosis. *Science.* August 28, 1998, 281(5381), pp. 1309-1312.

- GRIN Germplasm Resources Information Network. 2004.** [Online] USDA United States Department of Agriculture, 9 November 2004. [Cited: 30 November 2010.] <http://www.ars-grin.gov/cgi-bin/npgs/html/taxon.pl?104497>.
- Grindling, M, et al. 2009.** In vitro anti-cancer activity of two ethno-pharmacological healing plants from Guatemala *Pluchea odorata* and *Phlebodium decumanum*. *Int J Oncol.* April 2009, 34(4), pp. 1117-1128.
- Grisko, T, et al. 2006.** Persistent activation of stat3 signaling induces survivin gene expression and confers resistance to apoptosis in human breast cancer cells. *Clin Cancer Res.* January 1, 2006, 12(1), pp. 11-19.
- Gross, A, McDonnell, J M and Korsmeyer, S J. 1999.** BCL-2 family members and the mitochondria in apoptosis. *Genes Dev.* August 1, 1999, 13(15), pp. 1899-1911.
- Guengerich, F Peter. 2000.** Metabolism of chemical carcinogens. *Carcinogenesis.* 2000, 21(3), pp. 345-351.
- Gündogdu, M S, et al. 2010.** The haematopoietic GTPase RhoH modulates IL3 signalling through regulation of Stat activity and IL3 receptor expression. *Mol Cancer.* August 25, 2010, 9, p. 225.
- Gupta, R A and DuBois, R N. 2001.** Colorectal cancer prevention and treatment by inhibition of cyclooxygenase-2. *Nature Reviews Cancer.* October 2001, 1(1), pp. 11-21.
- Hanahan, D and Weinberg, R A. 2000.** The Hallmarks of Cancer. *Cell.* January 7, 2000, pp. 57-70. Review.
- Harris, C C. 1996.** p53 tumor suppressor gene: from the basic research laboratory to the clinic-an abridged historical perspective. *Carcinogenesis.* June 1996, 17(6), pp. 1187-1198.
- Hidaka, T, et al. 2010.** Increased leukocyte rho kinase (ROCK) activity and endothelial dysfunction in cigarette smokers. *Hypertens Res.* April 2010, 33(4), pp. 354-359.
- Hunter, T. 1997.** Oncoprotein networks. *Cell.* February 7, 1997, 88(3), pp. 333-346.
- IABIN Red Interamericana de Información sobre Biodiversidad. 2010.** [Online] IABINs Species and Specimen Thematic Network (SSTN), 2010. [Cited: 30 November 2010.] <http://ara.inbio.ac.cr/SSTN-IABIN/species/browse/taxon/262393>.
- IARC International Agency for Research on Cancer. 1987.** *IARC Monographx on the evaluation of the carcinogenic risk to humans.* Lyon, France : s.n., 1987.

- Ikebe, M and Hartshorne, D J. 1985.** Phosphorylation of smooth muscle myosin at two distinct sites by myosin light chain kinase. *J Biol Chem.* August 25, 1985, 260(18), pp. 10027-10031.
- Jackson, C B and Giraud, A S. 2009.** Stat3 as a prognostic marker in human gastric cancer. *J Gastroenterol Hepatol.* April 2009, 24(4), pp. 505-507.
- Jiang, J and Xu, Q. 2003.** Immunomodulatory activity of the aqueous extract from rhizome of *Smilax glabra* in the later phase of adjuvant-induced arthritis in rats. *J Ethnopharmacol.* March 2003, 85 (1), pp. 53-59.
- Jinawath, N, et al. 2010.** Oncoproteomic analysis reveals co-upregulation of RELA and Stat5 in carboplatin resistant ovarian carcinoma. *PLoS One.* June 18, 2010, 5(6), p. e11198.
- Johnson, T. 1999.** *CRC Ethnobotany Desk Reference.* London, New York, Washington D.C. : Boca Raton, 1999. p. 641.
- Kanda, N, et al. 2004.** Stat3 is constitutively activated and supports cell survival in association with survivin expression in gastric cancer cells. *Oncogene.* June 17, 2004, 23(28), pp. 4921-4929.
- Karlson, P, et al. 2005.** *Karlsons Biochemie und Pathobiochemie.* Fifteenth. Stuttgart : Thieme Verlag, 2005.
- Kastan, M B and Bartek, J. 2004.** Cell-cycle checkpoints and cancer. *Nature.* November 18, 2004, 432(7015), pp. 316-323.
- Kimura, K, et al. 1996.** Regulation of myosin phosphatase by Rho and Rho-associated kinase (Rho-kinase). *Science.* July 12, 1996, 273(5272), pp. 245-248.
- Kinzler, Kenneth W and Vogelstein, Bert. 1997.** Cancer-susceptibility genes. Gatekeepers. *Nature.* April 24, 1997, 386(6627), pp. 761-763.
- Kiyokawa, H and Ray, D. 2008.** In vivo roles of CDC25 phosphatases: biological insight into the anti-cancer therapeutic targets. *Anticancer Agents Med Chem.* December 2008, 8(8), pp. 832-836.
- Kundu, J K and Surh, Y J. 2008.** Inflammation: gearing the journey to cancer. *Mutat Res.* July-August 2008, 659(1-2), pp. 15-30.
- Leung, T, et al. 1996.** The p160 RhoA-binding kinase ROK alpha is a member of a kinase family and is involved in the reorganization of the cytoskeleton. *Mol Cell Biol.* October 1996, 16(10), pp. 5313-5317.

- Löffler, G and Petrides, P E. 1997.** *Biochemie und Pathobiochemie*. sixth. Heidelberg : Springer Medizin Verlag, 1997. pp. 1090-1109.
- MacDougall, J R and Matrisian, L M. 1995.** Contributions of tumor and stromal matrix metalloproteinases to tumor progression, invasion and metastasis. *Cancer Metastasis Rev.* December 1995, 14(4), pp. 351-362.
- Madlener, S, et al. 2009.** Short 42 degrees C heat shock induces phosphorylation and degradation of Cdc25A which depends on p38MAPK, Chk2 and 14.3.3. *Hum Mol Genet.* June 1, 2009, 18(11), pp. 1990-2000.
- Mallat, Z, et al. 2003.** Rho-associated protein kinase contributes to early atherosclerotic lesion formation in mice. *Circ Res.* October 31, 2003, 93(9), pp. 884-888.
- Markowitz, S, et al. 1995.** Inactivation of the type II TGF-beta receptor in colon cancer cells with microsatellite instability. *Science.* June 2, 1995, 268(5215), pp. 1336-1338.
- Matsui, T, et al. 1996.** Rho-associated kinase, a novel serine/threonine kinase, as a putative target for small GTP binding protein Rho. *EMBO J.* May 1, 1996, 15(9), pp. 2208-2216.
- Meeran, S M and Katiyar, S K. 2008.** Cell cycle control as a basis for cancer chemoprevention through dietary agents. *Front Biosci.* January 1, 2008, 13, pp. 2191-2202.
- Mehnert, A, Bergelt, C and Koch, U. 2003.** *Prädiktive genetische Brust- und Ovarialkrebsdiagnostik*. Stuttgart : Schattauer, 2003. pp. 15-23.
- Missouri Botanical Garden. 2010.** [Online] 2010. [Cited: November 30, 2010.] <http://www.mobot.org/MOBOT/Research/APWeb/orders/Lilialesweb.htm#Smilacaceae>
- Mui, A L, et al. 1995.** Interleukin-3, granulocyte-macrophage colony stimulating factor and interleukin-5 transduce signals through two Stat5 homologs. *EMBO J.* March 15, 1995, 14(6), pp. 1166-1175.
- Nakagawa, O, et al. 1996.** ROCK-I and ROCK-II, two isoforms of Rho-associated coiled-coil forming protein serine/threonine kinase in mice. *FEBS Lett.* August 26, 1996, 392(2), pp. 189-193.
- National Park Service. 2010.** Santa Monica Mountains National Recreation Area. [Online] U.S. Department of Interior, August 11, 2010. [Cited: November 30, 2010.] <http://www.researchlearningcenter.com/bloom/bloom.htm>

- Natural Resources Conservation Service. 2010.** [Online] USDA United States Department of Agriculture, 2010. [Cited: 30 November 2010.] <http://plants.usda.gov/java/ClassificationServlet?source=profile&symbol=PLODO&display=63#>.
- Nau, H, Steinberg, P and Kietzmann, M. 2003.** *Lebensmitteltoxikologie. Rückstände und Kontaminanten: Risiken und Verbraucherschutz*. Berlin : Parey Buchverlag, 2003. pp. 11-13.
- Navarro, M C, et al. 2003.** Antibacterial, antiprotozoal and antioxidant activity of five plants used in Ibazal for infectious. *Phytother Res*. April 2003, 17(4), pp. 325-329.
- Noma, K, Oyama, N and Liao, J K. 2006.** Physiological role of ROCKs in the cardiovascular system. *Am J Physiol Cell Physiol*. March 2006, 290(3), pp. C661-668.
- Parkin, D M, et al. 2005.** Global cancer statistics, 2002. *CA Cancer J Clin*. March-April 2005, 55(2), pp. 74-108.
- Paton, S and Calderon, O. 2010.** *Environmental Science Program (ESP)*. [Online] Smithsonian Tropical Research Institute, 2010. [Cited: 30 November 2010.] http://www.discoverlife.org/mp/20p?see=L_SP3223&res=640.
- Paulitschke, V, et al. 2010.** 3,3',4,4',5,5'-hexahydroxystilbene impairs melanoma progression in a metastatic mouse model. *J Invest Dermatol*. June 2010, 130(6), pp. 1668-16679.
- Paull, T T, et al. 2000.** A critical role for histone H2AX in recruitment of repair factors to nuclear foci after DNA damage. *Curr Biol*. July 27, 2000, 10(15), pp. 886-895.
- Pecorino, L. 2008.** *Molecular Biology of Cancer*. Second. New York : Oxford University Press, 2008. pp. 1-3, 95-98, 139-149, 217, 218.
- Pieper, A A, et al. 1999.** Poly (ADP-ribose) polymerase, nitric oxide and cell death. *Trends Pharmacol Sci*. April 1999, 20(4), pp. 171-181.
- Piperno, G, LeDizet, M and Chang, x J. 1987.** Microtubules containing acetylated alpha-tubulin in mammalian cells in culture. *J Cell Biol*. February 1987, 104(2), pp. 289-302.
- Pitti, R M, et al. 1998.** Genomic amplification of a decoy receptor for Fas ligand in lung and colon cancer. *Nature*. December 17, 1998, 396(6712), pp. 699-703.

- Rastogi, R P and Dhawan, B N. 1982.** Research on medicinal plants at the Central Drug Research Institute, Lucknow (India). *Indian J Med Res.* December 1982, 76(27-45).
- Sahai, E and Marshall, C J. 2003.** Differing modes of tumour cell invasion have distinct requirements for Rho/ROCK signalling and extracellular proteolysis. *Nat Cell Biol.* August 2003, 5(8), pp. 711-719.
- Salgia, R, et al. 1995.** Molecular cloning of human paxillin, a focal adhesion protein phosphorylated by P210BCR/ABL. *J Biol Chem.* March 10, 1995, 270(10), pp. 5039-5047.
- Satoh, S, et al. 2003.** Chronic inhibition of Rho kinase blunts the process of left ventricular hypertrophy leading to cardiac contractile dysfunction in hypertension-induced heart failure. *J Mol Cell Cardiol.* January 2003, 35(1), pp. 59-70.
- Schaller, M D. 2001.** Paxillin: a focal adhesion-associated adaptor protein. *Oncogene.* October 1, 2001, 20(44), pp. 6459-6472.
- Shay, J W and Bacchetti, S. 1997.** A survey of telomerase activity in human cancer. *Eur J Cancer.* April 1997, 33(5), pp. 787-791.
- Shoeb, M. 2006.** Anticancer agents from medicinal plants. *Bangladesh J Pharmacol.* 2006, 1, pp. 35-41.
- Stetler-Stevenson, W G. 1999.** Matrix metalloproteinases in angiogenesis: a moving target for therapeutic intervention. *J Clin Invest.* May 1, 1999, 103(9), pp. 1237-1241.
- Stewart, B W and Kleihues, P. 2003.** *World Cancer Report.* Lyon : IARC Press, 2003.
- Strasser, A, O'Connor, L and Dixit, V M. 2000.** Apoptosis signaling. *Annu Rev Biochem.* 2000, 69, pp. 217-245.
- Tan, J L, Ravid, S and Spudich, J A. 1992.** Control of nonmuscle myosins by phosphorylation. *Annu Rev Biochem.* 1992, 61, pp. 721-759.
- Taylor, L. 2005.** *The Healing Power of Rainforest Herbs: A Guide to Understanding and Using Herbal Medicinals.* New York : Square One Publishers, 2005.
- Thornberry, N A and Lazebnik, Y. 1998.** Caspases: enemies within. *Science.* August 28, 1998, 281(5381), pp. 1312-1316.
- Till, U. 1999.** *Pathophysiologie/Pathobiochemie. Systematisch.* Bremen : UNI-MED, 1999. pp. 91-93.

- Totsukawa, G, et al. 2000.** Distinct roles of ROCK (Rho-kinase) and MLCK in spatial regulation of MLC phosphorylation for assembly of stress fibers and focal adhesions in 3T3 fibroblasts. *J Cell Biol.* August 21, 2000, 150(4), pp. 797-806.
- Uehata, M, et al. 1997.** Calcium sensitization of smooth muscle mediated by a Rho-associated protein kinase in hypertension. *Nature.* October 30, 1997, 389(6654), pp. 990-994.
- Vagelos, P R. 1991.** Are prescription drug prices high? *Science.* May 24, 1991, 252(5010), pp. 1080-1084.
- Veikkola, T and Alitalo, K. 1999.** VEGFs, receptors and angiogenesis. *Semin Cancer Biol.* June 1999, 9(3), pp. 211-220.
- Vetterkind, S, et al. 2010.** Par-4: a new activator of myosin phosphatase. *Mol Biol Cell.* April 1, 2010, 21(7), pp. 1214-1224.
- Wang, H, Birkenbach, M and Hart, J. 2000.** Expression of Jun family members in human colorectal adenocarcinoma. *Carcinogenesis.* July 2000, 21(7), pp. 1313-1317.
- Weinberg, R A. 1995.** The retinoblastoma protein and cell cycle. *Cell.* May 1995, 81(3), pp. 323-330.
- WHO. 2009.** Cancer Fact sheet N°297. [Online] World Health Organization, February 2009. [Cited: November 13, 2010.] <http://www.who.int/mediacentre/factsheets/fs297/en/index.html>.
- **2008.** Traditional medicine Fact sheet N°134. [Online] World Health Organization, Dezember 2008. [Cited: November 13, 2010.] <http://www.who.int/mediacentre/factsheets/fs134/en/>.
- Wolf, D and Rotter, V. 1985.** Major deletions in the gene encoding the p53 tumor antigen cause lack of p53 expression in HL-60 cells. *Proc Natl Acad Sci USA.* February 1985, 82(3), pp. 790-794.
- World Cancer Research Fund International. 2007.** *Food, Nutrition, Physical Activity, and the Prevention of Cancer: a Global Perspective.* Washington DC : World Cancer Research Fund / American Institute for Cancer Research, 2007.
- Wyllie, A H, Kerr, J F and Currie, A R. 1980.** Cell death: the significance of apoptosis. *Int Rev Cytol.* 1980, 68, pp. 251-306.
- Zielinski, C and Jakesz, R. 1999.** *Onkologie heute. Mammakarzinom.* Wien : Springer-Verlag KG, 1999. pp. 13-17.

9 Indices

9.1 Index of Tables

Table 1 Stationary phase, mobile phases and detection methods used for TLC	24
Table 2 Explanation of the formula used for calculation of proliferation assay data	25
Table 3 Antibodies used for western blots <i>P. odorata</i> fractions and <i>S. spinosa</i> extracts	28
Table 4 Mobile phases used for VLC of the chlorophyll-rich dichloromethane extract.	31
Table 5 Mobile phases used for VLC of F1	32
Table 6 Mobile phases used for CC of F2.6.....	33
Table 7 Mobile phases used for CC of F3.2.....	33
Table 8 Mobile phases used for CC of F4.2.2.....	34
Table 9 Mobile phases used for CC of F4.3.1	35
Table 10 Mobile phases used for CC of F4.6.3.....	36
Table 11 Solvents used for extraction of <i>S. spinosa</i>	37
Table 12 Obtained amounts of fractions from VLC of the chlorophyll-rich dichloromethane extract	42
Table 13 Obtained amounts of fractions from VLC of F1	47
Table 14 Obtained amounts of fractions from CC of F2.6.....	50
Table 15 Obtained amount of fractions from CC of F3.2	51
Table 16 Obtained amount of fractions from CC of F4.2.2	53
Table 17 Obtained amount of fractions from CC of F5.2.2.1	54
Table 18 Obtained amount of fractions from CC of F4.3.1	56
Table 19 Obtained amount of fractions from CC of F5.3.6.7	58
Table 20 Obtained amount of fractions from CC of F3.6	60
Table 21 Obtained amount of fractions from CC of F4.6.3	62
Table 22 Obtained amounts of extracts of <i>S. spinosa</i>	70
Table 23 Obtained amounts of fractions after detannification of the methanol extract..	74

9.2 Index of Figures

Figure 1 Multistep model of carcinogenesis (own figure, based on Oliveira, et al., 2007)	4
Figure 2 The six hallmarks of cancer (own figure, based on Hanahan, et al., 2000)	8
Figure 3 Cell cycle (own figure, based on Pecorino, 2008)	10
Figure 4 Apoptosis and necrosis characteristic morphological changes (own figure, based on Stewart, et al., 2003)	12
Figure 5 Intrinsic and extrinsic apoptotic pathway (Stewart, et al., 2003)	14
Figure 6 <i>P. odorata</i> plant and flower (National Park Service, 2010)	20
Figure 7 <i>S. spinosa</i> leave (Paton, et al., 2010) and root (own picture)	21
Figure 8 Cell culture work (left), HL-60 cells (right) (own pictures)	24
Figure 9 Fluorescence microscope (Axiovert, Zeiss) (own picture)	26
Figure 10 VLC of the chlorophyll-rich dichloromethane extract (own picture)	31
Figure 11 Fractionation overview of <i>P. odorata</i>	38
Figure 12 Anti-proliferative effect of dichloromethane extract from 2005 and of the one from 2009	39
Figure 13 TLC of chlorophyll-rich (a) and	40
Figure 14 Anti-proliferative effect of chlorophyll-free and chlorophyll rich dichloromethane extract of <i>P. odorata</i>	41
Figure 15 TLC of F1-F3	41
Figure 16 TLC of F1-F3	42
Figure 17 Anti-proliferative effect of F1, F2 and F3	43
Figure 18 Induction of apoptosis by F1, F2 and F3	45
Figure 19 Analysis of proliferation of HL-60 cells pre-treated with F1, F2 and F3, respectively	45
Figure 20 Western blot analysis of F1 on caspase 3 and α -tubulin	46
Figure 21 TLC of F2.1-F2.10	47
Figure 22 Induction of apoptosis by F2.1-F2.10	48
Figure 23 TLC of F2.6-F2.10	48
Figure 24 TLC of F3.1-F3.10	49
Figure 25 TLC of F3.1-F3.10	49

Figure 26 Anti-proliferative effect of F3.1-F3.10	50
Figure 27 TLC of F4.2.1-F4.2.6.....	51
Figure 28 Anti-proliferative effect of F4.2.1, F4.2.3-F4.2.6.....	52
Figure 29 TLC of F5.2.2.1-F5.2.2.4.....	53
Figure 30 TLC of F6.2.2.1.1-F6.2.2.1.4.....	53
Figure 31 Anti-proliferative effect of F6.2.2.1.1-F6.2.2.1.4	54
Figure 32 TLC of F4.3.1	55
Figure 33 TLC of F5.3.6.1-F5.3.6.12.....	55
Figure 34 Anti-proliferative effect of F5.3.6.1-F5.3.6.12	56
Figure 35 Induction of apoptosis by F5.3.6.1, F5.3.6.2, F5.3.6.6, F5.3.6.7, F5.3.6.10 and F5.3.6.11	58
Figure 36 TLC of F6.3.6.7.1-F6.3.6.7.12.....	58
Figure 37 Induction of apoptosis by F6.3.6.7.1-F6.3.6.7.12.....	59
Figure 38 TLC of F4.6.1-F4.6.4.....	60
Figure 39 Induction of apoptosis by F4.6.1-F4.6.4.....	61
Figure 40 TLC of F5.6.3.1-F5.6.3.6.....	61
Figure 41 Induction of apoptosis by F5.6.3.1-F5.6.3.6.....	62
Figure 42 Analysis of cell cycle and checkpoint regulators.....	63
Figure 43 Analysis of apoptosis related proteins	65
Figure 44 Analysis of mobility proteins.....	66
Figure 45 Fractionation steps overview	69
Figure 46 Anti-proliferative effect of extracts (petroleum ether, dichloromethane, ethyl acetate, methanol and water).....	71
Figure 47 Anti-proliferative effect of methanol extract.....	72
Figure 48 Anti-proliferative effect of methanol extract.....	72
Figure 49 Anti-proliferative effect of methanol extract.....	72
Figure 50 Induction of apoptosis by methanol extract.....	73
Figure 51 Induction of necrosis by methanol extract.....	74
Figure 52 TLC of petroleum ether extract (1), petroleum ether fraction (2), water- methanol fraction (3) and chloroform fraction(4)	75
Figure 53 Proliferation assay of petroleum ether fraction, water-methanol fraction and chloroform fraction achieved from the detannification process.....	76

Figure 54 Induction of apoptosis by petroleum ether fraction, water-methanol fraction and chloroform fraction achieved from the detannification process	77
Figure 55 Analysis of cell cycle regulators	78
Figure 56 Analysis of apoptosis related proteins	79
Figure 57 Analysis of oncogenes	81

10 Danksagung

Ich danke besonders meinem Betreuer Ao. Univ. Prof. Dr. Georg Krupitza, dass ich dieses interessante Thema bearbeiten durfte, vor allem aber für die nette Unterstützung in wissenschaftlichen und persönlichen Angelegenheiten und für das angenehme Arbeitsklima während des gesamten Jahres.

Außerdem danke ich Univ. Prof. Mag. Dr. Brigitte Kopp für die Betreuung am Department für Pharmakognosie, sowie Dr. Ruxandra Popescu für die mutmachenden und humorvollen Stunden im dortigen Labor.

Besonderer Dank auch an Mag. Sabine Bauer für die hilfreichen Informationen zu *P. odorata*, sowie Mag. Benedikt Giessrigl, Mag. Katharina Viola, Mag. Christine Unger, Nicole Kretschy und Mathias Teichmann für die sehr gute Zusammenarbeit in der Arbeitsgruppe.

Abschließend danke ich meinen lieben Eltern und Geschwistern für die immer positive Unterstützung, und meinem Freund Daniel, dafür dass er mich unterstützt hat, obwohl ich diese Arbeit in Word verfasst habe.

11 Curriculum Vitae

Name: Mareike Seelinger
Date of Birth: 04/05/1985
Place of Birth: Worms, Germany
Nationality: German

Education

since 2008 University of Vienna (Austria):
Master in Molecular Nutrition
2004 - 2008 Justus-Liebig University Giessen (Germany):
Bachelor in Nutritional Science and Home Economics
2001 - 2002 Memorial High-School Victoria (Texas, USA)
1995 - 2004 Lessing-Gymnasium Lampertheim (Germany)
1991 - 1995 Schillerschule Lampertheim (Germany)

Practical Work

2007 / 2008 11 weeks practical work at Wollongong Hospital (Australia)
2006 4 weeks research experience at the Ege University Izmir (Turkey)
2006 5 weeks practical work at the Consumer Advice Centre Darmstadt
(Germany)

12 List of Publications

Mareike Seelinger, Ruxandra Popescu, Benedikt Giessrigl, Christine Unger, Bruno Wallnöfer, Karl-Heinz Wagner, Monika Fritzer-Szekeres, Thomas Szekeres, Rene Diaz, Foster M. Tut, Richard Frisch, Brigitte Kopp, Georg Krupitza.

Smilax spinosa extract with anti-neoplastic properties.

To: Oncol Rep.

Mareike Seelinger, Ruxandra Popescu, Benedikt Giessrigl, Christine Unger, Sabine Bauer, Karl-Heinz Wagner, Monika Fritzer-Szekeres, Thomas Szekeres, Rene Diaz, Foster M. Tut, Richard Frisch, Björn Feistel, Brigitte Kopp, Georg Krupitza.

The fractionation and purification of an apoptotic principle in the dichloromethane extract of *Pluchea odorata*.

To: Int. J. Oncol.

Sabine Bauer, Judith Singhuber, **Mareike Seelinger**, Christine Unger, Katharina Viola, Caroline Vonach, Benedikt Giessrigl, Sibylle Madlener, Nicole Stark, Bruno Wallnöfer, Karl-Heinz Wagner, Monika Fritzer-Szekeres, Thomas Szekeres, Rene Diaz, Foster M. Tut, Richard Frisch, Björn Feistel, Brigitte Kopp, Georg Krupitza, Ruxandra Popescu.

Separation of anti-neoplastic activities by fractionation of a *Pluchea odorata* extract.

Front. Biosci., submitted

Christine Unger, Ruxandra Popescu, Benedikt Giessrigl, Daniela Laimer, Susanne Heider, **Mareike Seelinger**, Rene Diaz, Foster M. Tut, Richard Frisch, Bruno Wallnöfer, Gerda Egger, Melanie Hassler, Martin Knöfler, Karl-Heinz Wagner, Monika Fritzer-Szekeres, Thomas Szekeres, Lukas Kenner, Brigitte Kopp, Georg Krupitza.

The dichloromethane extract of the anti-malarial plant *Neurolena lobata* specifically down-regulates the lymphoma-inducing NPM-ALK fusion product.

To: Leukaemia Lymphoma

Christine Unger, Ruxandra Popescu, Benedikt Giessrigl, **Mareike Seelinger**, Bruno Wallnöfer, Monika Fritzer-Szekeres, Thomas Szekeres, Rene Diaz, Foster M. Tut, Richard Frisch, Karl-Heinz Wagner, Brigitte Kopp, Georg Krupitza.

Critonia extracts exert strong anti-leukemic activity.

To: Int. J. Oncol.

Caroline Vonach, Katharina Viola, Benedikt Giessrigl, Nicole Huttary, Ingrid Raab, Romana Kalt, Sigurd Krieger, Than Phuong Nha Vo, Sibylle Madlener, Sabine Bauer, Marian Brigitte, Monika Hämmerle, Brigitte Hantusch, Susanne Stary, Christine Unger, **Mareike Seelinger**, Andreas Eger, Robert Mader, Walter Jäger, Helmut Dolznig, Wolfgang Mikulits, and Georg Krupitza.

12(S)-HETE-induced lymphendothelial cell motility is regulated by VE-Cadherin, ZEB1, and NF- κ B.

To: Br. J. Cancer